Report No. CDOT-CTI-96-1

LONG-TERM PERFORMANCE TESTS OF SOIL-GEOSYNTHETIC COMPOSITES

Kanop Ketchart
Jonathan T.H. Wu
University of Colorado at Denver

Colorado Department of Transportation
4201 E. Arkansas Ave.
Denver, CO 80222

January 1996

Prepared in cooperation with the
U.S. Department of Transportation
Federal Highway Administration

REPORT DOCUMENTATION PAGE

FORM APPROVED
OMB NO. 0704-0188

1. AGENCY USE ONLY (Leave Blank)	2. REPORT DATE	3. REPORT TYPE AND DATES COVERED
	Jauary, 1996	Final Report

4. TITLE AND SUBTITLE
Long-Term Performance Tests of Soil-Geosynthetic Composites

5. FUNDING NUMBERS
270.03

6. AUTHORS(S)
Kanop Ketchart, Jonathan T. H. Wu

7. PERFORMING ORGANIZATION NAME(S) AND ADDRESS(S)
Colorado Department of Transportation
4201 E. Arkansas Ave.
Denver, Colorado 80222

8. PERFORMING ORGANIZATION REPORT NUMBER
CDOT-CTI-96-1

9. SPONSORING/MONITORING AGENCY NAME(S) AND ADDRESS(S)
Colorado Department of Transportation
4201 E. Arkansas Ave.
Denver, Colorado 80222

10. SPONSORING/MONITORING AGENCY REPORT NUMBER
CDOT-CTI-96-1

11. SUPPLEMENTARY NOTES
Prepared in Cooperation with the U.S. Department of Transportation, Federal Highway Administration

12a. DISTRIBUTION/AVAILABILITY STATEMENT
No Restrictions: This report is available to the public through the National Technical Information Service. Springfield, VA 22161

12b. DISTRIBUTION CODE

13. ABSTRACT (Maximum 200 words)

Creep criteria for designing with geosynthetics as earth reinforcement was developed from in-air testing. It has been observed many times that geosynthetically reinforced soils (GRS) do not exhibit creep behavior predicted by the in-air tests. In fact, significant long-term geosynthetic creep in GRS features built with granular soils is unreported.

This paper describes development of a testing device and testing protocol to measure performance of GRS composite behavior. Testing included geosynthetically-reinforced granular and cohesive soils as well as unreinforced soils. Loads and reinforcements were varied.

Of the several conclusions, one of the more important is that geosynthetic creep will not occur in GRS composites with granular soils. In fact, loads in geosynthetics can become less with time in "typical" field constructions with granular soil.

14. SUBJECT TERMS
Geosynthetic Reinforcement
Geosynthetic Creep, Creep
Long Term Performance Testing

15. NUMBER OF PAGES
156

16. PRICE CODE

17. SECURITY CLASSIFICATION OF REPORT	18. SECURITY CLASSIFICATION OF THIS PAGE	19. SECURITY CLASSIFICATION OF ABSTRACT	20. LIMITATION OF ABSTRACT
Unclassified	Unclassified	Unclassified	

ABSTRACT

Creep behavior is of concern in the design of geosynthetic-reinforced soil (GRS) structures because geosynthetics, which are manufactured with various polymers, are generally considered creep-sensitive. In the current design methods for GRS structures, creep is accounted for by performing geosynthetic "element" creep tests in which sustained loads are applied directly to the geosynthetic under confined or unconfined conditions. However, measurement of field performance of GRS retaining walls has indicated that the backfill properties play a very significant role in the long-term performance. To investigate the long-term interactive deformation characteristics of soil-geosynthetic composites, Wu and Helwany devised a long-term soil-geosynthetic performance test. In the test, a sustained surcharge was applied to the soil. The stress induced in the soil was transferred to the geosynthetic. Deformation of the soil-geosynthetic composite occurred as a result of soil-geosynthetic interaction.

In the course of this study, a modified long-term soil-geosynthetic performance test was developed. The test simulates the soil-geosynthetic interactive behavior in a "worst" condition by allowing a soil-geosynthetic composite to deform in a plane strain condition without lateral confinement.

A series of performance tests were performed to examine test repeatability

and to investigate the effects of soil type, geosynthetic type and sustained load intensity on the behavior of soil-geosynthetic composite. One test was conducted with the geosynthetic reinforcement instrumented with strain gages. The measurement indicated stress relaxation occurring approximately 10 minutes after load application. Tests with soil only were also conducted for comparisons with soil-geosynthetic composite tests. In addition, a load-deformation test with a weak geosynthetic reinforcement was conducted to examine its failure mode. Many of the tests were conducted at an elevated temperature of 125°F. Element tests conducted on the geosynthetic indicated that the creep rate increased by 100 to 400 folds under 125°F temperature.

A finite element model was employed to analyze the performance test. The analytical results were compared with the measures values.

CONTENTS

Chapter			Page
1.	Introduction		1
	1.1	Problem Statement	1
	1.2	Research Objectives	5
	1.3	Method of Research	6
2.	Test Materials and Material Properties		10
	2.1	Soils	10
	2.2	Geosynthetics	12
	2.3	Acceleration of Geosynthetic Creep at an Elevated Temperature	20
3.	Test Apparatus, Test Procedure, and Test Program		27
	3.1	Test Apparatus	27
	3.2	Test Procedure	34
	3.3	Test Instrumentation	36
	3.4	Testing Program	40
4.	Test Results and Discussion of Results		49
	4.1	Verification of Test Method	50

4.1.1 Repeatability Test 50
4.1.2 Failure Mode of the Performance Test 56
4.2 Behavior Before Releasing Lateral Support 56
4.3 Long-Term Behavior of the Performance Test 62
4.3.1 Deformed Shape of Test Specimen and Strain Distribution along the Geosynthetic 62
4.3.2 Loads in Geosynthetic Reinforcement 64
4.3.3 The Role of Reinforcement 75
4.3.4 Effect of Geosynthetic Type 81
4.3.5 Effect of Soil Type 90
4.3.6 Effect of Temperature 93
4.3.7 Effect of Sustained Vertical Surcharge 94
5. Finite Element Analysis of the Performance Test 103
5.1 The Finite Element Model 103
5.1.1 Sekiguchi-Ohta Soil Model 104
5.1.2 Generalized Geosynthetic Creep Model 105
5.2 Evaluation of Model Parameters 107
5.2.1 Sekiguchi-Ohta Model Parameters 107
5.2.2 Generalized Geosynthetic Creep Model 112
5.3 Finite Element Simulation of the Performance Test .. 112
5.3.1 Finite Element Simulation 112

5.3.2 Results of Finite Element Analysis 115

6. Summary and Conclusions 120

6.1 Summary 120

6.2 Conclusions 122

Appendixes

A. Performance Test Results 127

B. Input Data of Finite Element Analysis 139

Bibliography 151

1. INTRODUCTION

1.1 Problem Statement

Geosynthetic-reinforced soil (GRS) retaining wall have become increasingly popular in the construction of retaining structure because of its many advantages over conventional reinforced concrete walls, including:

(1) GRS retaining structures are more flexible, hence more tolerant to foundation settlement.

(2) Construction of GRS retaining structure is rapid and requires only "ordinary" construction equipment.

(3) GRS retaining structures are generally less expensive to construct than their reinforced concrete counterparts.

When a geosynthetic is used as reinforcement in a "permanent" retaining structure, acceptable performance of the GRS retaining structure must be satisfied throughout its design life. The creep behavior is of concerned in evaluating the long-term performance of GRS retaining structure because geosynthetic, which are manufactured with various polymers, are generally

considered creep-sensitive.

Some current design methods (e.g., AASHTO, 1992) for GRS retaining structure evaluate the long-term creep potential of a GRS retaining structure by performing "element" creep tests on the geosynthetic reinforcement alone (in either a confined or unconfined mode). Other design methods simply apply a safety factor or a creep reduction factor to the ultimate strength of the geosynthetic reinforcement to account for creep. All these design methods tacitly assumed that creep of a GRS retaining structure is due entirely to the geosynthetic and not affected by the surrounding soil.

Field measurement of GRS retaining walls has indicated little or no creep when granular backfill is employed. Some examples of well-instrumented, well-monitored GRS retaining structure are:

(1) A 41-ft high geosynthetic-reinforced soil retaining wall constructed in Seattle in 1989 The creep strains in the geotextile 11 months after fill placement were very small (with a maximum creep strain of about 0.13%). The creep rate was 4.5×10^{-4}% per day after fill placement, and 2.0×10^{-4}% per day ten months after fill placement. The rates were approaching zero, 11 months

after placement. The backfill was gravelly sand (Allen, et al., 1992).

(2) Forty-six geogrid-reinforced soil retaining walls constructed in Tucson, Arizona in 1984 and 1985 Field measurement showed that despite the in-soil temperature was relatively high (97°F), the geogrid reinforcement experienced a maximum strain of approximately 1.0% and was stable with time. The measured creep of the reinforcement in 10-year after construction was negligible (Collin, et al., 1994).

(3) An 18-ft high geogrid-reinforced test wall constructed in Algonquin, Illinois A number of instruments were used to monitored the behavior of the test wall. Measured data indicated that the strain/load level remained constant(i.e. no creep) throughout the first five months after construction, and there were no other time-dependent phenomena deteriorating the geogrid performance. The backfill was well-graded sand gravel (Simac, et al., 1990; Bathurst, et al., 1993).

However, the creep reduction factors adopted in the current design methods are fairly low, regardless of the backfill type. For example, creep reduction factors ranging from 0.25 to 0.4, depending on the polymer type

of a geosynthetic, were specified in the AASHTO design method.

To characterized the soil-geosynthetic composite behavior, Wu (1994) and Wu and Helwany (1996) developed a soil-geosynthetic long-term performance test, in which the stresses applied to the soil are transferred to the geosynthetic in a manner similar to the typical load transfer mechanism in GRS retaining structures, and both the soil and the geosynthetic are allowed to deform in an interactive manner under a constant sustained load. They reported two carefully conducted long-term performance tests, one used a clayey backfill and the other a granular backfill. Using element test on the geosynthetic alone, the maximum strain in the geosynthetic was underestimated by 250% in the clay-backfill test, and over-estimated by 400% in the sand-backfill test. It was noted that creep deformation essentially ceased within 100 minutes after the sand-backfill test began; whereas, the clay-backfill test experienced creep deformation over the entire test period (18 days).

Wu and Helwany (1996) indicated that long-term creep of a soil-geosynthetic is a result of soil-geosynthetic interaction. If the confining soil has a tendency to

creep faster than the geosynthetic reinforcement along its axial direction, the geosynthetic will impose a restraining effect on the deformation of the soil through the friction and/or adhesion between the two materials. Conversely, if the geosynthetic reinforcement tends to creep faster than the confining soil, then the confining soil will restrain the reinforcement deformation through the friction/adhesion. This restraining effect is a direct result of soil-reinforcement interaction where redistribution of stresses in the confining soil and changes in axial forces in the reinforcement occur over time in an interactive manner.

In this study, a modified soil-geosynthetic long-term performance test was developed. The modified test was simpler to perform, yet represent a "worst" condition by providing no lateral constraint to the soil-geosynthetic composite.

1.2 Research Objectives

The objectives of this research were three-fold. The first objective was establish a consistent test procedure for the modified soil-geosynthetic long-term performance test so that long-term soil-geosynthetic interaction

creep behavior can be assessed in a reliable manner. The second objective was to examine the soil-geosynthetic interaction creep behavior for various soils and geosynthetics under different conditions, including accelerated creep at an elevated temperature. The third objective was to analyze the load transfer mechanism in the long-term performance test.

1.3 Method of Research

This research was divided into two phases: an experimental phase and an analytical phase.

1.3.1 Experimental Study

Long-term performance tests were performed to examine the soil-geosynthetic interactive creep behavior in various conditions of soils, geosynthetics, sustained vertical surcharges, and temperatures.

Two types of soil, a road base and a clayey soil with 43% of fines, were employed as backfill for the tests. The road base is a silty sandy gravel(GM). It has been widely used as backfill for construction of road ways and retaining walls. The clayey soil has a plasticity index of 11 and a higher tendency to deform

with time than the road base.

Three types of geosynthetic, Amoco 2044, Amoco 2002, and Typar 3301, were selected as reinforcement for the tests. Amoco 2044 and Amoco 2002 are woven-prolypropylene geotextile with tensile strength of 400 lb/in. and 120 lb/in.,respectively. Amoco 2044 presents a strong reinforcement, while Amoco 2002 presents a weak reinforcement. Typar 3301 is a heat-bonded nonwoven-prolypropylene geotextile. This fabric was selected because of its relatively smooth surface which make mounting of strain gages much easier.

The test specimen comprised a cuboid of soil and a layer of geosynthetic reinforcement embedded at the mid-height of the soil. The soil-geosynthetic composite was prepared inside the apparatus. The soil was prepared at 2% wet-of-optimum moisture and compacted to 95% relative density for every test conducted in this study. For comparison, tests without geosynthetic (i.e., soil only) were also conducted.

Six long-term performance tests were conducted at an elevated temperature of 125°F to accelerate creep of the geosynthetics. Tests under ambient temperature were also conducted to examine the effects of temperature on soil-

geosynthetic composites.

A sustained average vertical pressure of 15 psi was applied to all of the performance tests except one test which was subjected to a sustained pressure of 30 psi. The test under 30 psi pressure was performed to examine the effects pressure intensity on the soil-geosynthetic composites.

The lateral and vertical displacements of the soil-geosynthetic composite were monitored by LVDT's (Linear Voltage Displacement Transducers) and mechanical displacement dial gages. In one test, strain gages were installed along the length of the geosynthetic to measure the distribution of axial strain with time. The measured results were also used for verification of a finite element analytical model.

1.3.2 Analytical Study

A finite element model developed by Helwany and Wu (1995) was employed to analyze the experimental results. The finite element model incorporated an elasto-viscoplastic soil model and a generalized creep model. The generalized creep model was developed by Helwany and Wu(1992) to simulate creep characteristics of

geosynthetics. The elasto-viscoplastic soil model was developed by Sekigushi and Ohta (1977). The finite element model has been verified with the measured behavior by Iizuka and Ohta (1987), Chou (1992) and Helwany and Wu (1995).

2. TEST MATERIALS AND MATERIAL PROPERTIES

2.1 Soils

A Road Base and a clayey soil with 43% of fines were selected for the tests. The road base has been widely used as backfill for construction of roadways and retaining walls. The clayey soil represents a natural soil which deforms significantly with time.

2.1.1 The Road Base

This soil was classified as A-1-B(0). The grain size distribution curve is shown in Figure 2.1. The material has 76% passing the standard sieve No. 4 and 19% passing No. 200. The specific gravity of the soil solids was 2.67. The maximum dry unit weight of the soil was 134 lb/ft^3 and the optimum moisture content was 7.2%. The Road Base was prepared inside the test apparatus by compaction with a 8-pound Proctor hammer. The soil was compacted to 95% relative density and 2% wet-of-optimun moisture content.

Three consolidated-drained (CD) triaxial compression tests at confining pressures of 15, 30, 45 psi were

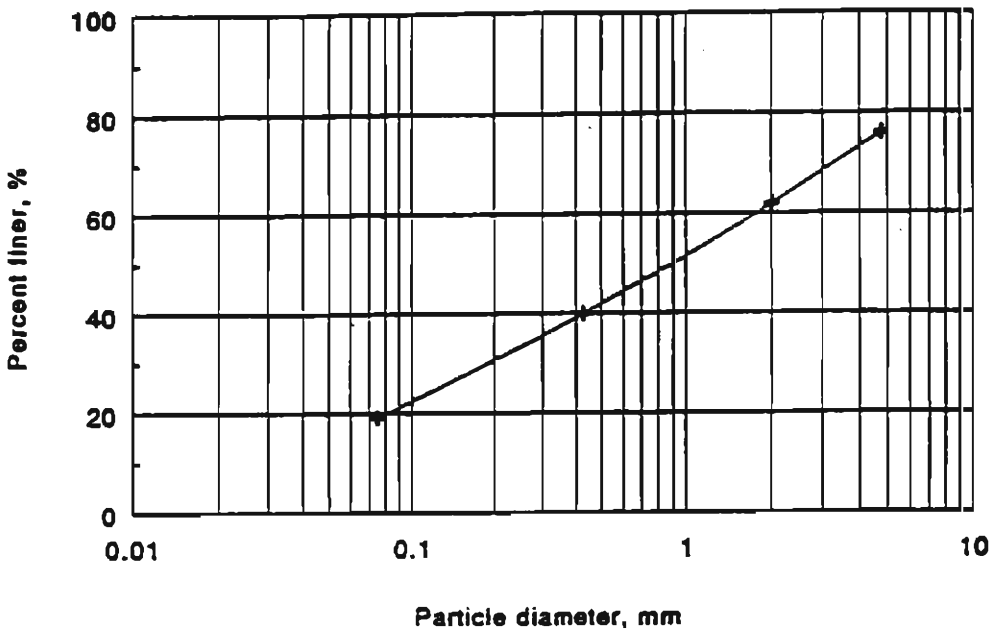

Figure 2.1 : Grain Size Distribution of the Road Base

conducted. The test specimen was prepared at a density of 126 lb/ft^3 and a moisture content of 8.5%. Each specimen was loaded at a constant deformation rate of $0.3x10^{-3}$in. per hour. The stress-strain relationship is shown in Figure 2.2. The internal friction angle of the road base was 32°.

2.1.2 The Clayey soil

This soil was classified as A-6. The grain size distribution curve is shown in Figure 2.3. The material has 100% passing the standard sieve No. 4 and 43% passing No. 200. The plasticity index and liquid limit were 11 and 26, respectively. The maximum dry unit weight was 120 lb/ft^3 and the optimum moisture content was 11%. The clayey soil was prepared inside the test apparatus in the same as that of the road base.

2.2 Geosynthetics

2.2.1 Amoco 2044

AMOCO 2044 is a woven polypropylene geotextile with some of its index properties listed in Table 2.1. The wide width Tensile test with Curtis Sure-Gripe with 16 inch gage length and 0.5 inch per minute cross head speed

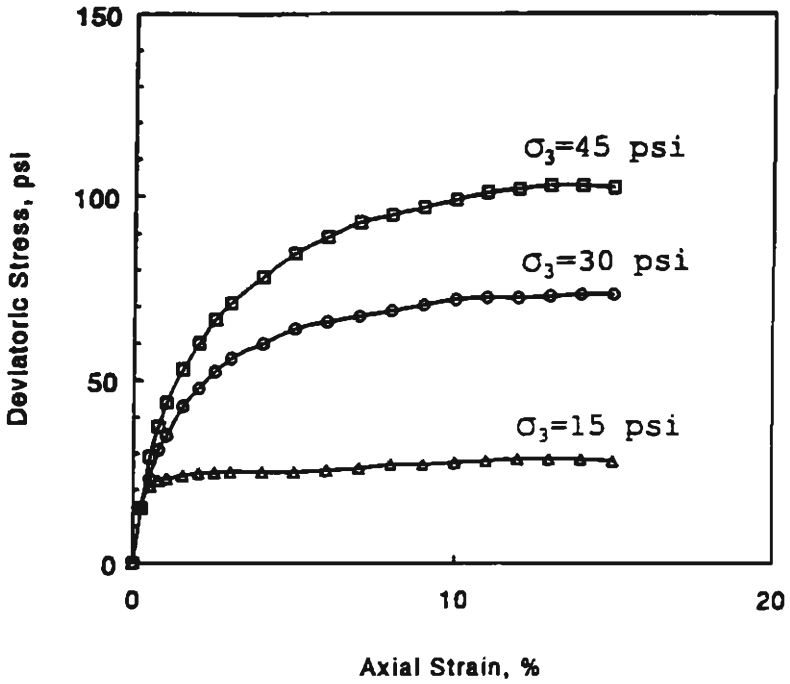

Figure 2.2 : Consolidated Drained Triaxial Test Results of the Road Base

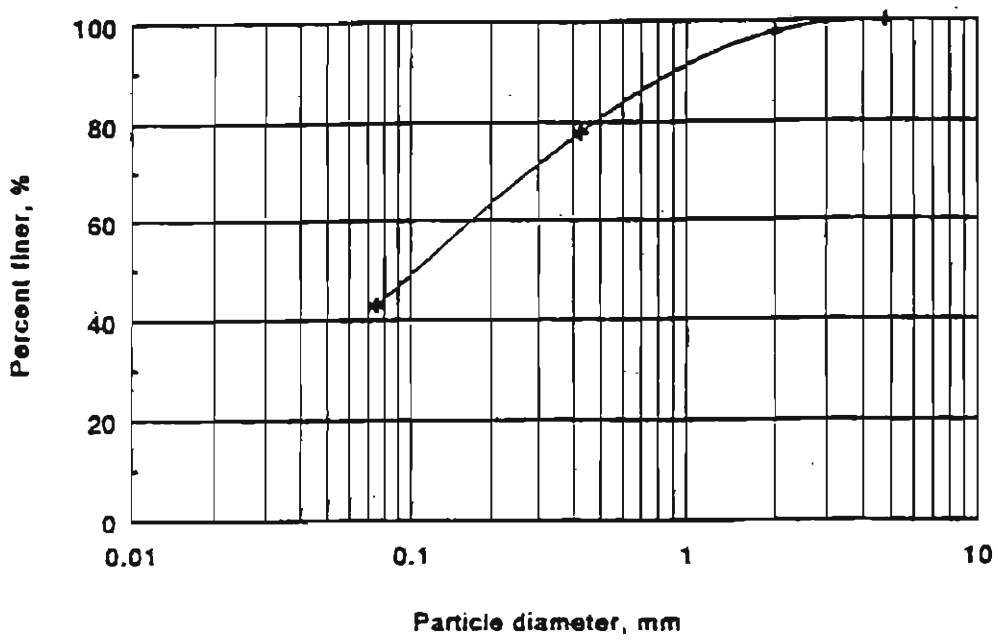

Figure 2.3 : Grain Size Distribution of the Clayey Soil

was conducted by the manufacturer. The load-deformation relationship is shown in Figure 2.4.

The element creep tests with 4-in. diameter roller grips and a 8-inch wide specimen have also been conducted by the manufacturer. These tests were conducted at temperatures of 70°F, 100°F, and 120°F, under constant loads corresponding to 22%, 25%, 30% of the ultimate load.

2.2.2 Amoco 2002

Amoco 2002 is a woven polypropylene geotextile. Creep test data was not available through the manufacturer because the main function of Amoco 2002 was not for reinforcement. The index properties of Amoco 2002 are listed in Table 2.1.

2.2.3 Typer 3301

Typar 3301 is a heat-bonded nonwoven polypropylene geotextile. This geotextile was selected because of easiness for strain gage installation and accuracy for measurement. The index properties of Typar 3301 are shown in Table 2.1.

The load-deformation behavior of Typar 3301 is shown

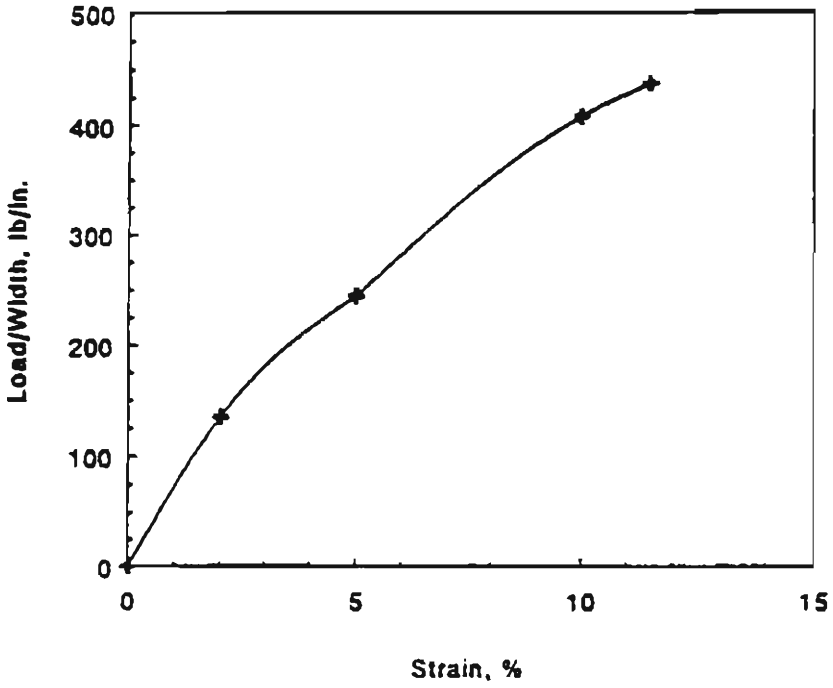

Figure 2.4 : Load-Deformation Behavior of Amoco 2044
(Courtersy of Rick Valentine,
Amoco Fabrics and Fibers Company)

Table 2.1 Some Index Properties of Geosynthetics

	Amoco 2044	Amoco 2002	Typar 3301
Polymer type	Polypropylene	Polypropylene	Polypropylene
Manufacturing Method	Woven	Woven	Non-woven
Wide width strength (ASTM D-4595)	400 lb/in.	120 lb/in.	35 lb/in.
Elongation at break (%) (ASTM D-4595)	18%	10%	60%
Grab tensile (ASTM D-4632)	600 lb	200 lb	120 lb
Elongation at break (%) (ASTM D-4632)	20%	15%	60%

in Figure 2.5. Specimens 30 cm in width and 3.75 cm in gage length were tested under three conditions: (1) unconfined (in-isolation), (2) confined by a sand, and (3) confined by a rubber membrane. For the confined tests (i.e. Test Conditions 2 and 3), an effective normal stress of 11 psi was applied on the geosynthetic. All the tests were conducted at a strain rate of 2% per minute (Wu, 1992).

The confined tests were conducted in a manner that the soil-reinforcement interface friction will not be inadvertently mobilized throughout the test. Detailed test procedures and test conditions have been presented by Wu (1991).

Since the load-deformation behavior of the heat-bonded geotextile is hardly affected by the confinement, as seen in Figure 2.5, the creep tests were conducted with the geotextile in isolation (unconfined). The specimen size used in the creep tests was 6 in. wide and 1 in. long. Both ends of the test specimen were glued between two sets of thin metal plates to facilitate application of loads. The sustained loads used in the tests were 96, 140, and 180 lb/ft (approximately 24%, 35%, and 45% of the short-term ultimate strength,

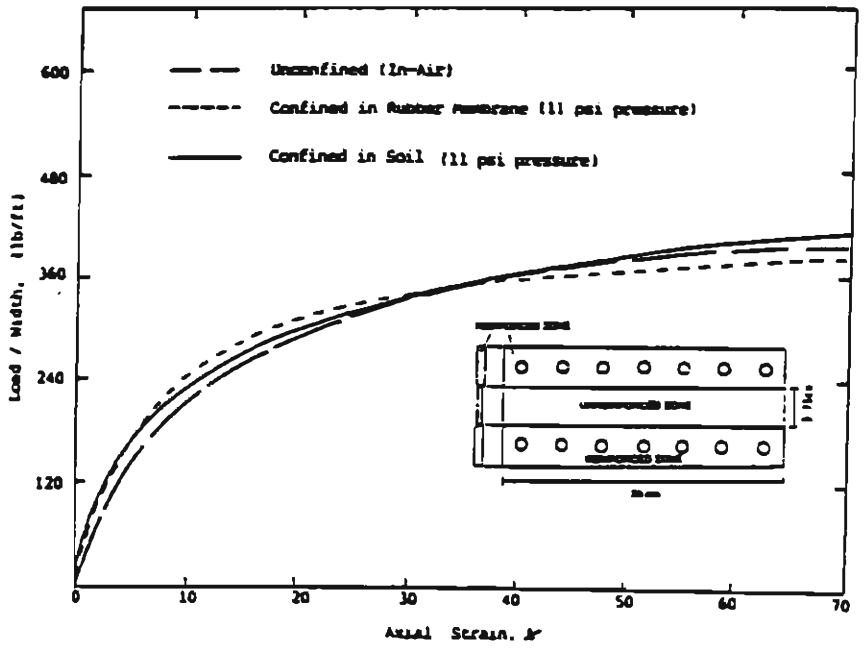

Figure 2.5 : Load-Deformation Behavior of Typar 3301 (Wu, 1992)

respectively). The results of the creep tests are shown in Figure 2.6.

2.3 Acceleration of Geosynthetic Creep at an Elevated Temperature

A Higher temperature has a tendency to accelerate creep in a polymer. Hence, creep tests should be conducted to cover a range of temperatures in the anticipated in-service condition of the structure. This does, however, require extensive testing at different temperatures over considerable time periods. In absence of such information, time-shifting techniques may be utilized (with caution) to account for the effect of temperature.

Morgan and Ward (1971) have indicated that the creep curves at a given temperature can be obtained by a simple horizontal shift of a creep curve obtained at different test temperature under the same sustained load. A number of element creep tests at different temperatures need to be conducted to establish the time shifting factor.

Element creep curves for Amoco 2044 subject to three different sustained loads at temperatures of 70°F, 100°F and 120°F, as described in Section 2.2.1, were used to

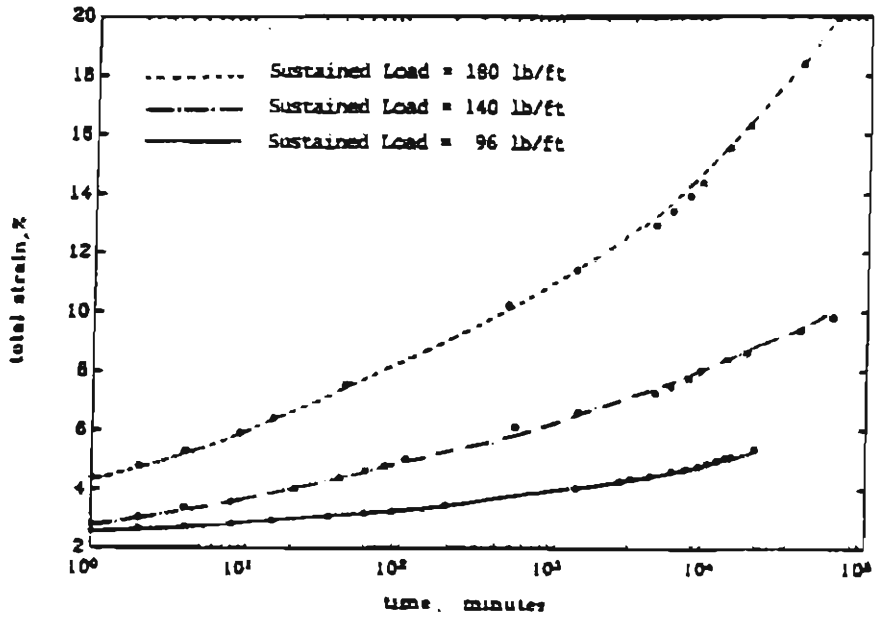

Figure 2.6 : Creep Behavior of Typar 3301 Geotextile (Wu, 1992)

evaluate the time shifting factor, as shown in Table 2.2.

The time shifting factor varies with the intensity of the sustained load, as well as the strains induced in Amoco 2044 geotextile. For instance, at 70°F and under a sustained load corresponding to 30% of the ultimate load, a strain of 5.0% was measured at an elapsed time of approximately 25 hours. At 120°F temperature, under otherwise identical conditions, 5.0% strain was reached at an elapsed time of 0.1 hour, which gives a time shifting factor of 250. Under a sustained load corresponding to 25% of the ultimate load, the elapsed time needed to reach 5% strain was about 110 hours at 70°F, and about 1.1 hour at 120°F, giving a time shifting factor of 100. At a strain of 7.5%, under 25% ultimate load, the shifting factor was 180. The value of the time shifting factor for Amoco 2044 typically varies tween 100 to 400 for temperatures raised from 70°F to 120°F. Namely, as temperature increases from 70°F to 120°F, the creep rate typically increases by 100 to 400 folds.

Table 2.2 Acceleration of Creep of Amoco 2044 for an increase of temperature from 70°F to 125°F

Sustained Load (% of ultimate Load)	Strain (%)	Elapsed Time (hours)		Time Shifting Factor
		70°F	120°F	
22%	4	100	0.2	500
	5	1,000	3	330
	6	4,500	15	300
25%	4.5	30	0.2	150
	5	110	1.1	100
	6.5	1,000	11	100
	7.5	5,400	30	180
30%	5	25	0.1	250
	6	200	1	200
	10	4,000	41	100

[B L A N K]

[B L A N K]

[B L A N K]

3. TEST APPARATUS, TEST PROCEDURE, AND TEST PROGRAM

3.1 Test Apparatus

Wu (1994) and Wu and Helwany (1996) developed a long-term soil-geosynthetic performance test to investigate long-term interactive behavior of soil-geosynthetic composite. A schematic diagram of the test device is shown in Figure 3.1, in which a reinforced soil unit was placed inside a rigid container with transparent plexiglass side walls. The reinforced soil unit comprised a geosynthetic reinforcement, two vertical flexible steel plates, and confining soil. The confining soil confined the geosynthetic reinforcement at both top and bottom. The two ends of the geosynthetic reinforcement were securely attached to the two vertical steel plates, each of 1 mm in thickness, at their mid-height. The transverse direction of the reinforced soil unit was fitted between two lubricated plexiglass side-wall of a rigid container in such a manner that the reinforced soil unit was restrained from movement in the direction perpendicular to the plexiglass side walls (i.e., in a plane strain

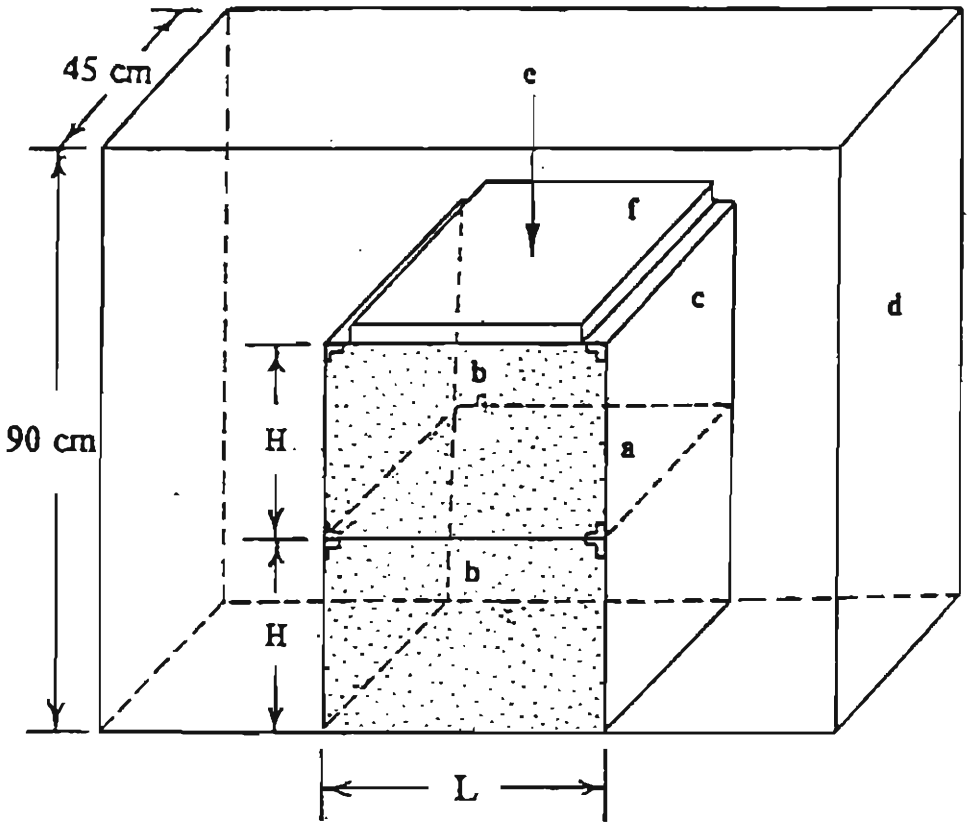

Dimensions:

Sand-Backfill Test:

L = 81.3 cm

H = 30.5 cm

Clay-Backfill Test:

L = 45.7 cm

H = 25.4 cm

Legends:

a	Geosynthetic Reinforcement
b	Soil
c	Steel Plate
d	Rigid Container with Lubricated Side Walls
e	Sustained Load
f	Rigid Plate

Figure 3.1 : Schematic Diagram of the Long-Term Soil-Geosynthetic Performance Test Device (Helwany and Wu, 1996)

configuration). On the top surface of the confining soil, another sheet of geosynthetic was used to connect the top edge of the vertical steel plates. Upon the application of a sustained vertical surcharge to the top surface of the reinforced soil unit, the geosynthetic reinforcement and its confining soil will deform in an interactive manner over time. Namely, there will be an interactive retraining effecting on deformation between the geosynthetic reinforcement and the soil.

To maintain plane strain condition throughout the test, the interface between the rigid plexiglass and the soil was minimized to near frictionless. This was accomplished by creating a lubrication layer at the interface of the plexiglass side-wall and the soil. The lubrication layer consists of a 0.02 mm thick membrane and a thin layer of a silicon grease. This procedure was developed by Tatsuoka at the University of Tokyo. The friction angle between the lubrication layer and plexiglass as determined by the direct shear test was less than one degree (Tatsuoka, et al., 1984).

In this study, a modified apparatus was developed to simplify sample preparation and load application. A photograph and a schematic diagram of the modified long-

term performance test apparatus are shown, respectively, in Figures 3.2 and 3.3. The modified apparatus differs from the original device in five aspects:

(a) Dimension of test apparatus The modified test apparatus is 1-ft high, 2-ft wide, and 2-ft long, which was smaller than the original apparatus depicted in Figure 3.1. Test specimen was reduced to 1-ft high, 1-ft wide, and 2-ft long. The test specimen was prepared at the center of the test apparatus.

(b) Moveable Lateral Supporting Panels The longitudinal direction of the test specimen was fitted between two lubricated plexiglass panels. These two lateral supporting panels can be moved horizontally. The movement was controlled by an air cylinder attached to each panel. After the lateral supporting panels were released (i.e., moved away from the soil) the test specimen was free to move in the longitudinal direction in an unconfined condition. This represents a "worst" condition as any lateral confinement will undoubtedly reduce lateral deformation of the soil-geosynthetic composite.

(c) Attachment of Geosynthetic The geosynthetic reinforcement at the mid-height as well as at the top surface were simply laid horizontally without attaching

to the vertical plates (not present in the modified apparatus) as in the original apparatus. Such a manner greatly simplifies sample preparation and eliminate possible bucking of the vertical plate.

(d) Load Application Mechanism In the modified test, the sustained vertical load was applied with a self-contained loading mechanism which consisted of a rigid frame and a Conbel pneumatic loader. The rigid loading frame was used as the reaction for the load application. To distribute a concentrate load to the top surface of the specimen, rigid plexiglass plates of different sizes were assembled in a pyramid configuration. The moveable supporting panels were released after the sustained vertical load was applied for a given period of time.

(e) Measurement of Lateral Deformation The lateral deformation of test specimen was measured by LVDT's (Linear Voltage Deformation Transducers) at the mid-height, where the geosynthetic reinforcement was located. Mechanical displacement dial gage was used to measure the vertical displacement of the specimen.

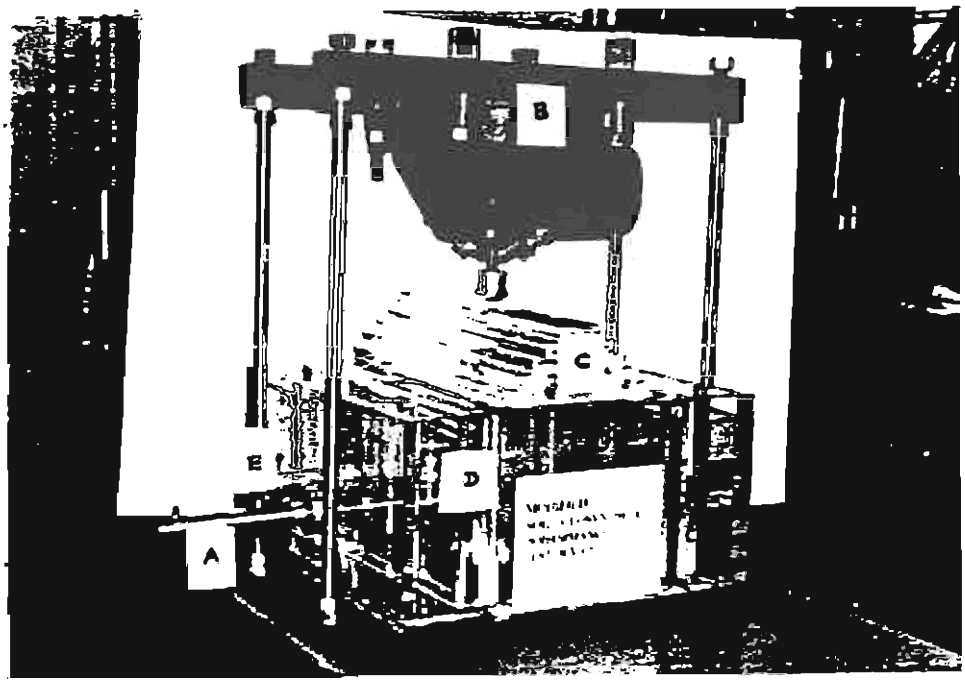

Legends:

A Air Cylinder

B Conbel Pneumatic Loading Device

C Loading Plate

D Lateral Movable Supporting Panel

E LVDT Supporting Tube

Figure 3.2 : The Modified Long-Term Soil-Geosynthetic Performance Test Device

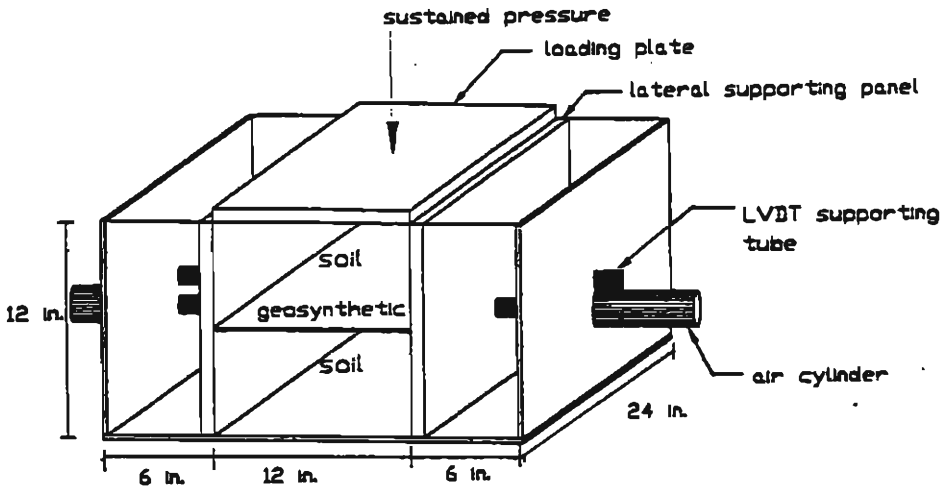

(a) Before Releasing Lateral Supporting Panels

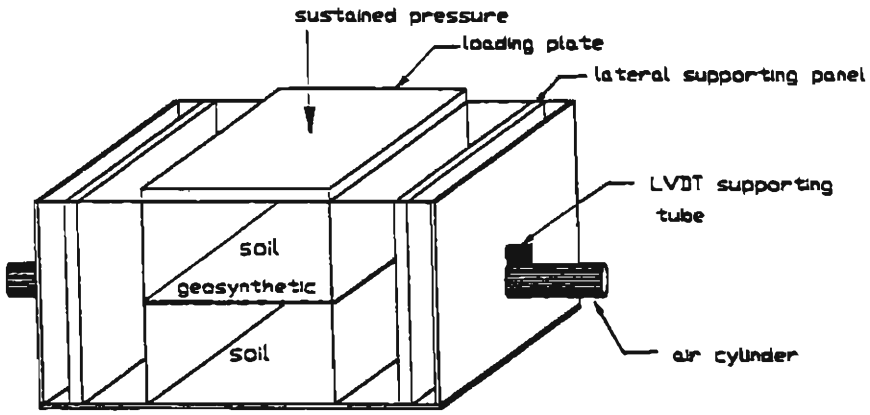

(b) After Releasing Lateral Supporting Panels

Figure 3.3 : Schematic Diagram of the Modified Long-Term Soil-Geosynthetic Performance Test Device

3.2 Test Procedure

The procedure for the Long-Term Soil-Geosynthetic Performance test can be described in the following steps:

1. prepare the soil at the desired moisture content (2% wet-of-optimum in this study) and cure the soil overnight in a sealed container inside a high humidity room.

2. apply lubrication layers, each consist of a latex membrane and a thin layer of a silicon grease, on all four sides of the plexiglass.

3. restrain movement of the moveable supporting panels with a high air pressure (80 psi) through air cylinders. A pair of carpenter's clamps were also used to prevent movement of the supporting panel during soil compaction. This creates a cuboidal volume of 1 ft by 1 ft by 2 ft, within which a sample can be prepared.

4. place a layer of geosynthetic (1 ft by 2 ft in size) at the bottom of the test device, and compact the soil in lifts until it reaches the mid-height (i.e., 0.5 ft), and lay a layer of geosynthetic (1 ft by 2 ft in size) covering the soil surface.

5. compact soil in lifts over the geosynthetic layer until it reaches 1 ft height, and cover the top surface

with a layer of geosynthetic.

6. remove the carpenter's clamps, and mount the LVDT's and dial indicator, and set the readings to zero.

7. cover the test specimen with a plastic sheet to keep a constant moisture content.

8. apply a sustained vertical load through a loading plate placed on the top surface of the geosynthetic layer (see Figure 3.3(a)).

9. release the moveable supporting panels (the supporting panels are retracted and the lateral confinement is removed) after the sustained vertical load has been applied for a given amount of time (see Figure 3.3(b)), and take a reading of the immediate response.

10. take measurement periodically by a data acquisition system.

In case of testing at elevated temperature (125□F), tests were performed in a heat chamber at constant temperature and humidity (provided by humidifier), as shown in Figure 3.4. In order to achieve consistent elevated temperature of test specimen, test specimen in test apparatus was placed in the heat chamber for 2 days before load application.

3.3 Test Instrumentation

The instruments used in the test are LVDT and mechanical displacement dial gage. With the exception of one test (Test D-1), two LVDT's were used to measure the lateral deformation of test specimen, a dial gage was used to measure the vertical displacement. A typical layout of instrumentation is depicted in Figure 3.5.

3.3.1 Linear Voltage Deformation Transducer (LVDT)

Linear Voltage Deformation Transducer (LVDT) was placed in a horizontal position used to measure lateral movement of the soil-geosynthetic composite. The stylus of LVDT was set to just touch the mid-height of the composite, where the reinforcement layer was placed. Two LVDT's were employed in each test, one on each side of the composite. Reading of the LVDT's was recorded periodically by an automated data acquisition interfaced with a personal computer.

3.3.2 Mechanical Displacement Dial Gage

Mechanical displacement dial gage was used to measure the vertical displacement of the soil-geosynthetic composite. The tip of the dial gage was set

Figure 3.4 : The Modified Long-Term Soil-Geosynthetic Performance Test Device at Elevated Temperature

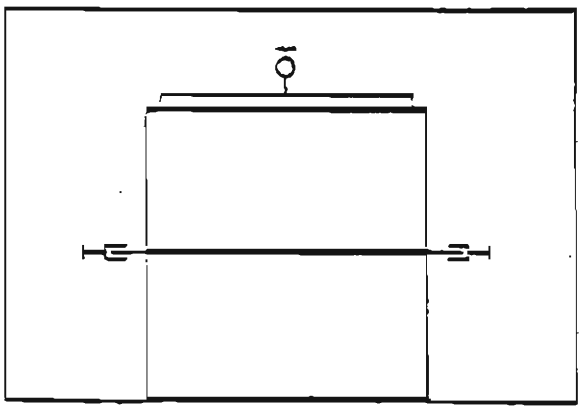

Legend

linear voltage displacement transducer

mechanical displacement dial gage

Figure 3.5 : Layout of Instrumentation

to touch the top of the loading plate. The accuracy of the dial gage was ±0.001 in.

3.3.3 Strain Gage

High-elongation strain gages were used to measure the strain distribution of the Typar geotextile in one of the tests (Test D-1). Two additional layout of the instruments in such test is depicted in Figure 3.6.

A total of 10 strain gages were mounted along the length of geosynthetic on two parallel lines to provide redundancy of the measurement. To avoid inconsistent local stiffening of the geotextile by the adhesive, the strain gage attachment technique developed by Billiard and Wu (1991) was employed by gluing only the two ends of a strain gage to the surface of geotextile with two-ton epoxy. This technique has been used successfully by Wu (1992) and Helwany (1994).

Because the soil contained gravel and was moist. A microcrystalline wax material was used to protect the gages from soil moisture. For five of the strain gages, an extensible neoprene rubber patch was used to cover each strain gage (see Figure 3.7) to prevent the expected mechanical damage during compaction. Helwany (1994)

conducted two uniaxial tension tests, one with and the other without the protective cover (wax material plus Neoprene patch), to examine the effect of the protective cover on the extensibility of the geotextile. The results indicated that the protective material had little effect on the extensibility of the geotextile.

A uniaxial tension test with two strain gages on a geotextile specimen was performed to obtain the calibration curve. The calibration curves for the two strain gages, as shown in Figure 3.8, are nearly identical.

3.4 Testing Program

The testing program was designed to examine the effects of various factors on long-term behavior of soil-geosynthetic composites. These factors included soil type, geosynthetic type, temperature, and sustained vertical surcharge. To demonstrate the validity of the test method, repeatability tests and load-deformation tests were also performed. A summary of these tests is presented in Table 3.1. The test conditions are described briefly as following:

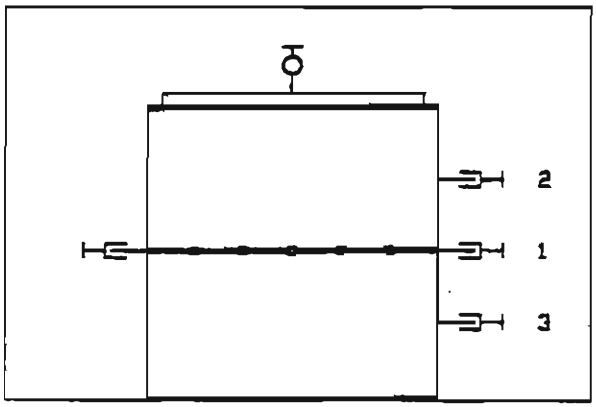

Legend

□ strain gage

linear voltage displacement transducer

mechanical displacement dial gage

Figure 3.6 : Layout of Instrumentation of Test D-1

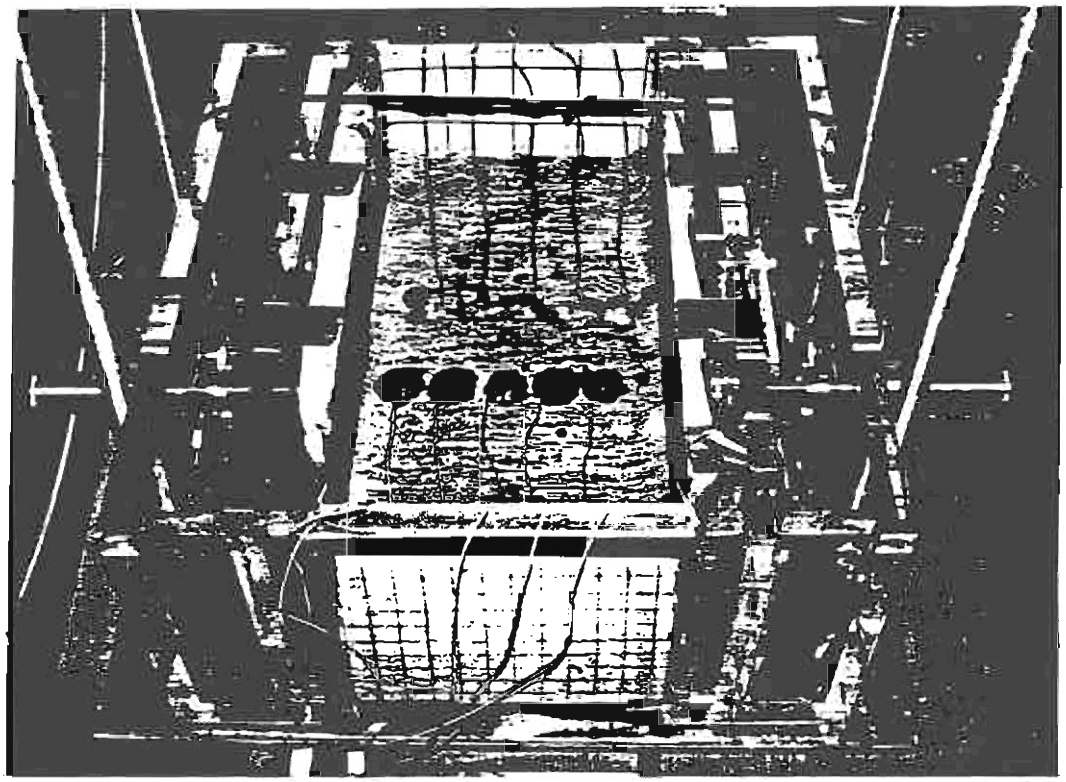

Figure 3.7 : Strain Gages Mounted along the Length of Geotextile

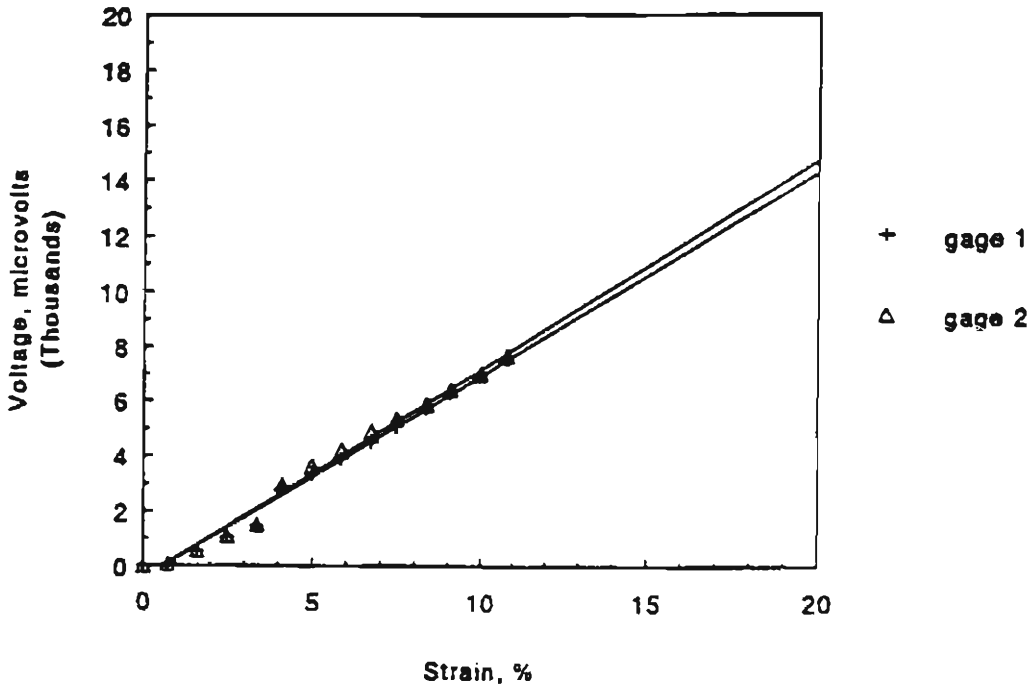

Figure 3.8 : Calibration Curves for Strain Gages on Typar 3301 Geotextile

Table 3.1 Test Program

Test Designation	Soil	Reinforcement	Temp. (°F)	Sustained Average Vertical Pressure (psi)	Total Elapsed Time (days)
C-1	C.S.	None	70	15	30
C-2	C.S.	Amoco 2044	70	15	30
D-1	R.B.	Typar 3301	70	15	15
H-1	R.B.	Amoco 2044	125	30	30
R-1	R.B.	Amoco 2044	70	15	30
R-2	R.B.	Amoco 2044	125	15	30
R-3	R.B.	Amoco 2044	125	15	30
S-1	R.B.	None	70	15	30
S-2	R.B.	None	125	15	30
U-1	R.B.	Amoco 2002	70	failure	failure
W-1	R.B.	Amoco 2002	125	15	30

Note: R.B.= road base

C.S.= a clayey soil with 43% of fines and PI=11

3.4.1 Repeatability Tests

Two tests were conducted in identical conditions to examine repeatability of the performance test. Tests R-2 and R-3 were conducted with the road base and Amoco 2044 reinforcement. The tests were conducted under a sustained average vertical pressure of 15 psi, and at a constant temperature of 125°F.

3.4.2 Failure Mode of the Performance Test

In order to investigate failure mode of the performance test, a soil-geosynthetic composite (with the road base and Amoco 2002) was subjected to an increasing applied load at a constant rate of 0.6 in. per minute, using a MTS-810 loading machine, until a failure condition developed. This test was designated as Test U-1.

3.4.3 Deformed Shape of Test Specimen and Strain Distribution along the Geosynthetic

To examine strain distribution along the geosynthetic reinforcement and deformed shape of the test specimen, a Test designated as Test D-1 was conducted.

The soil-geosynthetic composite consisted of the road base and Typar 3301 reinforcement. Ten strain gages were installed along the length of the geotextile to measure the distribution of strain with time under an average vertical pressure of 15 psi and at ambient temperature. LVDT's were used to measure horizontal displacement of the specimen at Points 1, 2, and 3, as shown in Figure 3.7. The vertical movement was measured by a mechanical displacement dial gage.

3.4.4 Roles of Reinforcement

Tests C-1, S-1 were conducted with the clayey soil and the road base only, respectively, under a sustained average vertical pressure of 15 psi at 70°F. Comparisons between Test C-2 and C-1, and between R-1 and S-1 were made to assess the role of reinforcement in the long-term performance test. Test C-2 and R-1 were conducted under the same conditions as Tests C-1 and S-1, except that Test C-1 and R-1 are with Amoco 2044 reinforcement. To investigate the roles of reinforcement at an elevated temperature, Test S-2 was performed with the road base only, under a sustained average vertical pressure of 15 psi at 125°F to compare with Test R-2 which was conducted

under the same conditions as Test S-2 except a sheet of Amoco 2044 was incorporated in Test R-2.

3.4.5 Effect of Soil Type

To assess the behavior of the performance test with different soil types, the clayey soil and the road base were employed in Tests C-2 and R-1, respectively. Both tests used Amoco 2044 reinforcement and were conducted under a sustained average pressure of 15 psi at 70°F.

3.4.6 Effect of Temperature

The creep behavior of the performance test at ambient and elevated temperatures was examined by Tests R-1 and R-2. Test R-1 was conducted at 70°F, while Test R-2 was at 125°F. Both Tests R-1 and R-2 used the road base and Amoco 2044 reinforcement and both were subjected to a sustained average pressure of 15 psi.

3.4.7 Effect of Geosynthetic Type

Amoco 2002 and Amoco 2044 are manufactured by the same method and with the same polymer except that the

same method and with the same polymer except that the ultimate tensile strength of Amoco 2002 is about 3 times lower than Amoco 2044. Test W-1, consisted of the road base and Amoco 2002 reinforcement, were conducted to assess the effect of reinforcement strength by with Test R-2 which was conducted under the same conditions except with Amoco 2044 reinforcement.

The effect of reinforcement type can be also be examined by comparing Tests D-1 and R-1 which were conducted under the same conditions (with the road base under a sustained average pressure of 15 psi at 70□F). Typar 3301 and Amoco 2044 were used as reinforcement in Test D-1 and R-1, respectively.

3.4.8 Effect of Sustained Vertical Surcharge

Test H-1 was designed to examine the behavior of the performance test under a higher sustained vertical load. An average sustained vertical pressure of 30 psi was applied in Test H-1 which was conducted under the same condition as test R-2 except for the average sustained vertical pressure.

4. TEST RESULTS AND DISCUSSION OF RESULTS

In this research, a number of performance tests were conducted with different soils, geosynthetics, sustained vertical surcharges, and at different temperatures. Lateral and vertical displacements of the soil-geosynthetic composite were recorded periodically throughout each test. The term lateral displacement, unless otherwise specified, is referred to the total lateral displacement on both sides of the test specimen at the mid-height of the soil-geosynthetic composite (i.e. at the location of the reinforcement). The time, t, is referred to the elapsed time after the supporting panels were removed. Strain distributions along geosynthetic with time were measured in one test only (Test D-1). The test data presented in this chapter are tabulated in Appendix A.

4.1 Verification of Test Method

4.1.1 Repeatability tests

Figures 4.1(a) and 4.1(b) show the lateral and vertical displacements versus time relationships of Tests R-2 and R-3, respectively. The two tests were conducted under the same condition (road base with Amoco 2044 reinforcement, under a sustained average pressure of 15 psi, at 125°F) to examine the repeatability of the performance test.

Because of the electrical interference of data acquisition system, significant reading scatters of LVDT readings were experienced. To examine the extent of the electrical interference, two LVDT's with their stylus touching a rigid wall (i.e., presumably a zero displacement) were tested in the heat chamber. The readings, as shown in Figure 4.2, are seem to deviate from zero with an accuracy of $\pm 0.4 \times 10^{-2}$ in. To accommodate these scatters, curve fittings were performed on the test data to allow comparison of lateral and vertical displacements versus time for Tests R-2 and R-3.

Initial vertical displacements at t= 10 min. of 0.018 in. and 0.020 in., and initial lateral displacements of 0.028 in. and 0.013 in. were measured

displacements of 0.028 in. and 0.013 in. were measured for Tests R-2 and R-3 after releasing of lateral supports, respectively. The differences are mostly due to the differences in the degree of restraint of the supporting panels.

The magnitudes of creep deformation over 43,200 min. (30 days) and the rates of creep in both directions for Tests R-2 and R-3 were similar. As shown in Table 4.1, the creep deformation in vertical and lateral directions at t=43,200 min. were, respectively, 0.054 in. and 0.055 in. for Test R-2; and were 0.055 in. and 0.054 in. for Test R-3. The creep rates decreased at fast decreasing rate in both vertical and lateral direction in both tests. The repeatability of the performance test is considered satisfactory.

It is of great important to note that, under the elevated temperature condition of which the creep rate accelerated more than 100 folds, the creep deformation was very small and essentially ceased after t=30,000 minutes. This behavior conferred with those observe in full-scale tests (see section problem statement in Chapter 1) that creep was negligible.

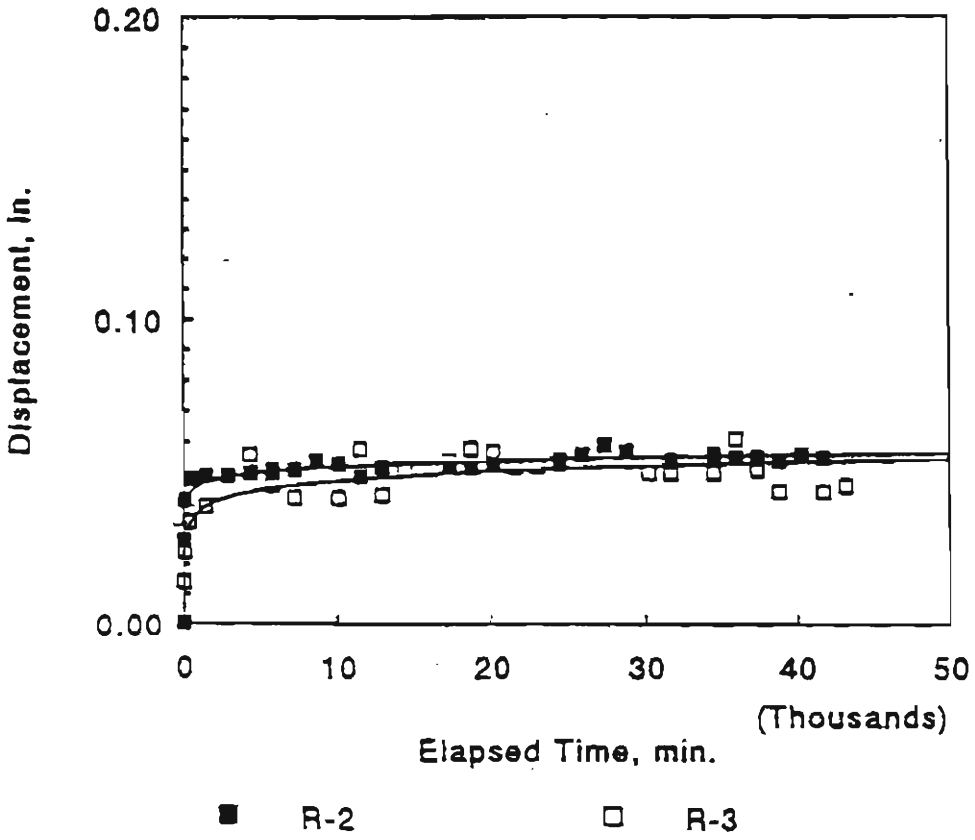

Figure 4.1(a) Lateral Displacements Versus Time Relationships of Tests R-2, R-3

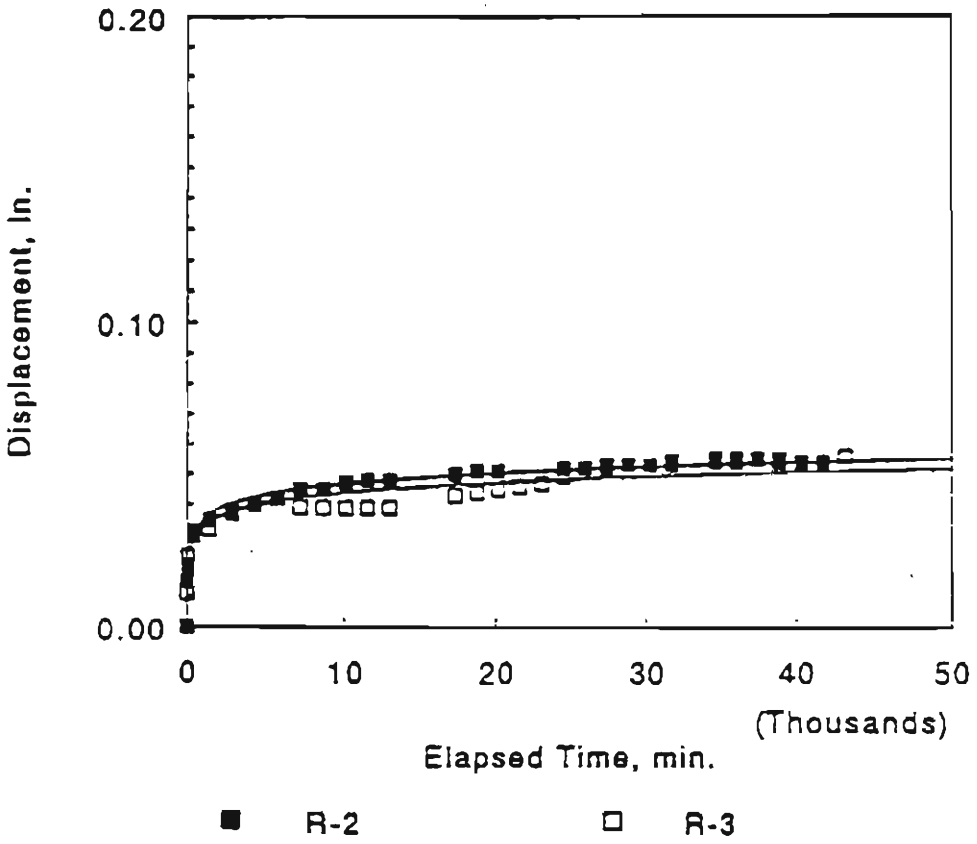

Figure 4.1(b) Vertical Displacements Versus Time Relationships of Tests R-2, R-3

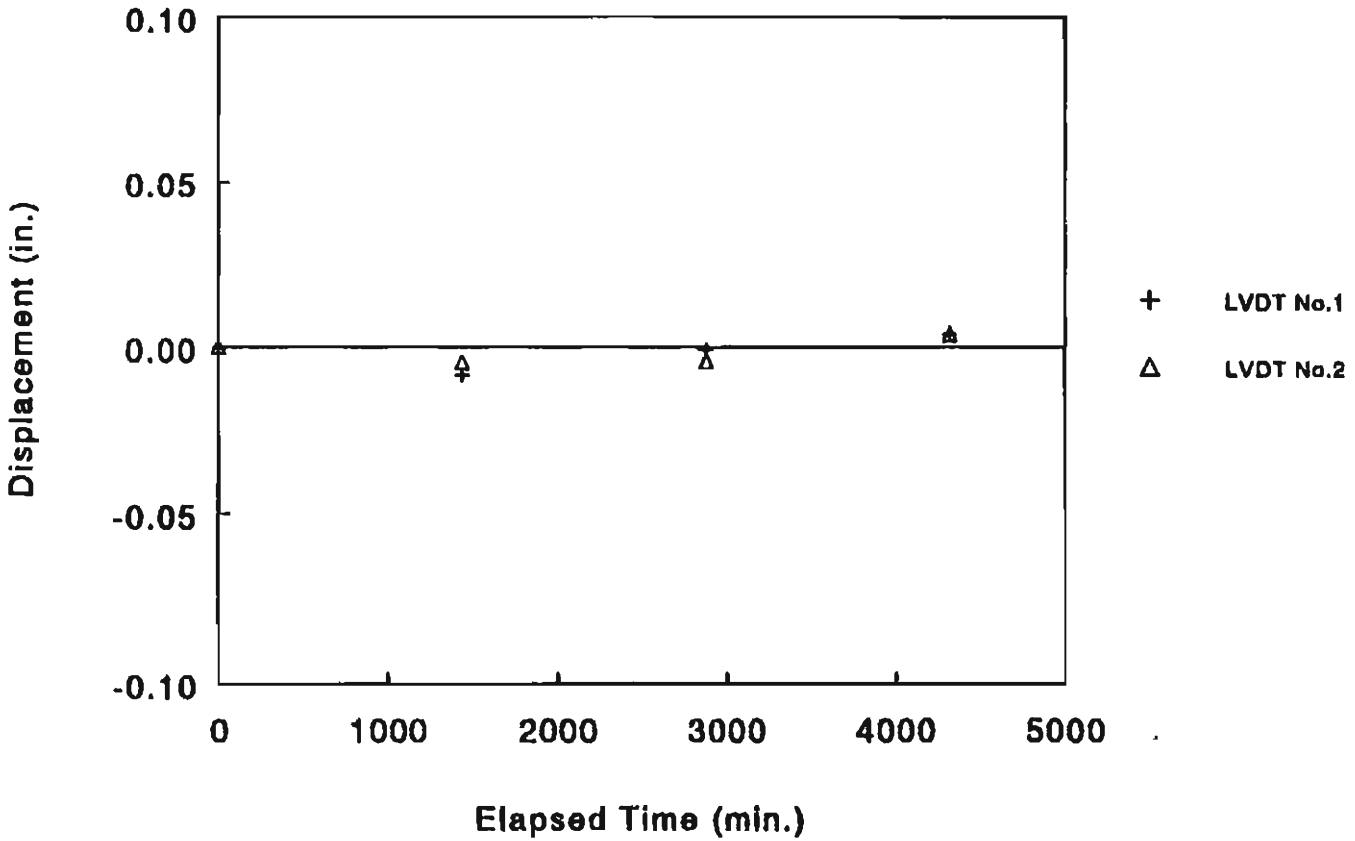

Figure 4.2 : Examination of Electrical Interference to LVDT

Elapsed Time (min.)	Test R-2 Lateral Disp. (in.)	Test R-2 Avg. Incremental Lateral Creep Rate (%/day)	Test R-2 Vertical Disp. (in.)	Test R-2 Avg. Incremental Vertical Creep Rate (%/day)	Test R-3 Lateral Disp. (in.)	Test R-3 Avg. Incremental Lateral Creep Rate (%/day)	Test R-3 Vertical Disp. (in.)	Test R-3 Avg. Incremental Vertical Creep Rate (%/day)
60	0.042	8.4E+00	0.028	5.6E+00	0.025	5.0E+00	0.028	5.6E+00
400	0.048	2.1E-01	0.030	7.1E-02	0.034	3.2E-01	0.036	2.8E-01
1000	0.049	2.0E-02	0.032	4.0E-02	0.037	6.0E-02	0.038	4.0E-02
10000	0.053	5.3E-03	0.048	1.9E-02	0.047	1.3E-02	0.039	1.3E-03
20000	0.054	1.2E-03	0.053	8.4E-03	0.051	4.8E-03	0.045	7.2E-03
30000	0.055	1.2E-03	0.054	1.2E-03	0.052	1.2E-03	0.053	9.6E-03
40000	0.055	0.0E+00	0.054	0.0E+00	0.054	2.4E-03	0.055	2.4E-03

Table 4.1 Displacements and Average Creep Strain Rates of Tests R-2, R-3

4.1.2 Failure Mode of the Performance Test

Figure 4.3 shows the applied vertical load versus time curve of Test U-1 (the road base with Amoco 2002 reinforcement). This test was conducted with a metal test apparatus because of the anticipate high load intensity. Part of the curve has to be estimated because the maximum load capacity of the MTS-810 machine was preset at 20 kips. The ultimate load was approximately 24 kips (i.e., an average pressure of 80 psi). As the force in the geotextile reached its ultimate strength, the geosynthetic reinforcement ruptured along the center line, as shown in Figure 4.4, which clearly indicated that the maximum force in reinforcement occurred along the center line of geosynthetic specimen. This behavior also conforms with the anticipated load distribution in the performance test.

4.2 Behaviors Before Releasing Lateral Support

After each test specimen was prepared, a sustained vertical load was applied. The transverse movement of the soil-geosynthetic composite was restrained by the side walls of the test device, while the longitudinal movement

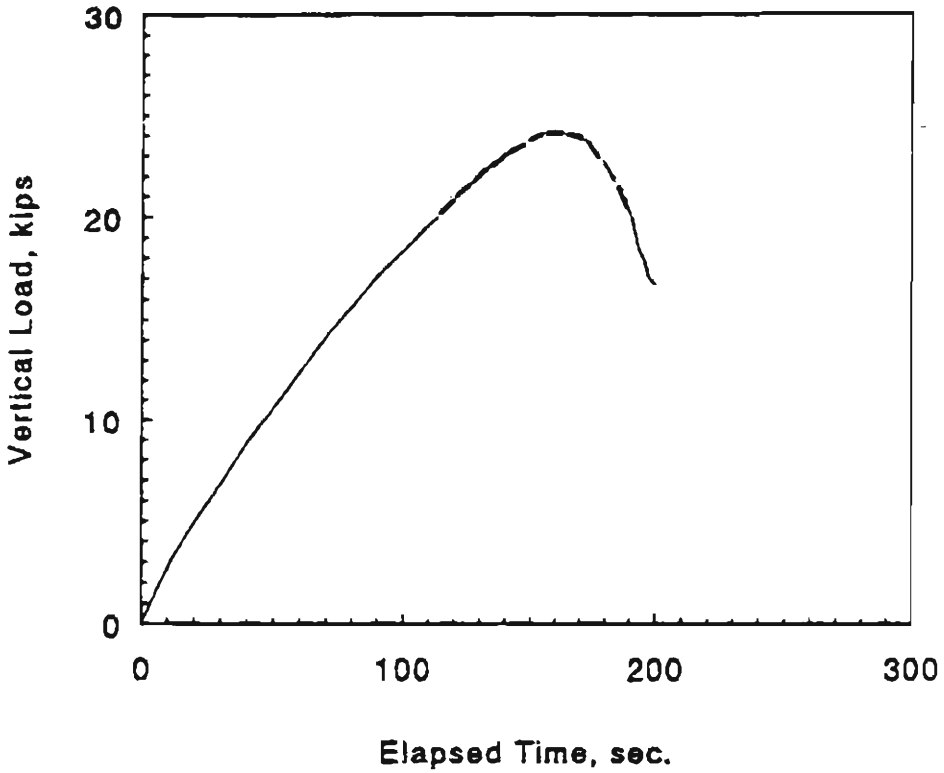

Figure 4.3: Applied Vertical Load Versus Time Relationships of Test U-1

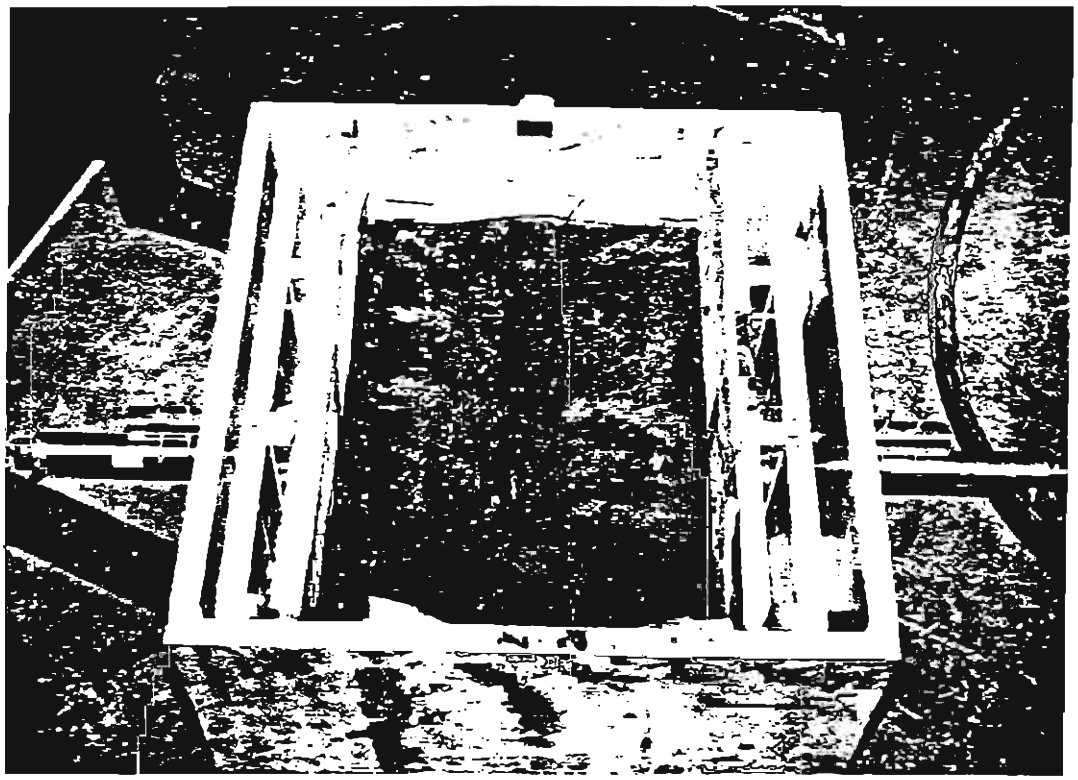

Figure 4.4 : Rupture of Amoco 2002 Geotextile, Test U-1

of the composite was restrained by the lateral supporting panels with an air pressure of 80 psi.

In addition to vertical displacement, because of the high vertical load, some appreciable (longitudinal) lateral displacements occurred before the lateral supporting panels were released due to soil compaction pressure. The measured displacements immediately before releasing the movable supporting panels are presented in Table 4.2. From Table 4.2, the following observations were made:

1. Comparisons of Test S-1 (the road base only, under a sustained average pressure of 15 psi, at 70°F), Test R-1 (same as Test S-1 except with Amoco 2044 reinforcement), and Test D-1 (as Test R-1 except with Typar 3301 reinforcement) indicated that the geosynthetic reinforcement played a significant role in restraining the lateral movement of the composite, but insignificant in reducing the vertical movement before releasing of the lateral supports.

2. Comparisons of Test C-2 (the clayey soil with Amoco 2044 reinforcement, under a sustained average pressure of 15 psi, at 70°F) and Test R-1 (same conditions as Test C-2 except with the road base)

Table 4.2 Lateral and Vertical Displacements Before Releasing Lateral Supports

Test Designation	Soil	Reinforcement	Temp. (°F)	Sustained Average Vertical Pressure (psi)	Lateral Disp. (in.)	Vertical Disp. (in.)
C-1	C.S.	None	70	15	0.122	0.36
C-2	C.S.	Amoco 2044	70	15	0.066	0.67
D-1	R.B.	Typar 3301	70	15	0.138	0.376
H-1	R.B.	Amoco 2044	125	30	0.24	0.464
R-1	R.B.	Amoco 2044	70	15	0.136	0.325
R-2	R.B.	Amoco 2044	125	15	0.066	0.268
R-3	R.B.	Amoco 2044	125	15	0.025	0.264
S-1	R.B.	None	70	15	0.329	0.416
S-2	R.B.	None	125	15	0.303	0.257
W-1	R.B.	Amoco 2002	125	15	0.396	0.238

Note: R.B.= road base

C.S.= a clayey soil with 43% of fines and PI=11

indicated that the clayey soil was more compressible than the road base, thus, Test C-2 exhibited about twice as much vertical displacement than Test R-1. The lateral displacement of Test C-2 was, however, only one half of that occurred in Test R-1. This may be because the compaction effect in Test C-2 was much smaller.

3. At ambient temperature, Test R-1 (the road base with Amoco 2044 reinforcement, under a sustained average pressure of 15 psi, at 70°F) and test D-1 (same condition as Test R-1 except Typar 3301 was used as reinforcement) exhibited nearly the same lateral and vertical displacements. However, at 125°F temperature, Test R-2 (same as R-1 except at 125°F) showed six times smaller lateral displacement than Test W-1 (under the same condition as Test R-2 except Amoco 2202 was used as reinforcement), although their vertical displacements were comparable.

4. Test R-1 (the road base with Amoco 2044 reinforcement, under a sustained average pressure of 15 psi, at 70°F) showed twice as much lateral displacement as Test R-2 (under the same condition as R-1 except at 125°F). The vertical displacement of Test R-1 was only slightly larger than Test R-2.

5. The effect of the sustained load can be assessed by comparing Test R-2 (the road base with Amoco 2044 reinforcement, under a sustained average pressure of 15 psi, at 125°F) with Test H-1 (same conditions as Test R-2 except under a sustained average pressure of 30 psi). Test H-1 showed larger displacement in both vertical and lateral direction. Note that the increase in the vertical displacement approximately proportional to the increase in the sustained average pressure increasing.

4.3 Long-Term Behavior of the Performance Test

4.3.1 Deformed Shape of Test Specimen and Strain Distribution along the Geosynthetic

Figure 4.5 shows the relationships of vertical and lateral displacements at three heights versus elapsed time of test D-1 (the road base with Typar 3301 reinforcement, under a sustained average pressure of 15 psi, at 70°F). As to be expected, the displacements at Points 2 and 3 were larger than those at Point 1. Points 2 and 3 showed very similar lateral creep displacement at the beginning of the test. Thereafter, however, Point 3 exhibited a larger creep displacement than point 2. The

the beginning of the test. Thereafter, however, Point 3 exhibited a larger creep displacement than point 2. The difference grew larger as time elapsed.

The vertical displacement was fairly close to the lateral displacement at Point 1. The creep rate at Point 1 was slightly lower than the vertical creep rate.

The lateral deformed shapes of the specimen at different elapsed times are shown in Figure 4.6. Larger displacements occurred at 1/4 and 3/4 heights (i.e., Points 2 and 3), while smaller displacements occurred at the top, the bottom, and the mid-height. At t=10 minutes, the upper part of the specimen was very similar to the lower part. As time progressed, the lower part showed more lateral deformation than the upper part. Point 3 experienced the largest creep rate.

Figure 4.7 shows the measured strain distribution along the length of geotextile of Test D-1 at t=10 min., 4,320 min. and 18,720 min. after releasing the lateral supports. The strain at the two ends of geotextile was zero, because there was no restraint at the ends.

The measured strains along the geotextile resembled a bell shape with an axis of symmetry at the center. The maximum strains occurred at the center of geosynthetic

strain versus time. The maximum measured strain was 2.0% at t=10 min., and at t=2,880 min. the maximum strain increased to 2.8%, then, remained constant for about 1,440 min.(1 day), i.e., at t=4,320 minutes, after that, the maximum strain decreased at an average rate of 0.005% per day.

Figure 4.9 shows the relationships between creep strain rates and elapsed time. It is seen that the creep rate decreased almost linearly with log(time), and that the rates of decrease in the vertical direction and different points in the lateral direction are fairly similar. The magnitude and rate of creep deformation at selected elapsed times are listed in Table 4.3.

4.3.2 Loads in Geosynthetic Reinforcement

Loads induced in the geotextile reinforcement are of significant interest in the design of GRS structures. The conventional approach for determining the loads is to apply the load-strain relationship of the geotextile , which was obtained from "element" load-deformation tests, to measured or computed strains. However, the load-strain behavior of geotextiles is affected significantly by, among other factors, the strain rate. In Test D-1 the

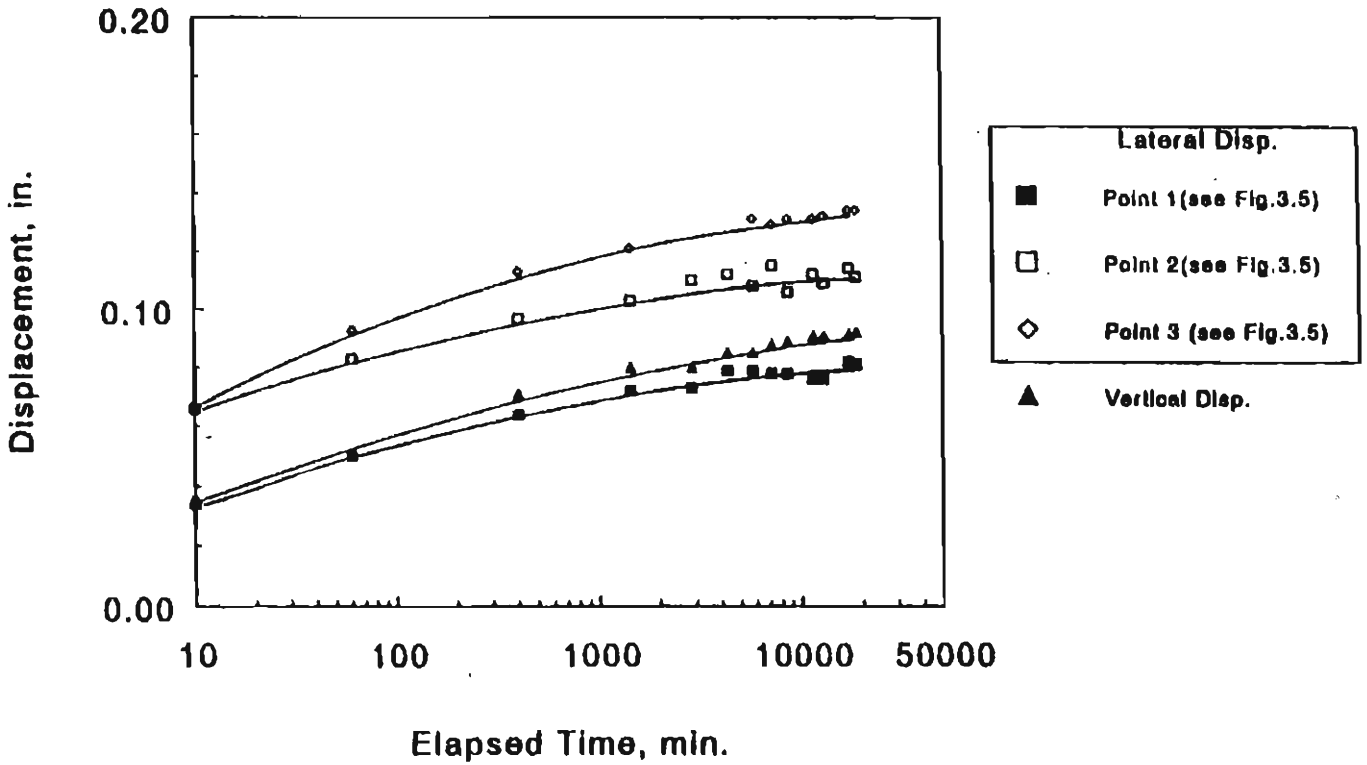

Figure 4.5 : Lateral and Vertical Displacements Versus Time Relationships of Test D-1

Elapsed Time (min.)	Lateral Direction						Vertical Direction	
	Point 1		Point 2		Point 3			
	Displacement (in.)	Creep Strain Rate (%/min.)	Displacement (in.)	Creep Strain Rate (%/min.)	Displacement (in.)	Creep Strain Rate (%/min.)	Displacement (in.)	Creep Strain Rate (%/min.)
60	0.050	1.0E+01	0.083	1.7E+01	0.093	1.9E+01	0.051	1.0E+01
400	0.064	4.9E-01	0.097	4.9E-01	0.113	7.1E-01	0.071	7.1E-01
1000	0.070	1.2E-01	0.102	1.0E-01	0.118	1.0E-01	0.078	1.4E-01
2000	0.074	4.8E-02	0.105	3.6E-02	0.122	4.8E-02	0.082	4.8E-02
4000	0.077	1.8E-02	0.108	1.8E-02	0.127	3.0E-02	0.086	2.4E-02
6000	0.078	6.0E-03	0.109	6.0E-03	0.128	6.0E-03	0.088	1.2E-02
8000	0.079	3.0E-03	0.110	6.0E-03	0.129	6.0E-03	0.089	3.0E-03
10000	0.079	3.0E-03	0.111	3.0E-03	0.130	6.0E-03	0.089	3.0E-03
20000	0.080	1.2E-03	0.111	6.0E-04	0.133	3.6E-03	0.090	1.2E-03

Table 4.3 Displacements and Average Creep Strain Rates of Test D-1

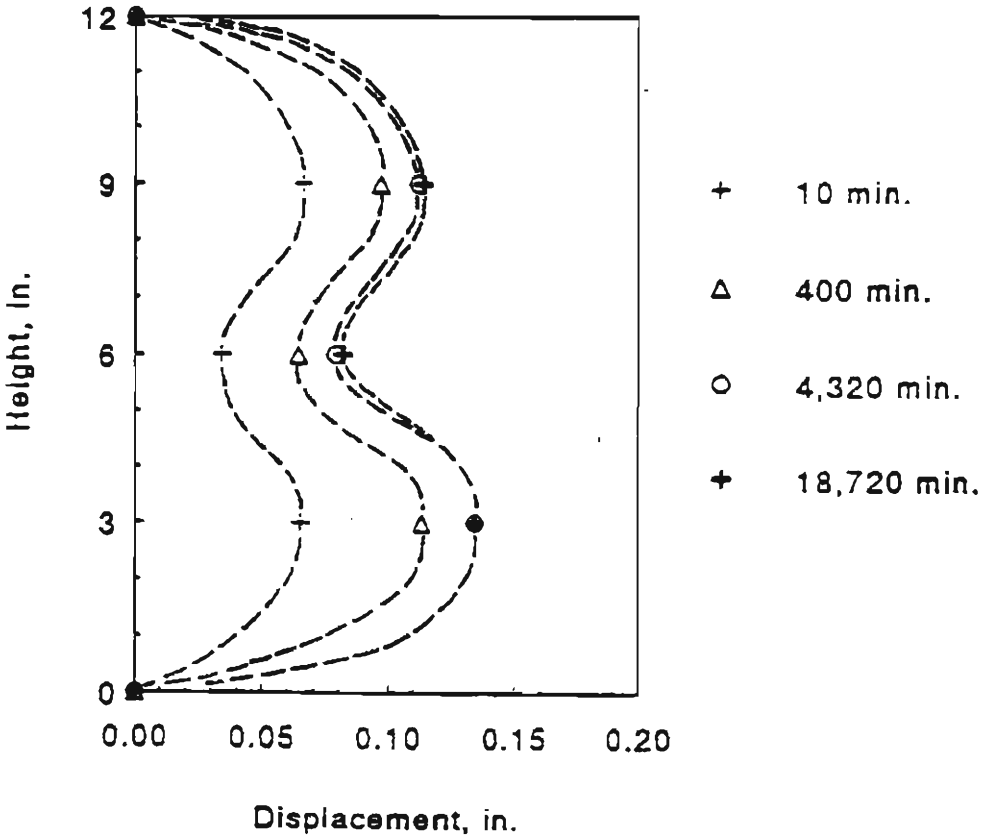

Figure 4.6: Lateral Deformed Shapes of Test D-1 at Different Elapsed Times

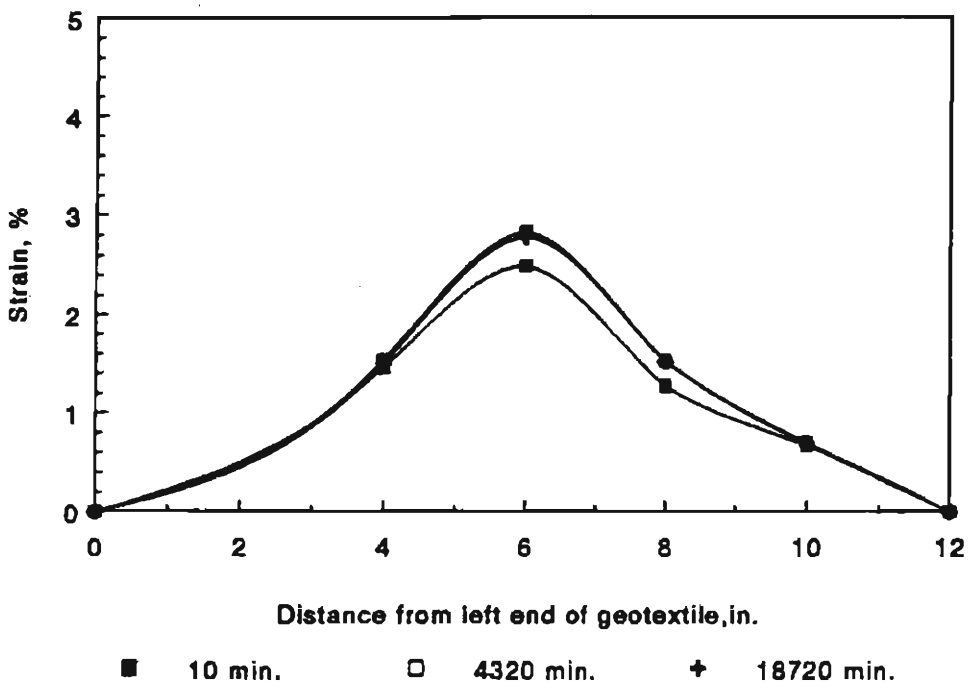

Figure 4.7 : Measured Strains along the Length of Geotextile of Test D-1 at t= 10 min., 4,320 min., 18,720 min.

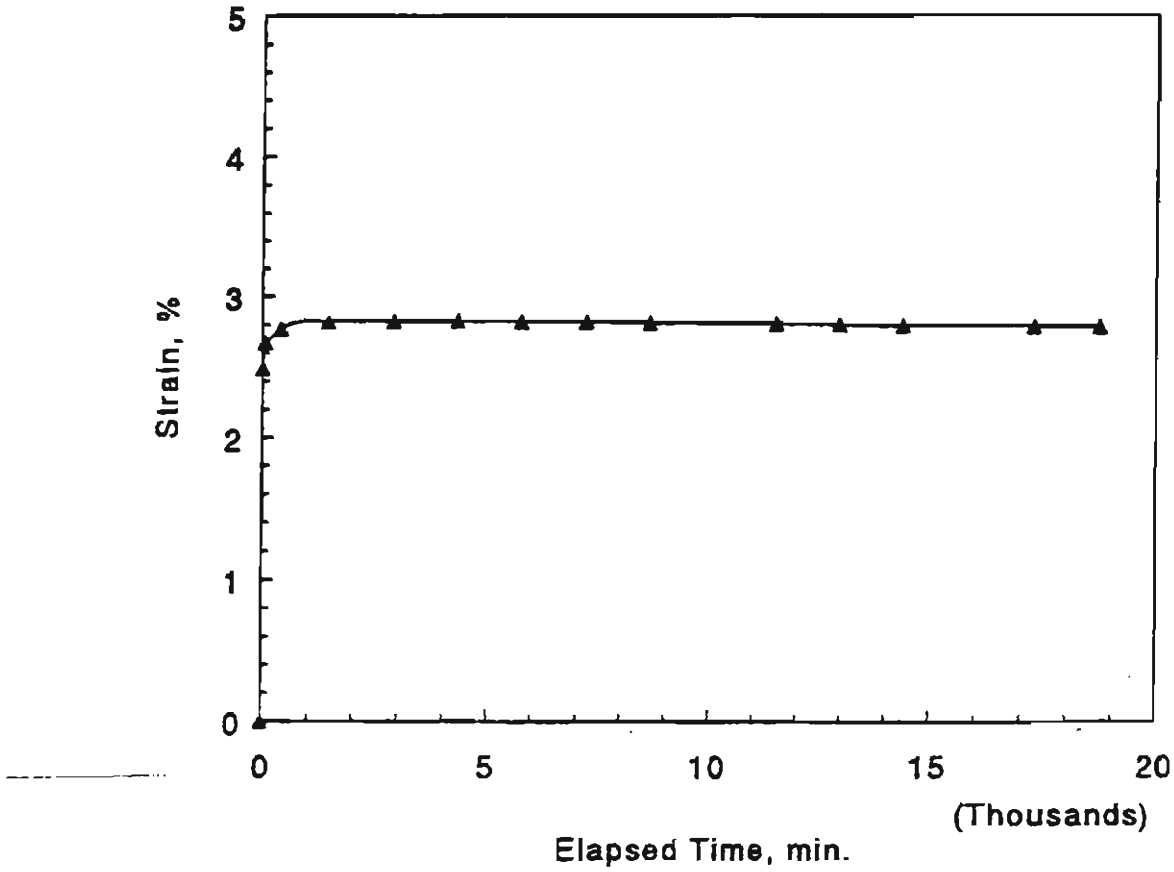

Figure 4.8: Maximum Strains Versus Time Relationships of Test D-1

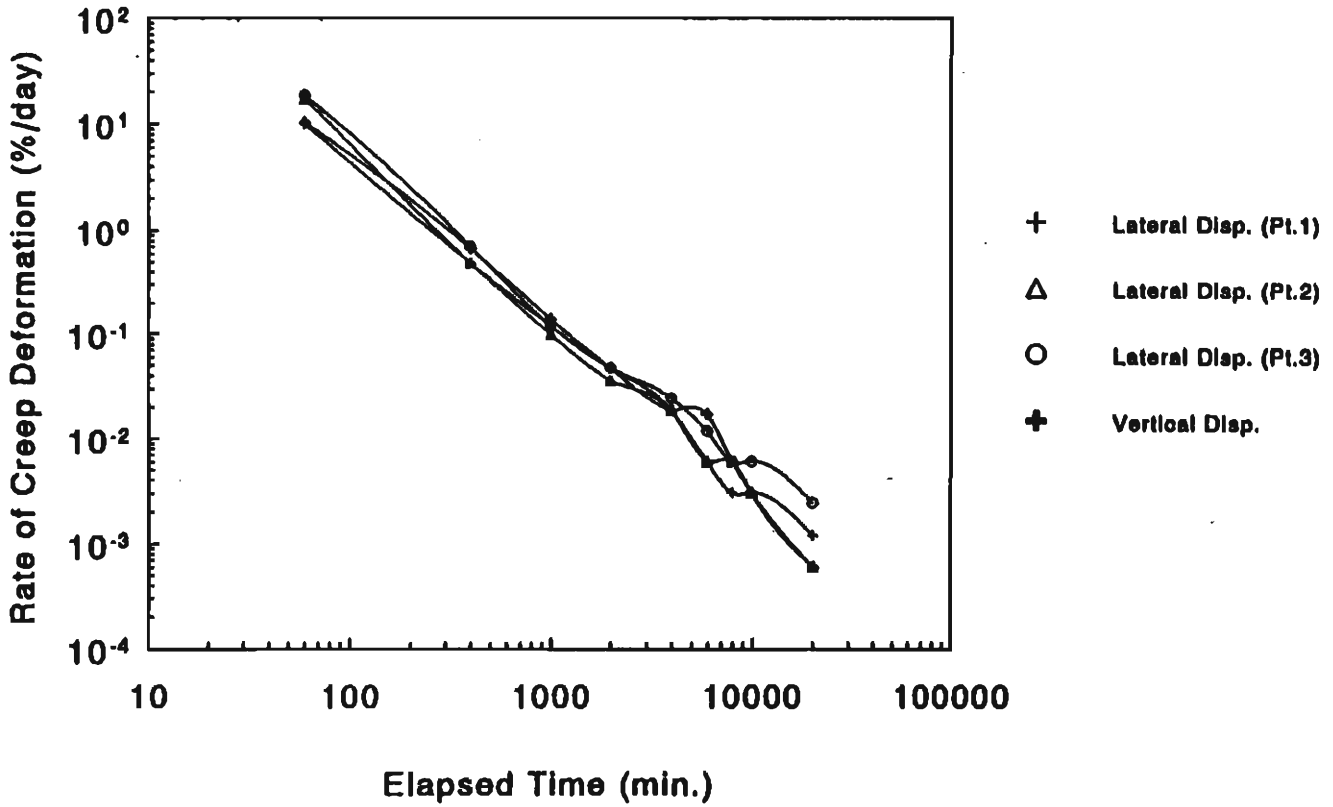

Figure 4.9 : Average Creep Strain Rates in the Vertical and Lateral Directions Versus Time Relationships of Tests D-1

strain rate was highly nonlinear, as seen in Figure 4.9. A different approach, using the isochronous load-strain curves, was used to determine the loads in the geotextile reinforcement.

Isochronous load-strain curves were first established as shown in Figure 4.10. The isochronous load-strain curve were deduced from the creep curves shown in Figure 2.9. Using Figure 4.10, the load in geosynthetic for a certain strain at a given time can be determined.

Figure 4.11 shows the calculated loads along the length of geotextile at different elapsed times. The maximum load occurred at the center of geotextile and decreased toward to two extremities. This is consistent with Test U-1 in which rupture occurred along the center line of the geotexile.

Figure 4.12 shows the relationships of loads versus time at different locations along the geotextile. The loads decreased at a decreasing rate as time elapsed. The rate of decrease was nearly the same at all locations. This decreasing load behavior in the geosynthetic could be the result of "stress relaxation". Stress relaxation is a term used to describe a behavior that the load in a

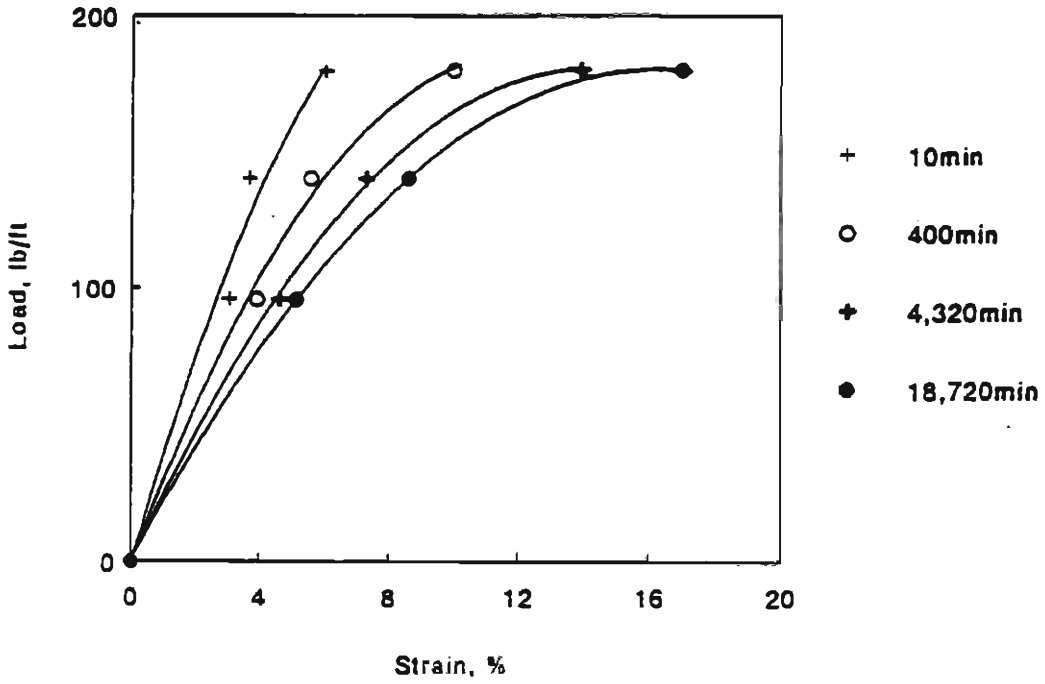

Figure4.10: Isochronous Load-Strain Curves

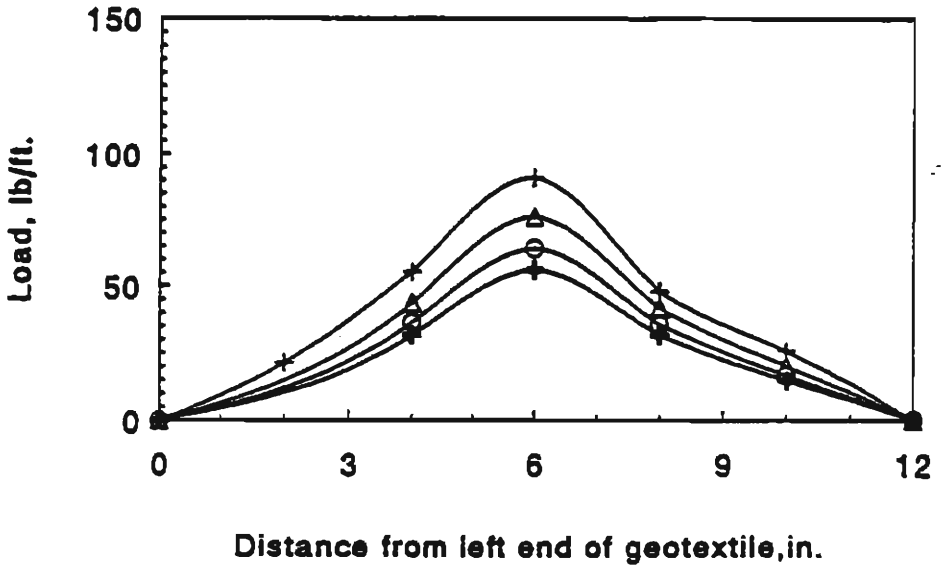

Figure 4.11 : Loads along the Length of Geotextile at Different Elapsed Times of Test D-1

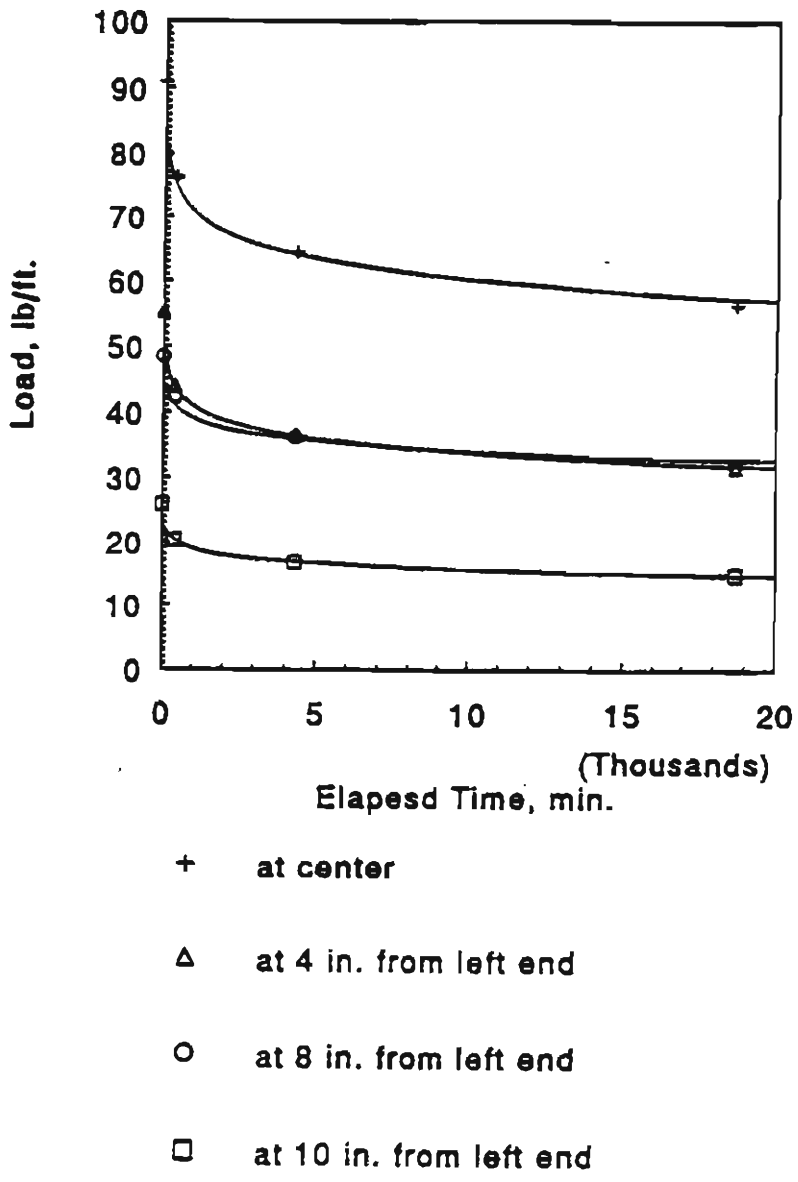

Figure 4.12 : Maximum Loads in Geotextile Versus Time at Different Distances from Left End of Geotextile of Test D-1

material, subject to a constant deformation, decreases with time. Stress relaxation may occur when the rate of deformation becomes small. In Test D-1, stress relaxation began at 10 minutes after releasing the lateral supports.

4.3.3 The Role of Reinforcement

Comparison of the lateral and vertical displacements versus time relationships between Tests S-1 and R-1 and between Tests S-2 and R-2 are shown in Figures 4.13 and 4.14, respectively. Test S-1 was conducted with the road base only, under a sustained average pressure of 15 psi, at 70°F while, Test R-1 was conducted under the same conditions as Test S-1 except Amoco 2044 reinforcement was used. Test S-2 and R-2 were conducted under the same conditions as Tests Test S-1 and R-1, respectively, except the temperature was 125°F.

The magnitude of creep deformation in the lateral and vertical directions of unreinforced tests (Tests S-1 and S-2) were markedly larger than reinforced soil tests (Tests R-1 and R-2) because the geosynthetic reinforcement restrained movement in lateral and as a result the vertical displacement was also reduced. The reduction of displacements in the lateral direction was

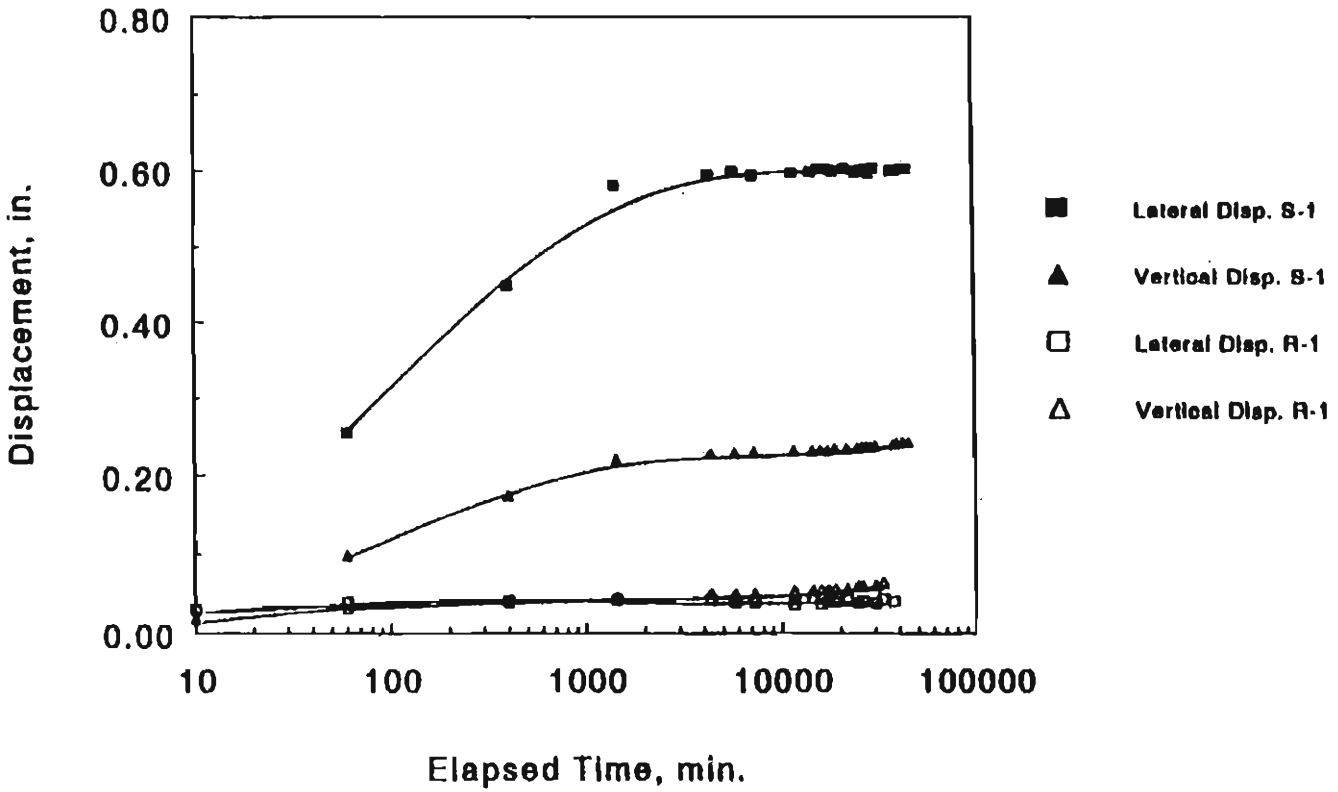

Figure 4.13 : Lateral and Vertical Displacements Versus Time Relationships of Tests S-1, R-1

Elapsed Time (min.)	Test S-1				Test R-1			
	Lateral Disp. (in.)	Avg. Incremental Lateral Creep Rate (%/day)	Vertical Disp. (in.)	Avg. Incremental Vertical Creep Rate (%/day)	Lateral Disp. (in.)	Avg. Incremental Lateral Creep Rate (%/day)	Vertical Disp. (in.)	Avg. Incremental Vertical Creep Rate (%/day)
60					0.039	7.8E+00	0.031	6.2E+00
400	0.448	1.6E+01	0.174	6.1E+00	0.040	3.5E-02	0.038	2.5E-01
1000	0.542	1.9E+00	0.210	7.2E-01	0.040	0.0E+00	0.042	8.0E-02
10000	0.600	7.7E-02	0.230	2.7E-02	0.040	0.0E+00	0.051	1.2E-02
20000	0.600	0.0E+00	0.233	3.6E-03	0.040	0.0E+00	0.056	6.0E-03
30000	0.601	1.2E-03	0.237	4.8E-03	0.040	0.0E+00	0.062	7.2E-03
40000	0.602	1.2E-03	0.241	4.8E-03	0.040	0.0E+00	0.067	6.0E-03

Table 4.4 Displacements and Average Creep Strain Rates of Tests S-1, R-1

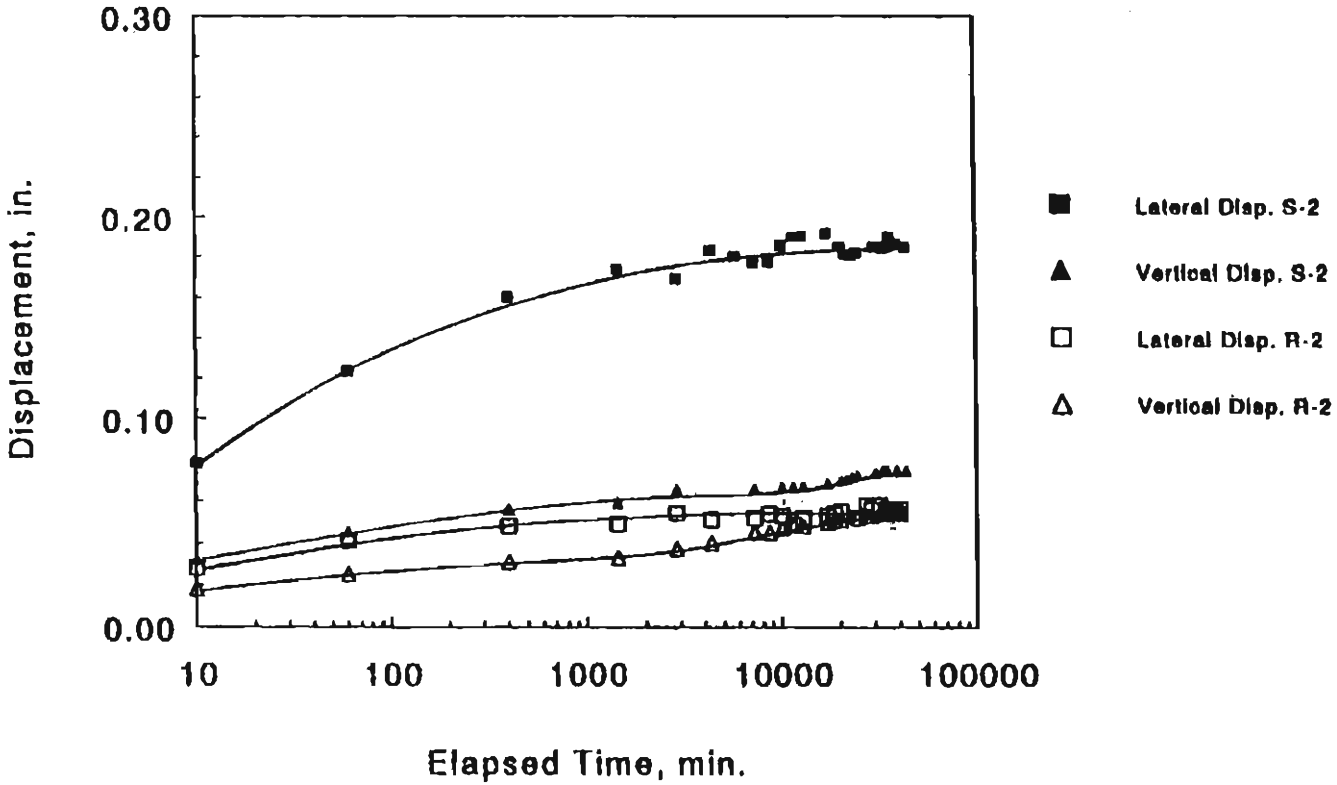

Figure 4.14 : Lateral and Vertical Displacements Versus Time Relationships of Tests S-2, R-2

Elapsed Time (min.)	Test S-2				Test R-2			
	Lateral Disp. (in.)	Avg. Incremental Lateral Creep Rate (%/day)	Vertical Disp. (in.)	Avg. Incremental Vertical Creep Rate (%/day)	Lateral Disp. (in.)	Avg. Incremental Lateral Creep Rate (%/day)	Vertical Disp. (in.)	Avg. Incremental Vertical Creep Rate (%/day)
60	0.123	2.5E+01	0.045	9.0E+00	0.042	8.4E+00	0.028	5.6E+00
400	0.160	1.3E+00	0.058	3.9E-01	0.048	2.1E-01	0.030	7.1E-02
1000	0.171	2.2E-01	0.058	4.0E-02	0.049	2.0E-02	0.032	4.0E-02
10000	0.185	1.9E-02	0.066	1.1E-02	0.053	5.3E-03	0.046	1.9E-02
20000	0.187	2.4E-03	0.070	4.8E-03	0.054	1.2E-03	0.053	8.4E-03
30000	0.187	0.0E+00	0.075	6.0E-03	0.055	1.2E-03	0.054	1.2E-03
40000	0.187	0.0E+00	0.075	0.0E+00	0.055	0.0E+00	0.054	0.0E+00

Table 4.5 Displacements and Average Creep Strain Rates of Tests S-2, R-2

much larger than that in the vertical direction. The magnitude of vertical creep displacements occurred between t=10 min. and t=43,200 min. were 0.144 in. and 0.05 in., for Tests S-1 and R-1, respectively. The lateral creep displacements in the same period of time were 0.347 in. and 0.008 in. for Tests S-1 and R-1, respectively.

At 70°F, the creep rates in both the vertical and lateral directions of Test S-1 were higher than Test R-1 up to t=1,440 min., thereafter, the creep rates were nearly the same. At 125°F, the creep rate of Test S-2 in the vertical direction was about equal to that of Test R-2 but significantly higher than Test R-2 in lateral direction up to t=4,000 minutes, thereafter, the creep rate of Tests S-2 and R-2 were similar. The creep rates of Tests S-1, R-1 and S-2, R-2 are shown in Tables 4.4 and 4.5, respectively.

Figure 4.15 and 4.16 show the lateral and vertical displacements versus time relationships of Test C-1 (the clayey soil only, under a sustained average pressure of 15 psi, at 70°F) and Test C-2 (under the same conditions as Test C-1 except Amoco 2044 reinforcement was used), respectively.

The test specimen in Test C-1 failed at t=17 minutes. The failure occurred due to shear failure. Some distinct shear bands were visible from the latex membrane as shown in Figure 4.17. Before failure creep in vertical and lateral directions occurred at about the same rate, although the lateral deformation was slightly higher.

With a sheet of reinforcement, Test C-2 exhibited about 0.1 in. lateral displacement after 40,000 min., at which time the test was terminated. The creep rate up to t=40,000 min. was nearly constant in the lateral direction. In the vertical direction, however, the creep deformation appeared to be experiencing tertiary creep from t=10,000 minutes to t=40,000 minutes.

4.3.4 Effect of Geosynthetic Type

Figure 4.18 shows the lateral displacements versus time relationships of Test R-2 (the road base with Amoco 2044 reinforcement, under a sustained average pressure of 15 psi, at 125 °F) and W-1 (under the same conditions as Test R-2 except Amoco 2002 was used). The lateral displacements of test S-2 (without reinforcement) were also plotted in the Figure for comparison. The vertical displacement of Test W-1 is not available because the

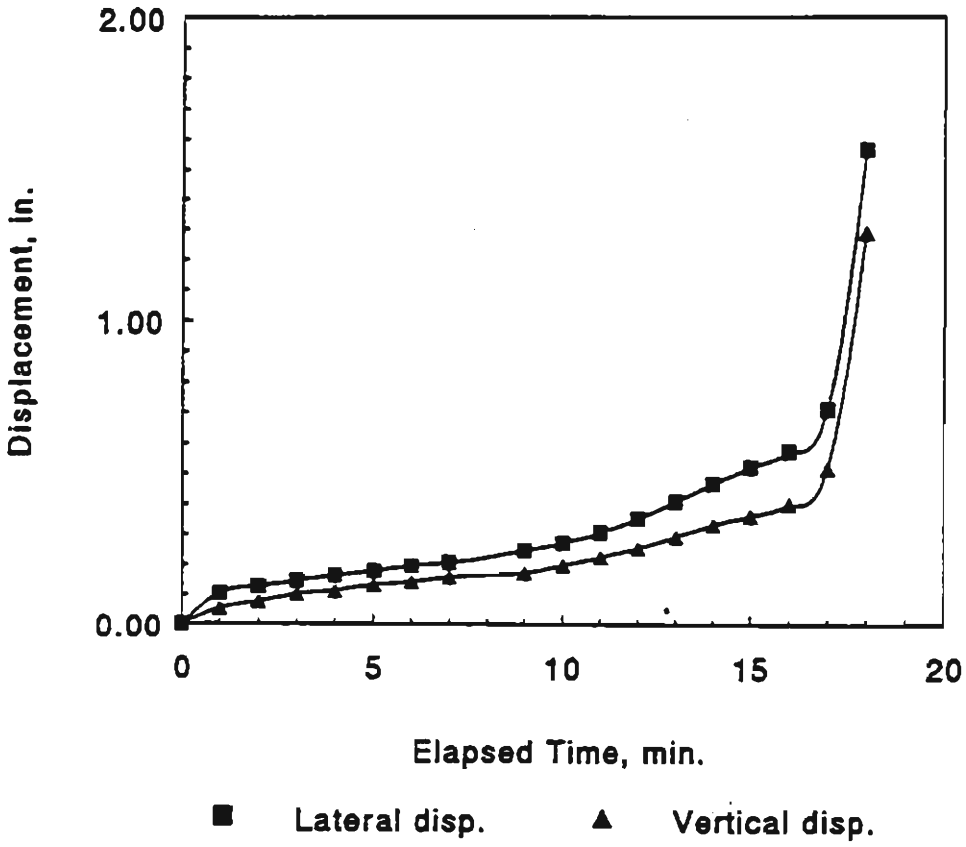

Figure 4.15 : Lateral and Vertical Displacements Versus Time Relationships of Test C-1

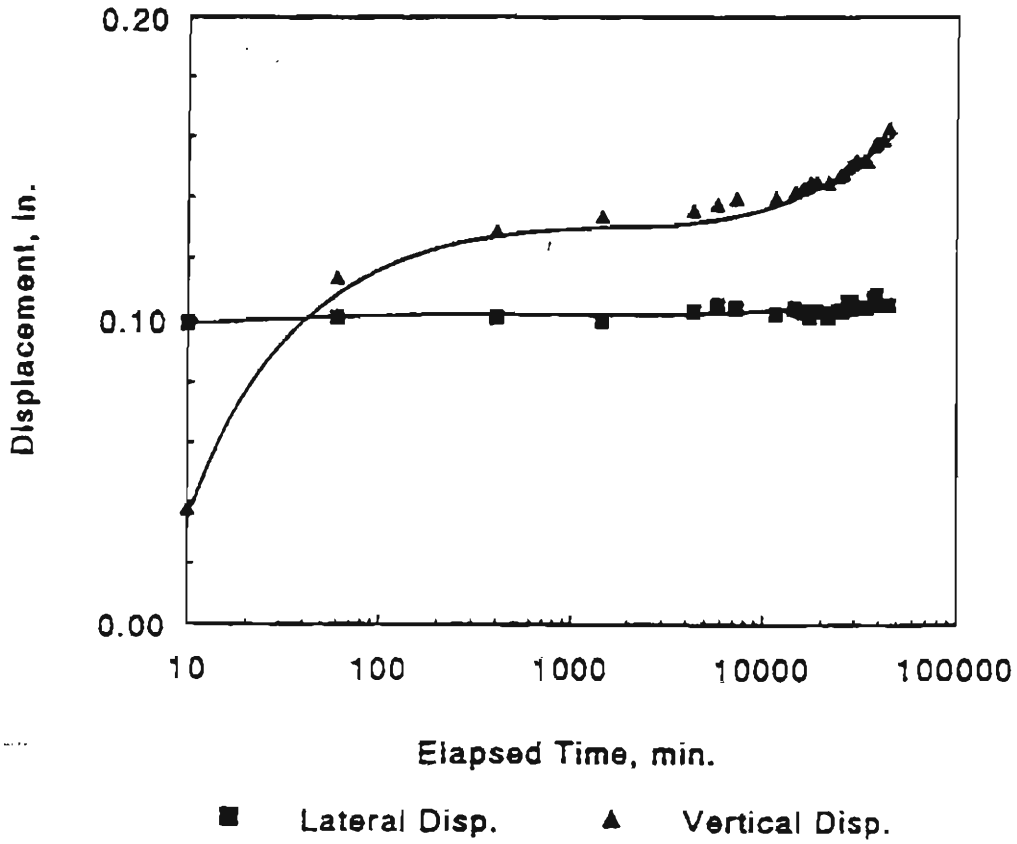

Figure 4.16 : Lateral and Vertical Displacements Versus Time Relationships of Test C-2

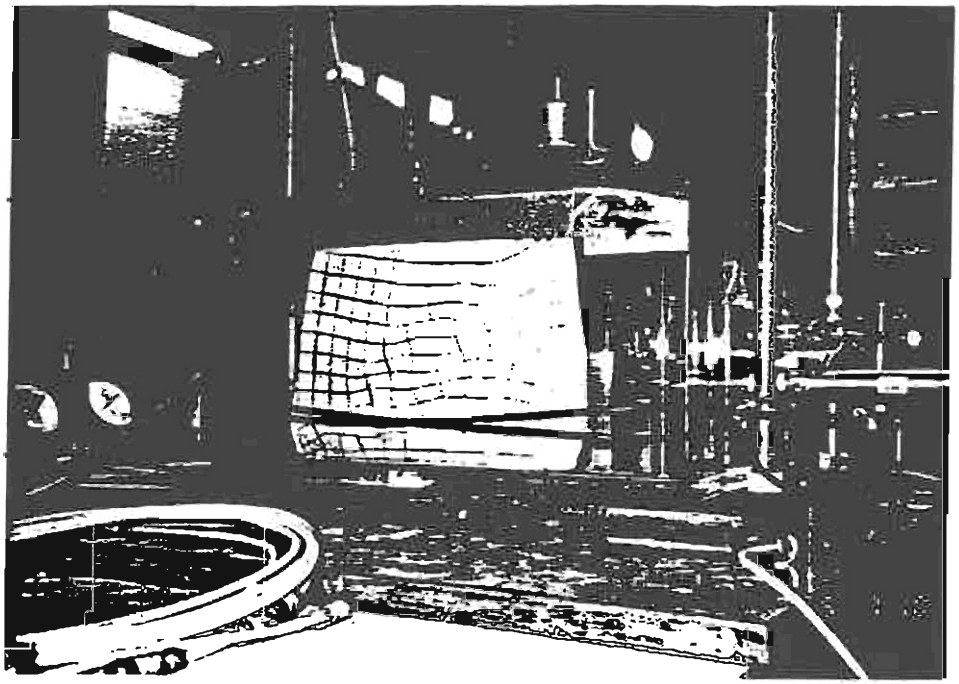

Figure 4.17 : Failure Mode of Test C-1

dial gage was found defective. As to be expected, the magnitude of creep deformation in the lateral direction was the largest in Test S-2 and the smallest in Test R-2. The creep rates in the lateral direction of Test W-1 were higher than Test R-2, yet Test W-1 and Test S-2 exhibited similar creep rate. The displacements and creep strain rates of Tests R-2, W-1, and S-2 are shown in Table 4.6.

Figure 4.19 shows the lateral and vertical displacements versus time relationships of Test D-1(the road base with Typar 3301 reinforcement, under a sustained average vertical pressure of 15 psi, at 70°F) and R-1 (under the same conditions as Test D-1 except Amoco 2044 was used as reinforcement). It is to be noted, as compared with those tests shown in Figure 4.18, these tests were conducted in ambient temperature.

The magnitude of creep deformation in the vertical direction of Test D-1 were larger than Test R-1 but the creep rates were comparable. The displacements and average creep strain rates of the two tests in the vertical direction are shown in Table 4.7.

The magnitudes of creep deformation in the lateral direction of Test D-1 were about the same as Test R-1 in the first 10 minutes and gradually became larger as time

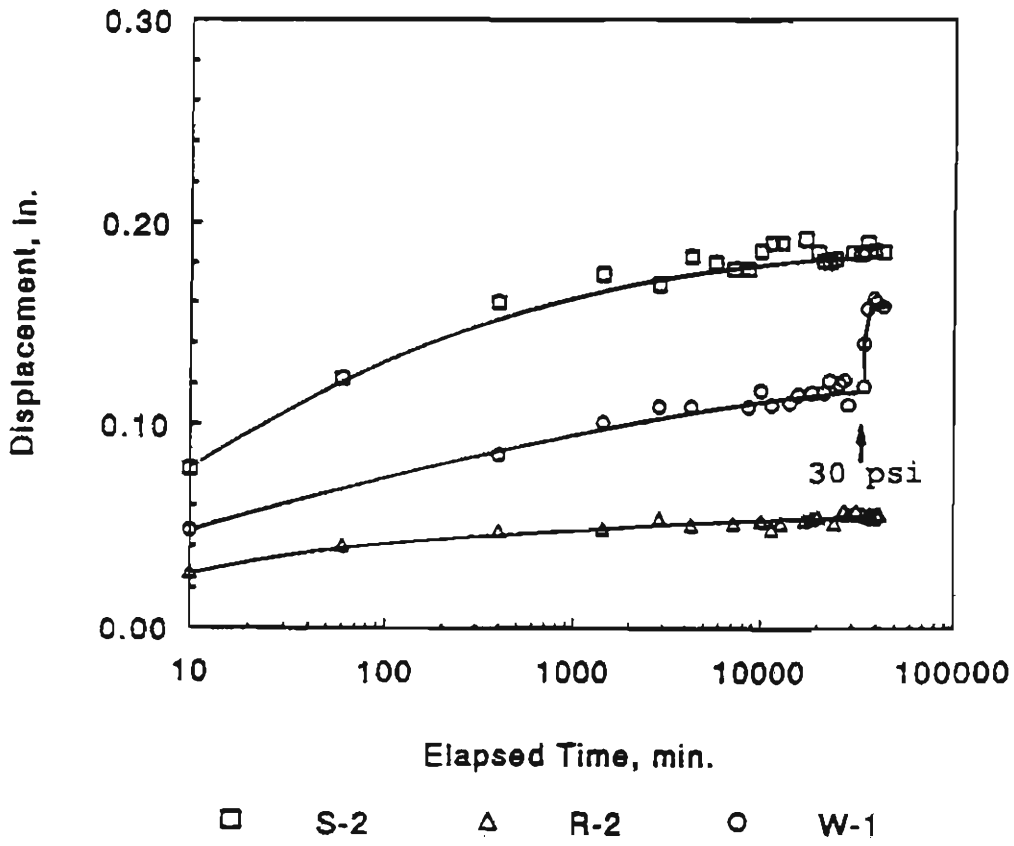

Figure 4.18: Lateral Displacements Versus Time Relationships of Tests S-2, R-2, W-1

Test S-2			Test R-2		Test W-1			
Elapsed Time (min.)	Lateral Disp. (in.)	Avg. Incremental Lateral Creep Rate (%/day)	Lateral Disp. (in.)	Avg. Incremental Lateral Creep Rate (%/day)	Elapsed Time (min.)	Sustained pressure (psi)	Lateral Disp. (in.)	Avg. Incremental Lateral Creep Rate (%/day)
60	0.123	2.5E+01	0.042	8.4E+00	60	15	0.067	1.3E+01
400	0.160	1.3E+00	0.048	2.1E-01	400	15	0.066	6.7E-01
1000	0.171	2.2E-01	0.049	2.0E-02	1000	15	0.096	2.0E-01
10000	0.185	1.9E-02	0.053	5.3E-03	10000	15	0.114	2.4E-02
20000	0.187	2.4E-03	0.054	1.2E-03	20000	15	0.118	4.8E-03
30000	0.187	0.0E+00	0.055	1.2E-03	30000	15	0.119	1.2E-03
40000	0.187	0.0E+00	0.055	0.0E+00	34560	15	0.120	2.6E-03
					34560	30	0.140	
					36000	30	0.157	1.4E-01
					40000	30	0.159	6.0E-03

Table 4.6 Displacements and Average Creep Strain Rates of Tests S-2, R-2, W-1

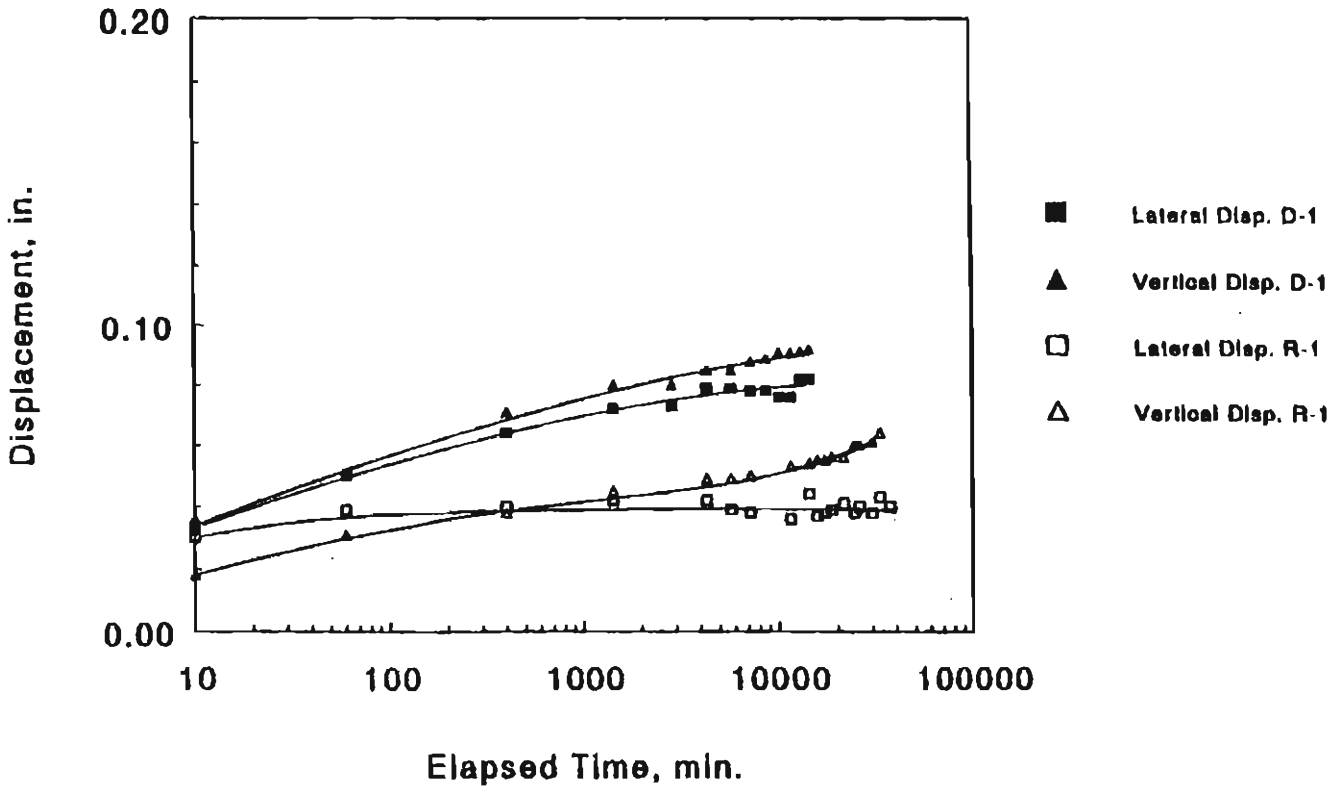

Figure 4.19 : Lateral and Vertical Displacements Versus Time Relationships of Tests D-1, R-1

Elapsed Time	Test R-1				Test D-1			
	Lateral Disp.	Avg. Incremental Lateral Creep Rate	Vertical Disp.	Avg. Incremental Vertical Creep Rate	Lateral Disp.	Avg. Incremental Lateral Creep Rate	Vertical Disp.	Avg. Incremental Vertical Creep Rate
(min.)	(in.)	(%/day)	(in.)	(%/day)	(in.)	(%/min.)	(in.)	(%/day)
60	0.039	7.8E+00	0.031	6.2E+00	0.050	1.0E+01	0.051	1.0E+01
400	0.040	3.5E-02	0.038	2.5E-01	0.064	4.9E-01	0.071	7.1E-01
1000	0.040	0.0E+00	0.042	8.0E-02	0.070	1.2E-01	0.078	1.4E-01
10000	0.040	0.0E+00	0.051	1.2E-02	0.079	1.2E-02	0.089	1.5E-02
20000	0.040	0.0E+00	0.056	6.0E-03				
30000	0.040	0.0E+00	0.062	7.2E-03				
40000	0.040	0.0E+00	0.067	6.0E-03				

Table 4.7 Displacements and Average Creep Strain Rates of Tests D-1, R-1

elapsed. The creep rates in the lateral direction of two tests were significantly different. The displacements and average creep strain rates of the two tests in the lateral direction are also shown in Table 4.7.

4.3.5 Effect of Soil Type

Figure 4.20 shows the lateral and vertical displacements versus time relationships of Test R-1 (the road base with Amoco 2044 reinforcement, under a sustained average pressure of 15 psi, at 70°F) and Test C-2 (the clayey soil in otherwise the same conditions as Test R-1). As to be expected, the magnitude of creep deformation in the vertical direction of Test C-2 were much larger than Test R-1. The creep rate in the vertical direction of Test C-2 was much higher than Test R-1 in the first 100 minutes; however, the creep rates of the two tests were similar after 100 minutes. The average creep rate in the vertical direction of Test C-2 was 9.6×10^{-3} % per day and 6.0×10^{-3} % per day in Test R-1 in 30 days.

Creep deformation in the lateral direction was negligible in both tests over 43,200 minutes. The tests, however, were conducted in ambient temperature. The test

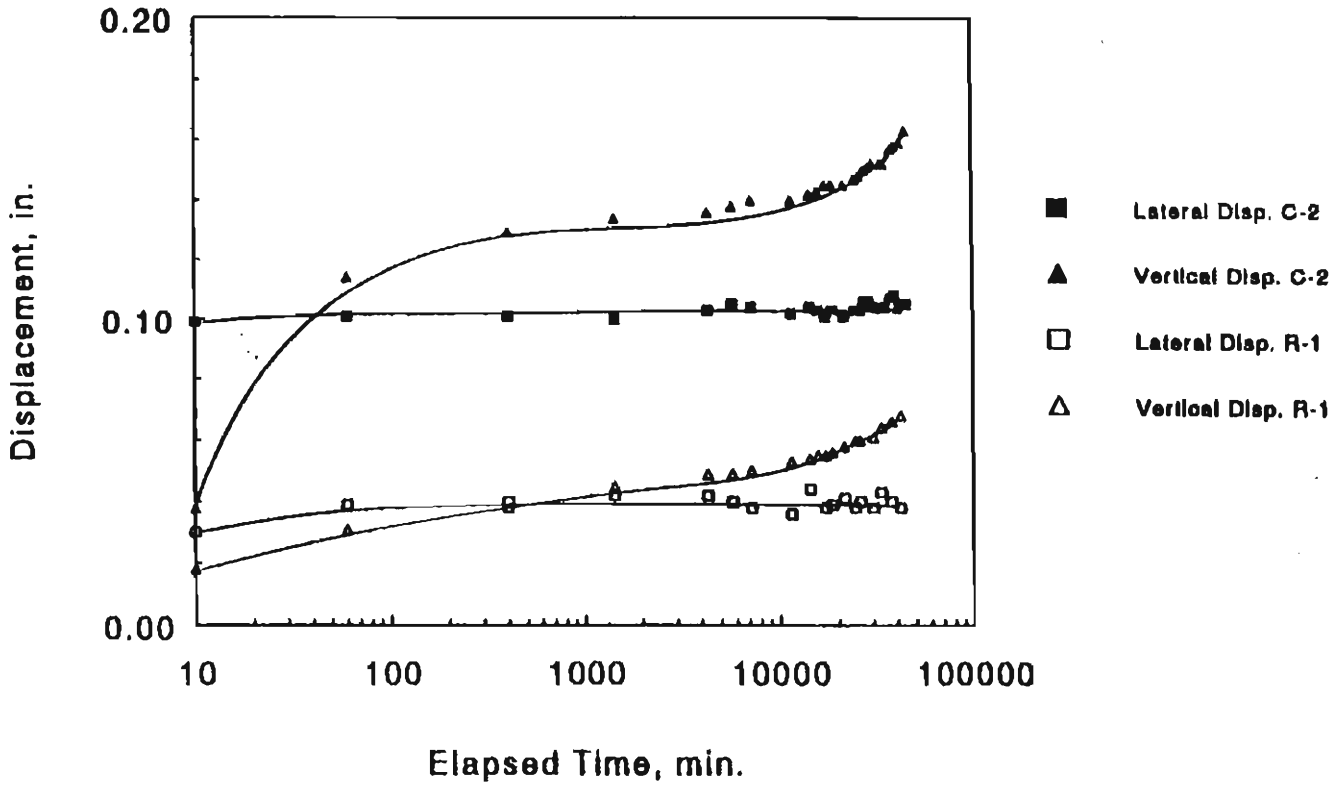

Figure 4.20: Lateral and Vertical Displacements Versus Time Relationships of Tests C-2, R-1

Elapsed Time (min.)	Test C-2				Test R-1			
	Lateral Disp. (in.)	Avg. Incremental Lateral Creep Rate (%/day)	Vertical Disp. (in.)	Avg. Incremental Vertical Creep Rate (%/day)	Lateral Disp. (in.)	Avg. Incremental Lateral Creep Rate (%/day)	Vertical Disp. (in.)	Avg. Incremental Vertical Creep Rate (%/day)
60	0.101	2.0E+01	0.114	2.3E+01	0.039	7.8E+00	0.031	6.2E+00
400	0.101	0.0E+00	0.129	5.3E-01	0.040	3.5E-02	0.036	2.5E-01
1000	0.101	0.0E+00	0.133	8.0E-02	0.040	0.0E+00	0.042	8.0E-02
10000	0.102	1.3E-03	0.139	8.0E-03	0.040	0.0E+00	0.051	1.2E-02
20000	0.104	2.4E-03	0.144	6.0E-03	0.040	0.0E+00	0.056	6.0E-03
30000	0.105	1.2E-03	0.150	7.2E-03	0.040	0.0E+00	0.062	7.2E-03
40000	0.106	1.2E-03	0.158	9.6E-03	0.040	0.0E+00	0.067	6.0E-03

Table 4.8 Displacements and Average Creep Strain Rates of Tests C-2, R-1

period of 43,200 min.(30 days) was relatively short. The displacement and average strain rates in both vertical and lateral directions for Tests C-2 and R-1 are shown in Table 4.8.

4.3.6 Effect of Temperature

Figure 4.21 and 4.22 show the lateral and vertical displacements versus time relationships of Test R-1 (the road base with Amoco 2044 reinforcement, under a sustained average pressure of 15 psi, at 70°F) and Test R-2 (under the same condition as Test R-1 except at 125°F temperature).

The magnitude of creep deformation in the lateral direction of Test R-2 were much larger than Test R-1. The creep rate of Test R-2 was higher than Test R-1 up to about 10,000 min., beyond which the creep rate became negligible, as was Test R-1.

The magnitudes of creep deformation in the vertical direction of Test R-1 and R-2 were slightly different at the beginning of the tests which was due mostly to different degrees of lateral restraint before releasing the supporting panels. The creep rates in the vertical direction for the two test were somewhat similar. By the

conclusion of the tests, however, Test R-2 had reached an equilibrium condition (i.e., creep rate become nearly zero), yet Test R-1 still exhibited continuing creep deformation in the vertical direction with a rate of about 6.0×10^{-3}% per day. The displacements and average creep strain rates of Test R-1 and R-2 are shown in Table 4.9.

It should be noted that the elevated temperature accelerated the creep rate of the geotextile by more than 100 folds (as discuss in section 2.3), whereas the effect on soil was negligible. Table 4.10 shows the displacements and average strain rates of Tests S-1 and S-2. It is seen that the elevated temperature has little effect on the creep rate of the soil.

4.3.7 Effect of Sustained Vertical Surcharge

Figures 4.23, 4.24 show, respectively, the lateral and vertical displacements versus time relationships for Test R-2 (the road base with Amoco 2044 reinforcement, under a sustained average pressure of 15 psi) and Test H-1 (under the same conditions as Test R-2 except at 30 psi

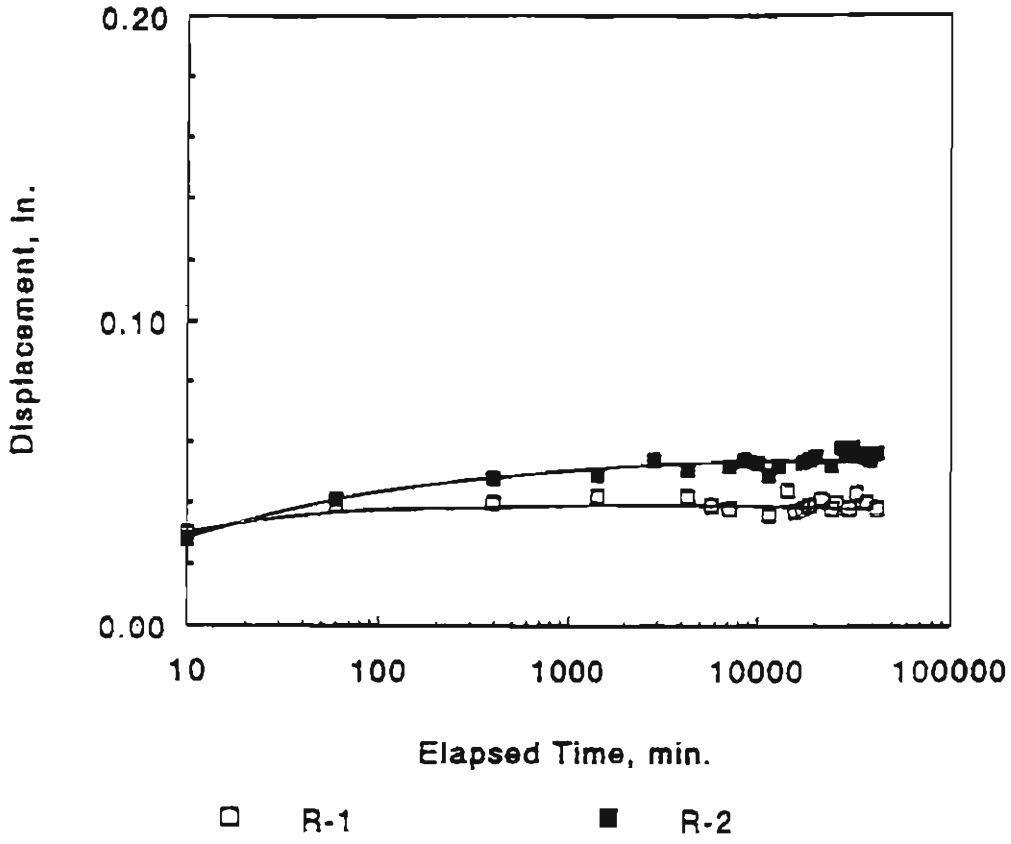

Figure 4.21: Lateral Displacements Versus Time Relationships of Tests R-1, R-2

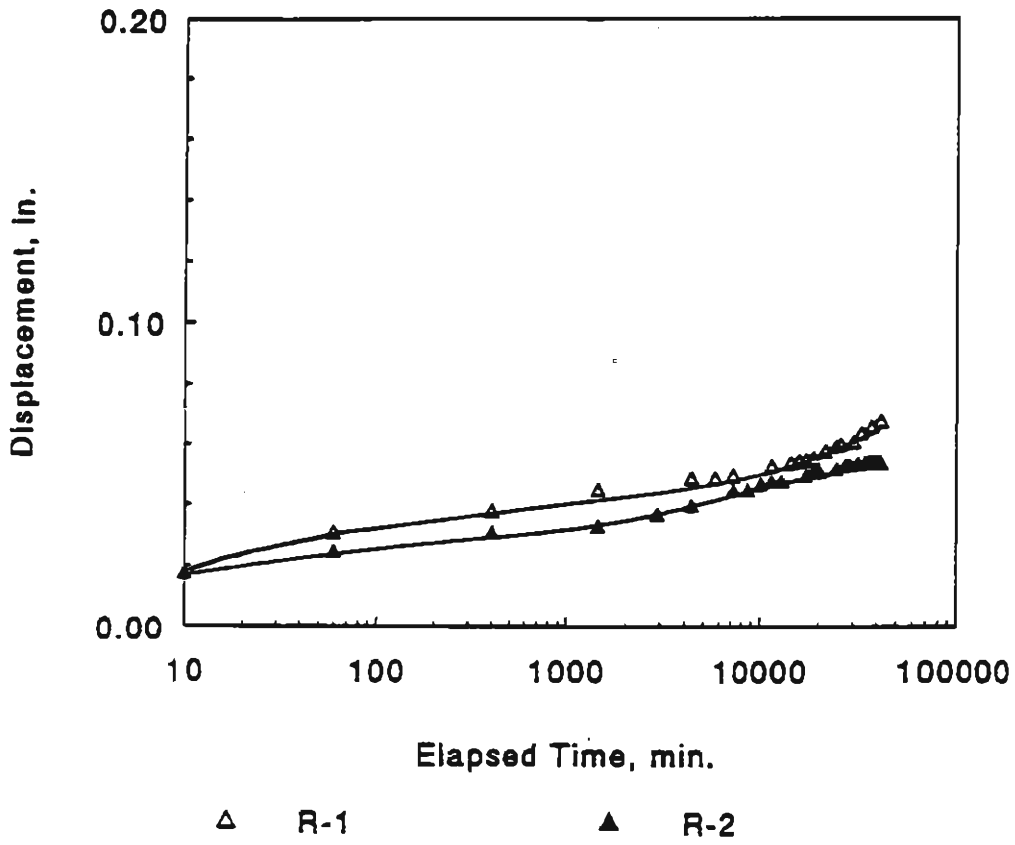

Figure 4.22 : Vertical Displacements Versus Time Relationships of Tests R-1, R-2

Elapsed Time (min.)	Test R-1				Test R-2			
	Lateral Disp. (in.)	Avg. Incremental Lateral Creep Rate (%/day)	Vertical Disp. (in.)	Avg. Incremental Vertical Creep Rate (%/day)	Lateral Disp. (in.)	Avg. Incremental Lateral Creep Rate (%/day)	Vertical Disp. (in.)	Avg. Incremental Vertical Creep Rate (%/day)
60	0.039	7.8E+00	0.031	6.2E+00	0.042	8.4E+00	0.028	5.6E+00
400	0.040	3.5E-02	0.038	2.5E-01	0.048	2.1E-01	0.030	7.1E-02
1000	0.040	0.0E+00	0.042	6.0E-02	0.049	2.0E-02	0.032	4.0E-02
10000	0.040	0.0E+00	0.051	1.2E-02	0.053	5.3E-03	0.046	1.9E-02
20000	0.040	0.0E+00	0.056	6.0E-03	0.054	1.2E-03	0.053	8.4E-03
30000	0.040	0.0E+00	0.062	7.2E-03	0.055	1.2E-03	0.054	1.2E-03
40000	0.040	0.0E+00	0.067	6.0E-03	0.055	0.0E+00	0.054	0.0E+00

Table 4.9 Displacements and Average Creep Strain Rates of Tests R-1, R-2

Elapsed Time (min.)	Test S-1 Lateral Disp. (in.)	Test S-1 Avg. Incremental Lateral Creep Rate (%/day)	Test S-1 Vertical Disp. (in.)	Test S-1 Avg. Incremental Vertical Creep Rate (%/day)	Test S-2 Lateral Disp. (in.)	Test S-2 Avg. Incremental Lateral Creep Rate (%/day)	Test S-2 Vertical Disp. (in.)	Test S-2 Avg. Incremental Vertical Creep Rate (%/day)
60					0.123	2.5E+01	0.045	9.0E+00
400	0.448	1.6E+01	0.174	6.1E+00	0.160	1.3E+00	0.056	3.9E-01
1000	0.542	1.9E+00	0.210	7.2E-01	0.171	2.2E-01	0.058	4.0E-02
10000	0.600	7.7E-02	0.230	2.7E-02	0.185	1.9E-02	0.066	1.1E-02
20000	0.600	0.0E+00	0.233	3.6E-03	0.187	2.4E-03	0.070	4.8E-03
30000	0.601	1.2E-03	0.237	4.8E-03	0.187	0.0E+00	0.075	6.0E-03
40000	0.602	1.2E-03	0.241	4.8E-03	0.187	0.0E+00	0.075	0.0E+00

Table 4.10 Displacements and Average Creep Strain Rates of Tests S-1, S-2

sustained average pressure).

The magnitude of creep deformation in the vertical direction of Test H-1 was higher than Test R-2. The change in vertical displacement with time for the two tests, however, were nearly the same.

Due to a difference in the degree of lateral restraint before releasing the lateral supports, the lateral displacement of Test H-1 was smaller than Test R-2 initially. After t=1,000 min., however, the displacements were larger in Test H-1. The creep rate of test H-1 was much higher than Test R-2. The displacements and creep strain rates of Test R-2 and Test H-1 are shown in Table 4.11.

In Test W-1, the sustained pressure was increased from 15 psi to 30 psi after 20 days, as shown in Figure 4.18. The initial increase in lateral displacement due to additional 15 psi pressure was 0.021 in. which was much smaller than that due to the first 15 psi pressure (0.48 in. at t=10 min.). This is because the soil-geosynthetic composite had been prestressed under 15 psi pressure for 20 days.

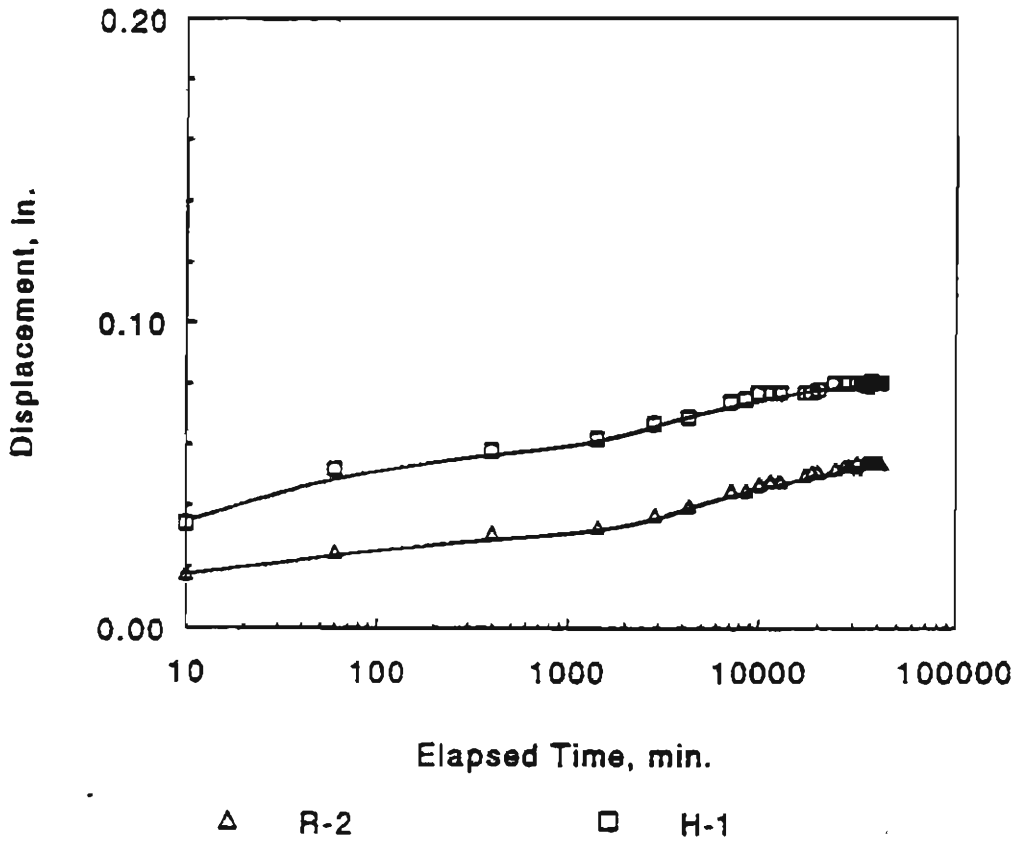

Figure 4.23: Vertical Displacements Versus Time Relationships of Tests R-2, H-1

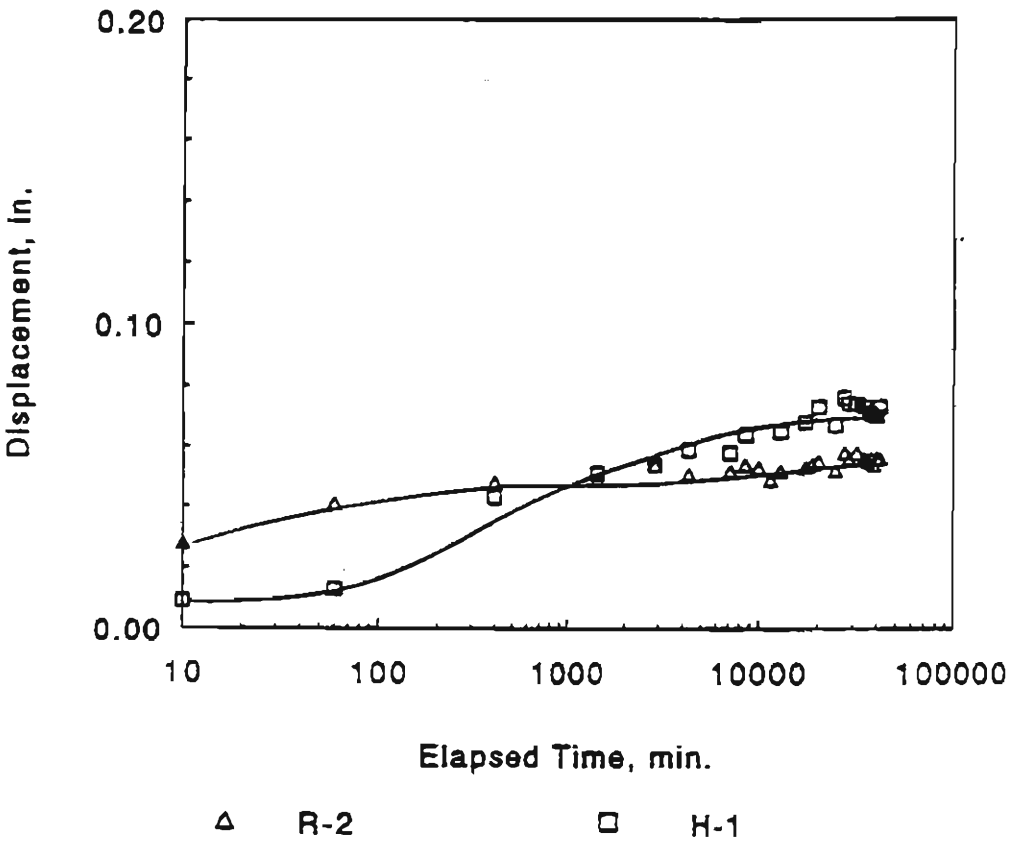

Figure 4.24: Lateral Displacements Versus Time Relationships of Tests R-2, H-1

Elapsed Time (min.)	Test R-2 Lateral Disp. (in.)	Test R-2 Avg. Incremental Lateral Creep Rate (%/day)	Test R-2 Vertical Disp. (in.)	Test R-2 Avg. Incremental Vertical Creep Rate (%/day)	Test H-1 Lateral Disp. (in.)	Test H-1 Avg. Incremental Lateral Creep Rate (%/day)	Test H-1 Vertical Disp. (in.)	Test H-1 Avg. Incremental Vertical Creep Rate (%/day)
60	0.042	8.4E+00	0.028	5.6E+00	0.012	2.4E+00	0.052	1.0E+01
400	0.048	2.1E-01	0.030	7.1E-02	0.043	1.1E+00	0.058	2.1E-01
1000	0.049	2.0E-02	0.032	4.0E-02	0.050	1.4E-01	0.061	6.0E-02
10000	0.053	5.3E-03	0.046	1.9E-02	0.065	2.0E-02	0.076	2.0E-02
20000	0.054	1.2E-03	0.053	8.4E-03	0.070	6.0E-03	0.078	2.4E-03
30000	0.055	1.2E-03	0.054	1.2E-03	0.072	2.4E-03	0.080	2.4E-03
40000	0.055	0.0E+00	0.054	0.0E+00	0.073	1.2E-03	0.080	0.0E+00

Table 4.11 Displacements and Average Creep Strain Rates of Tests R-2, H-1

5. FINITE ELEMENT ANALYSIS OF THE PERFORMANCE TEST

In this chapter a finite element model with a time-marching scheme was employed to analyze the behavior of Test D-1. The results of the analyses were compared with the measurement of Test D-1.

5.1 The Finite Element Model

A finite element program, DACSAR (Deformation Analysis Considering Stress Anisotropy and Reorientation), capable of analyzing long-term soil-geosynthetic interaction, was used by Helwany and Wu (1995) to analyze the original long-term performance test. The finite element model has been shown to give a very good simulation of the tests. In this study, the finite element model was employed to analyze the modified long-term performance test.

The finite element model incorporates an elasto-viscoplastic soil model and a generalized geosynthetic creep model. The elasto-viscoplastic soil model was developed by Sekiguchi and Ohta (1977) at the University

of Kyoto for simulation of consolidation and creep behavior of soils. The generalized creep model was developed by Helwany and Wu (1992) based on a nonlinear visco-elastic model proposed by Findley, et al.(1976).

5.1.1 Sekiguchi-Ohta Soil Model

The Sekiguchi-Ohta model (1977) is an incremental elasto-viscoplastic constitutive model of soils. The model is capable of describing time-independent and time-dependant characteristics of normally consolidated and lightly overconsolidated clays.

The Sekiguchi-Ohta model is an extension of the model developed by Ohta (1971) based on the dilatancy theory proposed by Shibata (1963). This model reduces to the model proposed by Ohta and Hata (1971) in the case of axisymmetric stress conditions. It further reduces to the original Cam-clay model proposed by Roscoe, Schofield and Thurairajah (1963) under an isotropic stress condition. The Sekiguchi-Ohta model can, therefore, be considered a "generalized" Cam-clay model.

The Sekiguchi-Ohta model has been verified using results of laboratory tests, such as K_o-triaxial compression/extension tests under different strain rates (Sekiguchi, 1989; Chou, 1992). The model has also been

verified through field tests, such as embankments on soft foundations (Iizuka and Ohta, 1987).

Six soil parameters are needed in Sekiguchi-Ohta model, i.e.,λ, κ, e_o, D, α and $\dot{v}_o$. The parameters λ and κ are related to the compression index and the swelling index, respectively, e_o is void ratio at the preconsolidated state, D is the coefficient of dilatancy as defined by Shibata (1963), α is the coefficient of secondary compression, and $\dot{v}_o$ is the initial volummetric strain rate. Detail description of the soil model can be found in Sekiguchi and Ohta (1977) and Iizuki and Ohta (1987).

5.1.2 Generalized Geosynthetic Creep Model

Findley, et al.(1976) represented creep of a nonlinear viscoelastic material by a series of multiple integral.

For uniaxial creep, the following expression results:

$$\epsilon(t) = F_1P+F_2P^2+F_3P^3 \qquad (1)$$

where $\epsilon(t)$: total strain

P: applied uniaxial load

F_1, F_2 and F_3: kernel functions

(time-dependant functions)

From Equation (1), the following expressions can be established for three uniaxial tests at constant sustained loads, P_a, P_b, and P_c covering the range of loads of interest.

$$\epsilon_a(t) = F_1P_a+F_2P_a^2+F_3P_a^3$$
$$\epsilon_b(t) = F_1P_b+F_2P_b^2+F_3P_b^3 \qquad (2)$$
$$\epsilon_c(t) = F_1P_c+F_2P_c^2+F_3P_c^3$$

Helwany and Wu (1992) developed a numerical procedure to determine the kernel functions. In the procedure, three measured creep strains (ϵ_a, ϵ_b and ϵ_c) at a selected time are first introduced into Equation (2), and the corresponding kernel functions F_1, F_2, and F_3 are determined by solving the three simultaneous equations. This is repeated at different elapsed times to obtain a series of kernel functions. A cubic spline function is then used to correlate the kernel functions with time. Since the values of the kernel functions at any given time can be determined from the cubic spline function, creep strains at any time t under a specified

sustained load P can be readily calculated by Equation (1). Typically, creep curves under three different sustained loads are needed to characterize the creep behavior of a geosynthetic.

5.2 Evaluation of Model Parameters

5.2.1 Sekiguchi-Ohta Model Parameters

Iizuka and Ohta (1987) developed a flow chart, together with empirical equation, for evaluating of the input parameters of the Sekiguchi-Ohta model, as shown in Figure 5.1. The soil model was developed for simulation of normally consolidated and lightly overconsolidated clays. In this study, however, the model was employed to simulate the behaviors of the compacted road base material.

The material parameters for the road base were determined by the following procedure:

(1) ϕ' value was determined from the results of the triaxial test at confining pressures of 15, 30, and 45 psi;

(2) M, the critical state parameter, was calculated as:

$$M=\frac{6\sin\phi'}{3-\sin\phi'}$$

(3) the ratio of κ/λ was calculated by an empirical equation,

$$\frac{\kappa}{\lambda}=1-\frac{M}{1.75}$$

(4) conduct a series of trial-and-error analyses on an axisymmetric element representing a soil element in a triaxial test until a good fit was obtained. For the road base, it was determined that λ= 0.12 and κ= 0.024 gave a good agreement with the consolidated drained triaxial test results as shown in Fig 5.2.

(5) D, the coefficient of dilatancy, was calculated as:

$$M=\frac{\lambda-\kappa}{D(1+e_o)}$$

Small values of creep parameters α and $\dot{v}_o$ were assumed for the road base since its creep is known to be negligible. Table 5.1 summarizes the values of the soil parameters used in the analysis.

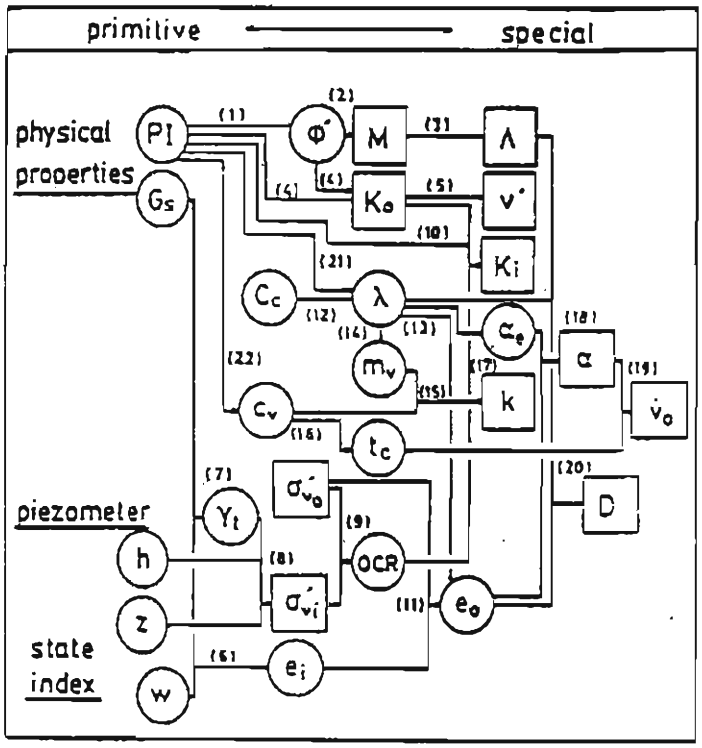

(1) $\sin\phi = 0.81 - 0.233 \log PI$ — Kenney (1959)

(2) $M = 6\sin\phi'/(3-\sin\phi')$

(3) $\Lambda = M/1.75$ — Karube (1975)

(4) $K_a = 0.44 - 0.42 \cdot 10^{-2} PI$ — Massarsch (1979)

$K_a = 1 - \sin\phi'$ — Jáky (1944)

(5) $\nu' = K_a/(1-K_a)$

(6) $e_i = w G_s$

(7) $\gamma_t = G_s\gamma_w(1+w)/(1+G_s w)$

(8) $\sigma'_{vi} = \gamma_t z - p_w$

(9) $OCR = \sigma'_{vo}/\sigma'_{vi}$

(10) $K_i = K_a(OCR)^{0.54 - 0.001 PI/133}$ — Alpan (1967)

(11) $e_o = e_i - \lambda(1-\Lambda)\ln(\overline{OCR})$ $\quad \overline{OCR} = \frac{1-2K_a}{1-2K_i} OCR$

(12) $\lambda = 0.4343\, C_c$

(13) $C_\varepsilon = 1.78\lambda - 0.155$

(14) $m_v = 3\lambda/[(1+e_o)(1-2K_a)\sigma'_{vo}]$

(15) $k = m_v c_v \gamma_w$

(16) $t_c = t_{90} = H^2 T_v(U=90\%)/c_v$

(17) $\alpha_\varepsilon/\lambda = 0.05 \pm 0.02$ (clay) $= 0.07 \pm 0.02$ (peat) — Mesri & Godlewski (1977)

(18) $\alpha = \alpha_\varepsilon/(1+e_o)$ — Sekiguchi (1977)

(19) $\dot{\nu}_o = \alpha/t_c$ — Sekiguchi (1977)

(20) $D = \lambda\Lambda/[M(1+e_o)]$ — Ohta (1971)

(21) $\lambda = 0.015 + 0.007 PI$

(22) $\log c_v\,(cm^2/min) = -0.025 PI + 0.25 \pm 1$

Figure 5.1 : Procedure for Determining Parameters for Sekiguchi-Ohta Model (Iizuka and Ohta, 1987)

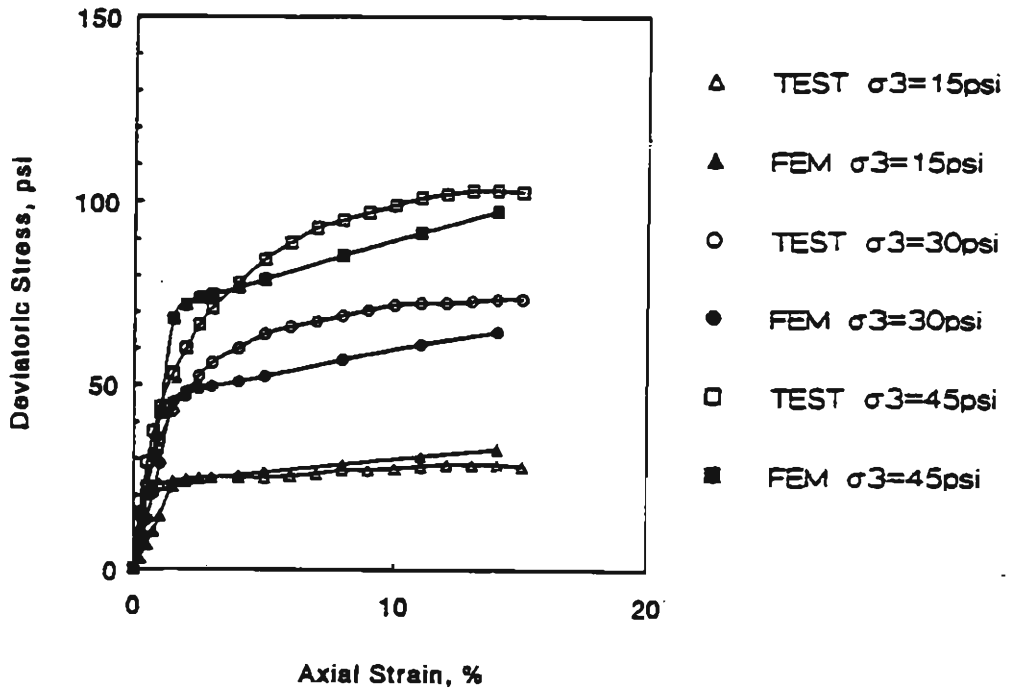

Figure 5.2: Consolidated Drained Triaxial Test:
Test Results Versus Model Simulation

Table 5.1 Soil parameters for Sekiguchi-Ohta soil model

Parameters	Value
λ	0.12
κ	0.024
M	1.4
D	0.056
e_o	0.223
$\acute{u}$	0.3
$\dot{v}_o$	0.004
α	0.0008

5.2.2 Generalized Geosynthetic Creep Model

Typar 3301 was the geotextile used in test D-1. The creeps test results of the geotextile and evaluation of the creep parameters have been presented by Helwany and Wu (1992). A comparison of creep model simulation and creep test results is shown in Figure 5.3. An excellent agreement was noted between the experimental results and the model simulation.

5.3 Finite Element Simulation of the Performance Test

5.3.1 Finite Element Simulation

Figure 5.4 depicts the finite element discretization for analysis of Test D-1. Because of symmetry, only one-half of the geometry was analyzed. A total of 192 quadrilateral elements with Sekiguchi-Ohta model were used to represent the soil, 12 truss elements with the generalized creep model to represent geosynthetic.

The lateral supports, which were used to restrain lateral movement of soil-geosynthetic composite during sample preparation and during load application, were simulated by 16 truss elements. These truss elements were connected to the soil elements along the vertical face of

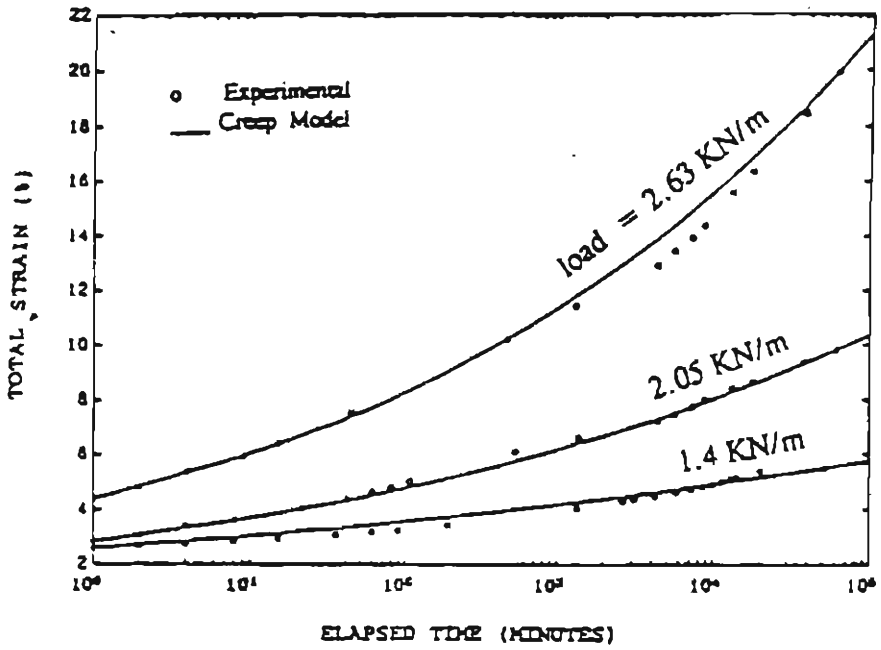

Figure 5.3 : Creep Test Results on Reinforcement: Experiment Versus Creep Model (Helwany and Wu, 1992)

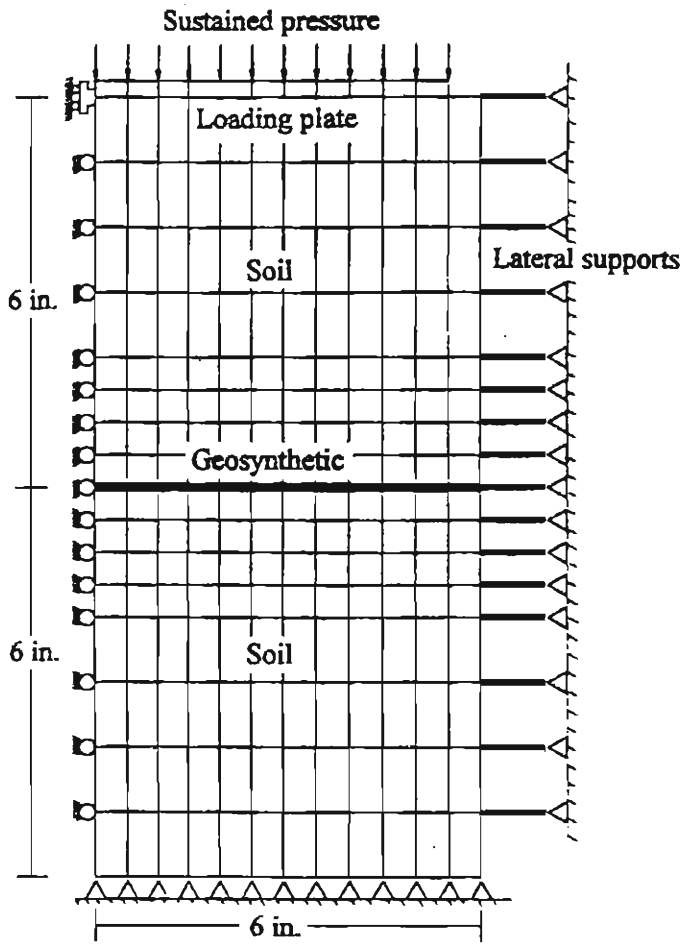

Figure 5.4: Finite Element Discretization

the composite. The removal of the lateral supports was simulated by removing the truss elements from the system.

The analysis was carried out with a time-marching procedure. After the sustained vertical load of 15 psi was applied to the top surface, the analysis was continued for a period of 13 days. Input data for the finite element analysis are presented in Appendix B.

5.3.2 Results of Finite Element Analysis

Figure 5.5 shows the calculated and measured lateral displacements versus time relationships of the geotextile reinforcement after releasing the lateral supports. A good agreement between the calculated and measured lateral displacements was obtained, although the measured displacement was slightly larger than the calculated value. The average measure creep rate was 2.4×10^{-3}% per day, while the average calculated creep rate was 1.6×10^{-3}% per day.

Figure 5.6 shows the calculated and measured lateral displacements along the side of the soil-geosynthetic composite after 18,720 min.(13 days). The calculated displacements were somewhat lower than the measured values. The calculated lateral displacement at

the mid-height was 0.07 inch, whereas the measured displacement was 0.11 inch. The deformed shapes of the calculated and measured displacements, however, were similar.

Figures 5.7 shows the calculated and the measured distribution of strains along the geosynthetic at 10, 4,320 and 18,720 minutes. It is seen that finite element simulation was less than satisfactory. The calculated strain did show a maximum value at the center but decreased toward the extremities at a much slower rate than the measured strains. The discrepancies may be caused by the limitation of the soil model in the finite element analysis, which was developed for simulation of normally consolidated or lightly consolidated clays.

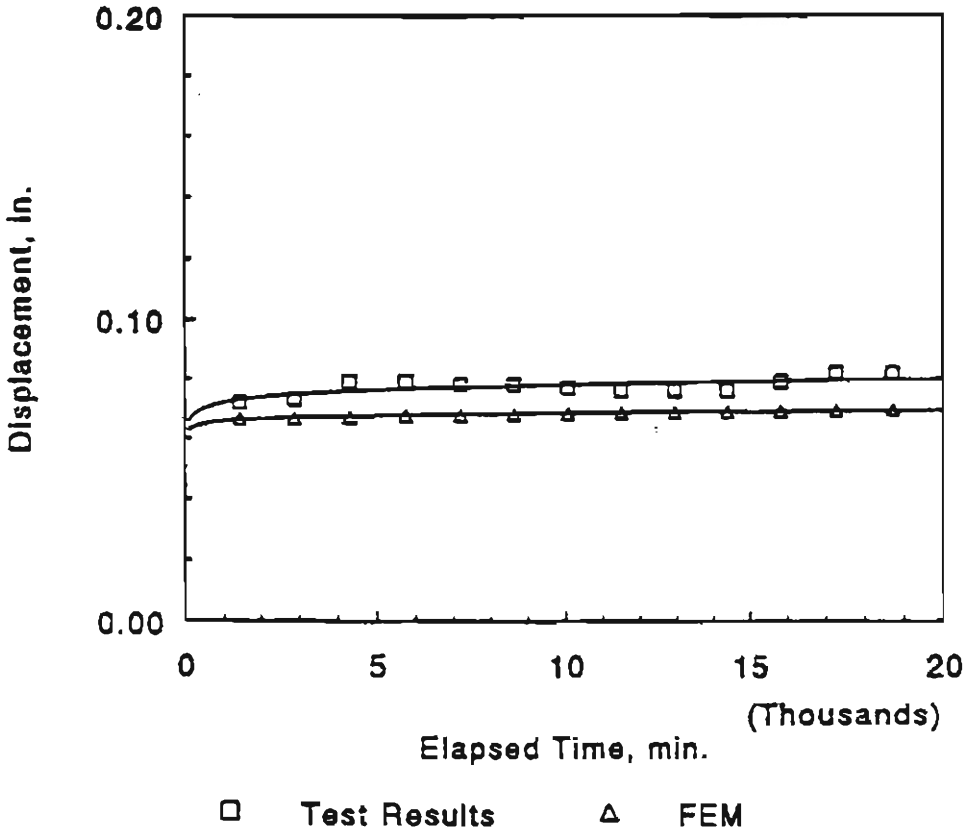

Figure 5.5 : Lateral Displacements after Releasing of Lateral Supports Versus Time- Test Results Versus FEM

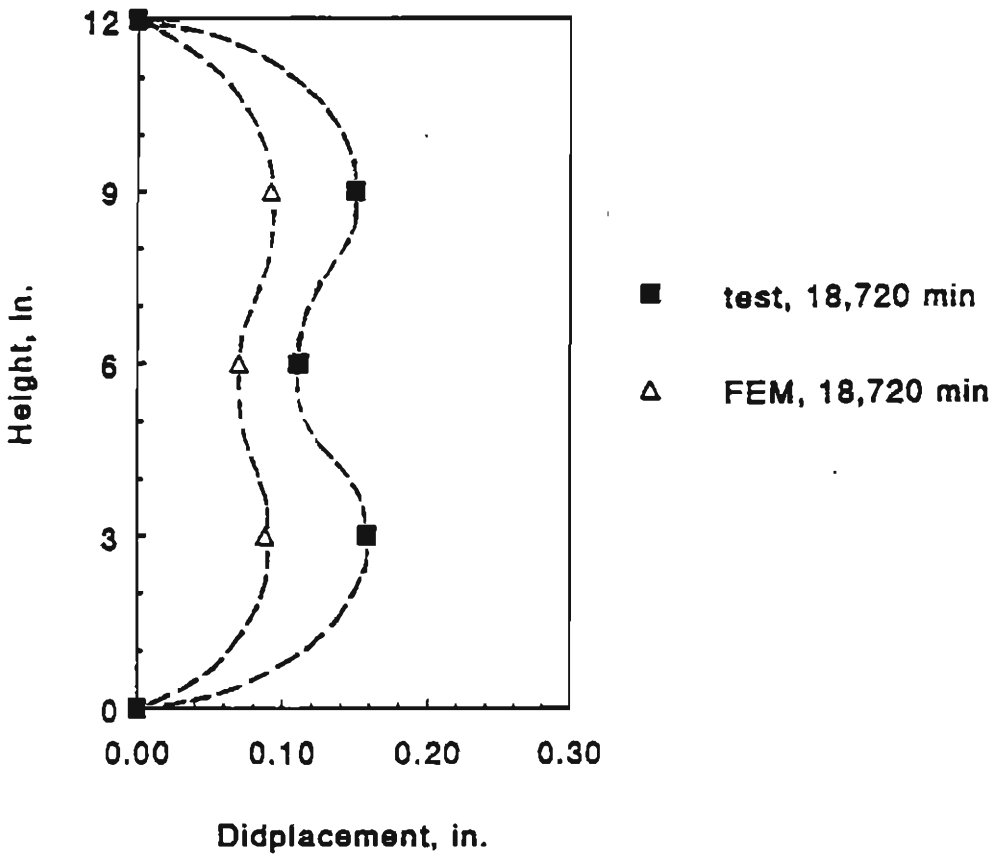

Figure 5.6: Lateral Shapes at 18,720 min.-
Test Results Versus FEM

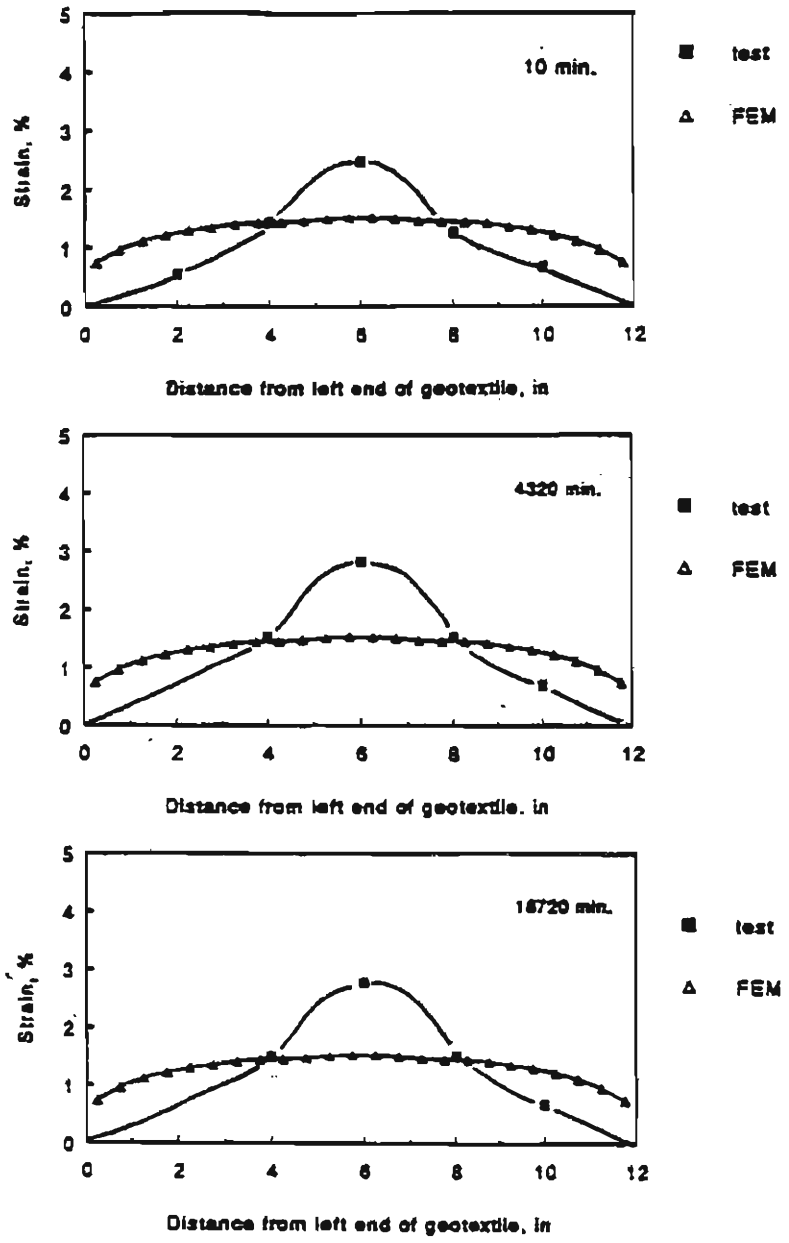

Figure 5.7 : Distribution of Strains along the Length of Geotextile: Test Results Versus FEM

6. SUMMARY AND CONCLUSIONS

6.1 Summary

In this study a modified performance test as well as test procedure for investigation of long-term behavior of soil-geosynthetic composites was developed. The modified test was easier to perform than the test developed by Wu and Helwany (1996) and represented a "worst" condition in the deformation behavior of the soil-geosynthetic composite.

In the modified test, a soil-geosynthetic composite was prepared inside the test apparatus in a plane strain condition. A sustained load was applied on the top surface of the soil-geosynthetic composite for a long period of time. The applied load was transferred from the soil to the geosynthetic, which was allowed to deform in an interactive manner with the confining soil.

During specimen preparation and during load application, longitudinal movement of the soil-geosynthetic composite was restrained by a pair of plexiglass panels, one on each side of the specimen,

which were released to begin the test. Lateral and vertical movements of the soil-geosynthetic composite were monitored by LVDT's and dial indicators from the instant the lateral support was released.

A series of performance tests were performed to examine test repeatability and to investigate the effects of soil type, geosynthetic type and sustained load intensity on the behavior of soil-geosynthetic composite. A test was instrumented with strain gages to measure deformation along the length of the geosynthetic. Tests with soil only were also conducted for comparisons with soil-geosynthetic composite. In addition, a load-deformation test with a weak geosynthetic was conducted to examine the failure mode of the soil-geosynthetic composites. Many of the tests were conducted at an elevated temperature of 125°F. Element test on the geosynthetics indicated that the elevated temperatures typically accelerated creep of the geosynthetic by 100 to 400 folds.

A finite element model was employed to analyze one of the performance tests. The analytical results were compared with the measured values.

6.2 Conclusions

Base on the tests conducted in this study, the following conclusions are advanced:

1) The repeatability of the performance test is considered satisfactory. Other than scatter of test data due to electrical interference, the major discrepancy of the tests occurred immediately after releasing the lateral support, which was due to a difference in the degree of lateral restraint during specimen preparation.

2) A test with Amoco 2002, a weak reinforcement, reached a failure condition with rupture along the centerline of the geotextile which conformed with the anticipated location of maximum force in the reinforcement.

3) A soil-geosynthetic composite, which consisted of a road base and Amoco 2044, subjected to an average vertical pressure of 15 psi, exhibited about 0.03 in. of lateral displacement at the release of the lateral support. In the next 30 days, an additional lateral movement of 0.025 in. occurred *in an elevated temperature*

environment of 125°F. The creep deformation decreased with time at a decreasing rate. The lateral deformation essentially ceased at 30,000 minutes after release of lateral support. Similar deformation behavior was measured in the vertical direction.

4) A soil-geosynthetic composite with a clayey soil and Amoco 2044, subjected to an average vertical pressure of 15 psi, also exhibited negligible creep in the lateral direction over the testing period of 30 days *in ambient temperature*. Creep deformation in the vertical direction, however, was significant and continue to increase at the end of the test. It is to be noted that the clayey soil without a reinforcement in otherwise the same test conditions failed within 17 minutes after released of the lateral support.

5) With the use of Amoco 2002 (a weaker reinforcement), the soil- geosynthetic composite, which employed the road base, subjected to 15 psi average vertical pressure

and 125°F temperature, exhibited about 0.05 in. at the release of the lateral support. Over the next 20 days, the lateral displacement increased by 0.06 in., which was more than two times as much as the composite with Amoco 2044 reinforcement.

6) At an average vertical pressure of 30 psi, the soil-geosynthetic composite, which employed the road base and Amoco 2044 reinforcement in a 125°F environment, exhibited about 0.01 in. lateral displacement at the release of the lateral support. The lateral displacement increased by 0.06 in. in the next 30 days, which is more than twice the increase in lateral displacement with 15 psi pressure (0.025 in. increase in lateral displacement). The vertical displacements at the release of the lateral support were about 0.018 in. and 0.035 in. under 15 psi and 30 psi, respectively. The increase in vertical displacements over the next 30 days were about the same under 15 psi and 30 psi (about 0.04 in.)

7) In the test which the strains along the geosynthetic reinforcement were measured, the soil-geosynthetic composite comprising the road base and Typar 3301 reinforcement, and subjected to an average vertical pressure of 15 psi and 70°F temperature. The maximum strain occurred at the center of the reinforcement, and decreased, in a nonlinear fashion, to zero at the two extremities. The maximum strain was 2.0% at the release of the lateral support. The maximum strain increased to 2.8% after 2 days and remained constant for about 1 day then decreased at an average rate of 0.005% per day.

The maximum lateral displacement of the soil-geosynthetic occurred near the quarter point, i.e., at 3 in. above the base. The rate of lateral deformation was also the highest at the quarter point.

Using isochronous load-strain curves, the forces along the length of the reinforcement can readily be determined. The loads decreased, as a result of stress relaxation, soon after the lateral support was released. The decrease

of loads occurred at a decreasing rate. The rate of decrease was about the same along the length of the reinforcement.

8) The agreement between the finite element analysis and measured test results was fairly good in terms of the magnitude of creep deformation and rate of creep in the lateral direction. The strains obtained from the finite element analysis were markedly different from the measured value. The discrepancy was attributed to the inability of the soil model for simulation of compacted soil.

APPENDIX A

PERFORMANCE TEST RESULTS

TEST: C-1
REINFORCEMNENT: None
SOIL: Clayey Soil
TEMPERATURE: 70 F
SUSTAINED VERTICAL LOAD: 15 psi
DATE: 07/07/95

Elapsed time	Displacement			
	Horizontal			Vertical
	left side	right side	Total	
(min.)	(in.)	(in.)	(in.)	(in.)
0	0.000	0.000	0.000	0.000
5	0.113	0.009	0.122	0.360
0	0.000	0.000	0.000	0.000
1	0.070	0.033	0.103	0.053
2	0.078	0.049	0.127	0.076
3	0.087	0.059	0.146	0.102
4	0.100	0.064	0.164	0.113
5	0.105	0.074	0.179	0.132
6	0.114	0.082	0.196	0.142
7	0.124	0.083	0.207	0.159
9	0.151	0.097	0.248	0.174
10	0.167	0.107	0.274	0.199
11	0.191	0.117	0.308	0.227
12	0.228	0.127	0.355	0.257
13	0.271	0.140	0.411	0.295
14	0.314	0.155	0.469	0.335
15	0.351	0.173	0.524	0.365
16	0.383	0.192	0.575	0.403
17	0.452	0.260	0.712	0.520
18	0.890	0.679	1.569	1.293

TEST: C-2
REINFORCEMNENT: Amoco 2044
SOIL: Clayey Soil
TEMPERATURE: 70 F
SUSTAINED VERTICAL LOAD: 15 psi
DATE: 10/06/95

Elapsed time	Displacement			
	Horizontal			Vertical
	left side	right side	Total	
(min.)	(in.)	(in.)	(in.)	(in.)
0	0.000	0.000	0.000	0.000
10	0.024	0.042	0.066	0.670
0	0.000	0.000	0.000	0.000
10	0.055	0.044	0.099	0.038
60	0.055	0.046	0.101	0.114
400	0.056	0.045	0.101	0.129
1440	0.055	0.045	0.100	0.134
4320	0.057	0.046	0.103	0.136
5760	0.057	0.048	0.105	0.138
7200	0.055	0.049	0.104	0.140
11520	0.055	0.048	0.103	0.140
14400	0.058	0.046	0.104	0.142
15840	0.057	0.047	0.104	0.143
17280	0.055	0.046	0.101	0.145
18720	0.056	0.047	0.103	0.145
21600	0.056	0.045	0.101	0.145
24480	0.056	0.048	0.104	0.147
25920	0.055	0.047	0.102	0.148
27360	0.057	0.049	0.106	0.150
28800	0.056	0.050	0.106	0.151
30240	0.056	0.048	0.104	0.152
33120	0.055	0.049	0.104	0.152
34560	0.056	0.048	0.104	0.152
37440	0.055	0.052	0.107	0.157

TEST: D-1
REINFORCEMNENT: Typar 3301
SOIL: Road Base
TEMPERATURE: 70 F
SUSTAINED VERTICAL LOAD: 15 psi
DATE: 09/06/95

Elapsed time	Displacement			
	Total Horizontal			Vertical
	Point 1	Point 2	Point 3	
(min.)	(in.)	(in.)	(in.)	(in.)
0	0.000	0.000	0.000	0.000
10	0.138	0.192	0.175	0.376
0	0.000	0.000	0.000	0.000
5	0.027	0.063	0.055	0.031
10	0.034	0.066	0.065	0.036
60	0.050	0.083	0.093	0.051
400	0.064	0.097	0.113	0.071
1440	0.072	0.103	0.121	0.080
2880	0.073	0.110	0.134	0.080
4320	0.079	0.112	0.134	0.085
5760	0.079	0.108	0.131	0.085
7200	0.078	0.115	0.129	0.088
8640	0.078	0.106	0.131	0.089
11520	0.076	0.112	0.131	0.091
12960	0.076	0.109	0.132	0.091
17280	0.082	0.114	0.134	0.0915
18720	0.082	0.113	0.134	0.0922

TEST: H-1
REINFORCEMNENT: Amoco 2044
SOIL: Road Base
TEMPERATURE: 125 F
SUSTAINED VERTICAL LOAD: 30 psi
DATE: 09/27/95

Elapsed time	Displacement			
	Horizontal			Vertical
	left side	right side	Total	
(min.)	(in.)	(in.)	(in.)	(in.)
0	0.000	0.000	0.000	0.000
10	0.114	0.126	0.240	0.470
0	0.000	0.000	0.000	0.000
10	0.004	0.005	0.009	0.034
60	0.006	0.007	0.013	0.052
400	0.031	0.012	0.043	0.058
1440	0.036	0.015	0.051	0.062
2880	0.039	0.015	0.054	0.067
4320	0.040	0.019	0.059	0.069
7200	0.041	0.017	0.058	0.074
8640	0.044	0.020	0.064	0.075
10080	0.039	0.017	0.056	0.077
11520	0.044	0.018	0.062	0.077
12960	0.045	0.020	0.065	0.077
17280	0.045	0.023	0.068	0.077
18720	0.042	0.021	0.063	0.077
20160	0.050	0.023	0.073	0.078
24480	0.047	0.020	0.067	0.080
27360	0.050	0.026	0.076	0.080
28800	0.048	0.026	0.074	0.080
31680	0.048	0.026	0.074	0.080
34560	0.047	0.026	0.073	0.080
36000	0.048	0.025	0.073	0.079
37440	0.047	0.024	0.071	0.081
38880	0.047	0.023	0.070	0.080
40320	0.048	0.022	0.070	0.080
41760	0.047	0.026	0.073	0.080

TEST: R-1
REINFORCEMNENT: Amoco 2044
SOIL: Road Base
TEMPERATURE: 70 F
SUSTAINED VERTICAL LOAD: 15 psi
DATE: 10/06/95

Elapsed time	Displacement			
	Horizontal			Vertical
	left side	right side	Total	
(min.)	(in.)	(in.)	(in.)	(in.)
0	0.000	0.000	0.000	0.000
10	0.052	0.084	0.136	0.325
0	0.000	0.000	0.000	0.000
10	0.014	0.016	0.030	0.018
60	0.017	0.022	0.039	0.031
400	0.019	0.021	0.040	0.038
1440	0.021	0.021	0.042	0.045
4320	0.020	0.022	0.042	0.049
5760	0.018	0.021	0.039	0.049
7200	0.020	0.018	0.038	0.050
11520	0.018	0.018	0.036	0.053
14400	0.023	0.021	0.044	0.054
15840	0.018	0.019	0.037	0.055
17280	0.021	0.017	0.038	0.055
18720	0.021	0.018	0.039	0.056
21600	0.022	0.019	0.041	0.058
24480	0.022	0.016	0.038	0.060
25920	0.019	0.021	0.040	0.060
30240	0.021	0.017	0.038	0.061
33120	0.025	0.018	0.043	0.064
37440	0.020	0.020	0.040	0.066

TEST:	R-2
REINFORCEMNENT:	Amoco 2044
SOIL:	Road Base
TEMPERATURE:	125 F
SUSTAINED VERTICAL LOAD:	15 psi
DATE:	09/27/95.

Elapsed time	Displacement			
	Horizontal			Vertical
	left side	right side	Total	
(min.)	(in.)	(in.)	(in.)	(in.)
0	0.000	0.000	0.000	0.000
10	0.036	0.030	0.066	0.262
0	0.000	0.000	0.000	0.000
10	0.012	0.016	0.028	0.018
60	0.016	0.025	0.041	0.025
400	0.019	0.029	0.048	0.031
1440	0.020	0.029	0.049	0.033
2880	0.020	0.034	0.054	0.037
4320	0.020	0.031	0.051	0.040
7200	0.020	0.032	0.052	0.045
8640	0.021	0.033	0.054	0.045
10080	0.019	0.034	0.053	0.047
11520	0.020	0.029	0.049	0.048
12960	0.020	0.032	0.052	0.048
17280	0.023	0.030	0.053	0.050
18720	0.024	0.030	0.054	0.051
20160	0.022	0.033	0.055	0.051
24480	0.022	0.030	0.052	0.052
27360	0.024	0.034	0.058	0.053
28800	0.023	0.033	0.056	0.053
31680	0.026	0.032	0.058	0.054
34560	0.023	0.033	0.056	0.054
36000	0.024	0.031	0.055	0.054
37440	0.026	0.030	0.056	0.055
38880	0.026	0.028	0.054	0.054
40320	0.026	0.030	0.056	0.054
41760	0.024	0.032	0.056	0.054

TEST: R-3
REINFORCEMNENT: Amoco 2044
SOIL: Road Base
TEMPERATURE: 125 F
SUSTAINED VERTICAL LOAD: 15 psi
DATE: 08/09/95

Elapsed time	Displacement			
	Horizontal			Vertical
	left side	right side	Total	
(min.)	(in.)	(in.)	(in.)	(in.)
0	0.000	0.000	0.000	0.000
10	0.016	0.009	0.025	0.264
0	0.000	0.000	0.000	0.000
10	0.007	0.006	0.013	0.020
60	0.016	0.009	0.025	0.028
400	0.018	0.016	0.034	0.030
1440	0.020	0.019	0.039	0.038
5760	0.021	0.025	0.046	0.038
7200	0.019	0.023	0.042	0.039
10080	0.019	0.023	0.042	0.039
12960	0.020	0.023	0.043	0.040
14400	0.030	0.021	0.051	0.041
17280	0.028	0.026	0.054	0.043
18720	0.030	0.029	0.059	0.044
20160	0.030	0.027	0.057	0.045
21600	0.031	0.021	0.052	0.046
23040	0.028	0.024	0.052	0.047
24480	0.030	0.024	0.054	0.049
28800	0.030	0.024	0.054	0.052
30240	0.028	0.022	0.050	0.053
31680	0.029	0.021	0.050	0.053
34560	0.029	0.021	0.050	0.055
37440	0.028	0.023	0.051	0.055

TEST: S-1
REINFORCEMNENT: None
SOIL: Road Base
TEMPERATURE: 70 F
SUSTAINED VERTICAL LOAD: 15 psi
DATE: 10/06/95

Elapsed time	Displacement			
	Horizontal			Vertical
	left side	right side	Total	
(min.)	(in.)	(in.)	(in.)	(in.)
0	0.000	0.000	0.000	0.000
10	0.164	0.264	0.428	0.416
0	0.000	0.000	0.000	0.000
10	0.120	0.135	0.255	0.098
400	0.189	0.259	0.448	0.174
1440	0.231	0.349	0.580	0.220
4320	0.235	0.359	0.594	0.227
5760	0.234	0.364	0.598	0.228
7200	0.234	0.360	0.594	0.229
11520	0.235	0.362	0.597	0.231
14400	0.236	0.362	0.598	0.231
15840	0.239	0.363	0.602	0.232
17280	0.237	0.365	0.602	0.232
18720	0.238	0.362	0.600	0.233
21600	0.237	0.365	0.602	0.234
24480	0.236	0.362	0.598	0.235
25920	0.235	0.365	0.600	0.236
27360	0.237	0.364	0.601	0.236
28800	0.236	0.361	0.597	0.236
30240	0.236	0.367	0.603	0.237
37440	0.238	0.362	0.600	0.240
38880	0.236	0.364	0.600	0.241
41760	0.237	0.365	0.602	0.242
44640	0.238	0.364	0.602	0.2422

TEST: S-2
REINFORCEMNENT: None
SOIL: Road Base
TEMPERATURE: 125 F
SUSTAINED VERTICAL LOAD: 15 psi
DATE: 08/09/95

Elapsed time	Displacement			
	Horizontal			Vertical
	left side	right side	Total	
(min.)	(in.)	(in.)	(in.)	(in.)
0	0.000	0.000	0.000	0.000
10	0.124	0.179	0.303	0.300
0	0.000	0.000	0.000	0.000
10	0.038	0.041	0.078	0.032
60	0.061	0.062	0.123	0.045
400	0.080	0.080	0.160	0.056
1440	0.089	0.085	0.174	0.059
2880	0.086	0.083	0.169	0.065
4320		0.091	0.183	0.065
5760		0.090	0.180	0.066
7200		0.088	0.177	0.066
8640		0.089	0.177	0.066
10080	0.095	0.090	0.186	0.067
11520	0.097	0.093	0.190	0.067
12960	0.099	0.092	0.190	0.067
17280	0.100	0.091	0.192	0.069
20160	0.096	0.089	0.185	0.070
21600	0.094	0.087	0.181	0.071
23040	0.094	0.086	0.180	0.072
24480	0.096	0.086	0.182	0.072
30240	0.097	0.088	0.185	0.075
33120	0.093	0.091	0.184	0.075
34560	0.089	0.096	0.185	0.075
36000	0.092	0.098	0.190	0.075
38880	0.092	0.095	0.186	0.075
43200	0.088	0.097	0.185	0.075

TEST: U-1
REINFORCEMENT: Amoco 2002
SOIL: Road Base
TEMPERATURE: 70 F

Elapsed Time (sec.)	Vertical Load (kips)	Equivalent Vertical Pressure (psi)
0.00	0.00	0.00
10.44	2.73	9.49
20.87	4.93	17.12
30.26	6.85	23.77
40.70	8.88	30.82
50.09	10.62	36.86
60.53	12.43	43.17
70.96	14.17	49.20
80.36	15.63	54.25
90.79	17.12	59.44
100.19	18.37	63.78
110.62	19.64	68.19
111.66	19.76	68.60
112.71	19.87	69.00
113.75	20.00	69.44
190.98	20.00	69.44
192.02	19.41	67.41
193.06	18.83	65.38
194.11	18.39	63.85
195.15	18.14	63.00
196.19	17.88	62.09
197.24	17.32	60.15
198.28	17.02	59.10
199.33	16.87	58.56
200.37	16.71	58.02

TEST: W-1
REINFORCEMNENT: Amoco 2002
SOIL: Road Base
TEMPERATURE: 125 F
SUSTAINED VERTICAL LOAD: 15 psi , after 20 days increase to 30 psi
DATE: 08/15/95

Elapsed time	Displacement		
	Horizontal		
	left side	right side	Total
(min.)	(in.)	(in.)	(in.)
0	0.000	0.000	0.000
10		0.020	0.040
0	0.000	0.000	0.000
10		0.024	0.048
400		0.043	0.085
1440	0.051	0.050	0.101
2880	0.055	0.055	0.109
4320	0.055	0.055	0.109
8640	0.056	0.053	0.109
10080	0.059	0.058	0.117
11520	0.056	0.054	0.110
14400		0.056	0.111
15840		0.058	0.115
18720		0.058	0.116
21600		0.058	0.116
23040		0.061	0.122
25920		0.060	0.120
27360		0.061	0.122
30240		0.055	0.110
34560		0.060	0.119
34560	30 psi	0.070	0.140
36000		0.078	0.157
38880		0.081	0.162
40320		0.080	0.160
43200		0.079	0.158

APPENDIX B

INPUT DATA OF FINITE ELEMENT ANALYSIS

lb in min Modified Long-Term Soil- Geosynthetic Performance Test

```
0  0  0  0  0  0
0  0  0  1  1  1
0  0  0  0  0  0  0  0  0
0.0361,   0.0
0  1   0.042   0.800   1.40   0.3   1000.   1000.
       20.00   0.56   0.966   1.0   .004   .0008
       0.12   .6500    0.0
0  2   0.042   0.800   1.40   0.3   1000.   1000.
       20.00   0.56   0.882   1.0   .004   .0008
       0.12   .6500    0.0
0  3   0.042   0.800   1.40   0.3   1000.   1000.
       20.00   0.560   0.798   1.0   .004   .0008
       0.12   .6500    0.0
0  4   0.042   0.800   1.40   0.3   1000.   1000.
       20.00   0.560   0.714   1.0   .004   .0008
       0.12   .6500    0.0
0  5   0.042   0.800   1.40   0.3   1000.   1000.
       20.00   0.560   0.630   1.0   .004   .0008
       0.12   .6500    0.0
0  6   0.042   0.800   1.40   0.3   1000.   1000.
       20.00   0.560   0.546   1.0   .004   .0008
       0.12   .6500    0.0
0  7   0.042   0.800   1.40   0.3   1000.   1000.
       20.00   0.560   0.462   1.0   .004   .0008
       0.12   .6500    0.0
0  8   0.042   0.800   1.40   0.3   1000.   1000.
       20.00   0.560   0.378   1.0   .004   .0008
       0.12   .6500    0.0
0  9   0.042   0.800   1.40   0.3   1000.   1000.
       20.00   0.560   0.294   1.0   .004   .0008
       0.12   .6500    0.0
0  10   0.042   0.800   1.40   0.3   1000.   1000.
       20.00   0.560   0.210   1.0   .004   .0008
       0.12   .6500    0.0
0  11   0.042   0.800   1.40   0.3   1000.   1000.
       20.00   0.560   0.126   1.0   .004   .0008
       0.12   .6500    0.0
```

```
  0  12    0.042   0.800    1.40    0.3    1000.    1000.
          20.00   0.560   0.042   1.0    .004     .0008
           0.12   .6500     0.0
  3  13   150.    1.0
  3  14    50.    1.0
  2  16 450000.   1.7      2.0
E  6  15  37570.   0.011
 50   7.996     11.70.   15.0      1.0
  0.0000   2.6000   2.8500   4.4000
  0.1000   2.6417   2.9246   4.5412
  0.2000   2.6840   3.0012   4.6869
  0.3000   2.7270   3.0798   4.8372
  0.4000   2.7707   3.1604   4.9925
  0.5000   2.8151   3.2432   5.1526
  0.6000   2.8603   3.3281   5.3180
  0.7000   2.9061   3.4153   5.4886
  0.8000   2.9527   3.5047   5.6647
  0.9000   3.0000   3.5965   5.8465
  1.0000   3.0481   3.6907   6.0341
  1.1000   3.0970   3.7874   6.2277
  1.2000   3.1466   3.8865   6.4275
  1.3000   3.1970   3.9883   6.6337
  1.4000   3.2483   4.0928   6.8466
  1.5000   3.3004   4.2000   7.0663
  1.6000   3.3533   4.3099   7.2930
  1.7000   3.4070   4.4228   7.5270
  1.8000   3.4616   4.5386   7.7685
  1.9000   3.5171   4.6575   8.0178
  2.0000   3.5735   4.7795   8.2750
  2.1000   3.6307   4.9046   8.5406
  2.2000   3.6889   5.0331   8.8146
  2.3000   3.7481   5.1649   9.0974
  2.4000   3.8081   5.3001   9.3893
  2.5000   3.8692   5.4389   9.6906
  2.6000   3.9312   5.5814  10.0015
  2.7000   3.9942   5.7276  10.3224
  2.8000   4.0582   5.8775  10.6536
  2.9000   4.1233   6.0315  10.9955
```

```
3.0000   4.1894   6.1894  11.3483
3.1000   4.2565   6.3515  11.7124
3.2000   4.3248   6.5178  12.0882
3.3000   4.3941   6.6885  12.4761
3.4000   4.4645   6.8637  12.8764
3.5000   4.5361   7.0434  13.2895
3.6000   4.6088   7.2279  13.7159
3.7000   4.6827   7.4172  14.1560
3.8000   4.7577   7.6114  14.6103
3.9000   4.8340   7.8108  15.0790
4.0000   4.9115   8.0153  15.5629
4.1000   4.9902   8.2252  16.0622
4.2000   5.0702   8.4406  16.5776
4.3000   5.1514   8.6617  17.1095
4.4000   5.2340   8.8885  17.6585
4.5000   5.3179   9.1213  18.2251
4.6000   5.4031   9.3601  18.8099
4.7000   5.4897   9.6053  19.4134
4.8000   5.5777   9.8568  20.0363
4.9000   5.6671  10.1149  20.6792
5.0000   5.7580  10.3798  21.3427
39
0.0001
  1.
  2.
  3.
  4.
  5.
  6.
  7.
  8.
  9.
 10.
1440.
2880.
4320.
5760.
7200.
```

```
 8640.
 10080.
 11520.
 12960.
 14400.
 15840.
 17280.
 18720.
 20160.
 21600.
 23040.
 24480.
 25920.
 27360.
 28800.
 30240.
 31680.
 33120.
 34560.
 36000.
 37440.
 38880.
 40320.
12
193  85  97
194  86  98
195  87  99
196  88  100
197  89  101
198  90  102
199  91  103
200  92  104
201  93  105
202  94  106
203  95  107
204  96  108
  1   1   1   1   1   0   1    1.0     1
  1    0.0      0.0     13   6.0      0.0
```

```
   14  7.0     0.0
   15  0.0     1.0     27  6.0     1.0
   28  7.0     1.0
   29  0.0     2.0     41  6.0     2.0
   42  7.0     2.0
   43  0.0     3.0     55  6.0     3.0
   56  7.0     3.0
   57  0.0     4.0     69  6.0     4.0
   70  7.0     4.0
   71  0.0     4.5     83  6.0     4.5
   84  7.0     4.5
   85  0.0     5.0     97  6.0     5.0
   98  7.0     5.0
   99  0.0     5.5    111  6.0     5.5
  112  7.0     5.5
  113  0.0     6.0    125  6.0     6.0
  126  7.0     6.0
  127  0.0     6.5    139  6.0     6.5
  140  7.0     6.5
  141  0.0     7.0    153  6.0     7.0
  154  7.0     7.0
  155  0.0     7.5    167  6.0     7.5
  168  7.0     7.5
  169  0.0     8.0    181  6.0     8.0
  182  7.0     8.0
  183  0.0     9.0    195  6.0     9.0
  196  7.0     9.0
  197  0.0    10.0    209  6.0    10.0
  210  7.0    10.0
  211  0.0    11.0    223  6.0    11.0
  224  7.0    11.0
  225  0.0    12.0    237  6.0    12.0
E 238  7.0    12.0
  1   1   2   16  15  1   12
  13  15  16  30  29  2   24
  25  29  30  44  43  3   36
  37  43  44  58  57  4   48
  49  57  58  72  71  5   60
```

```
   61  71  72  86  85  5   72
   73  85  86  100 99  6   84
   85  99  100 114 113 6   96
   97  113 114 128 127 7   108
   109 127 128 142 141 7   120
   121 141 142 156 155 8   132
   133 155 156 170 169 8   144
   145 169 170 184 183 9   156
   157 183 184 198 197 10  168
   169 197 198 212 211 11  180
   181 211 212 226 225 12  192
   193 113 114         15  204
   205 13  14          13  205
   206 27  28          13  206
   207 41  42          13  207
   208 55  56          13  208
   209 69  70          14  209
   210 83  84          14  210
   211 97  98          14  211
   212 111 112         14  212
   213 139 140         14  213
   214 153 154         14  214
   215 167 168         14  215
   216 181 182         14  216
   217 195 196         13  217
   218 209 210         13  218
   219 223 224         13  219
   220 237 238         13  220
   221 125 126         14  221
E  222 225 226         16  232
   1   13  1   1
   15      1   0
   29      1   0
   43      1   0
   57      1   0
   71      1   0
   85      1   0
   99      1   0
```

```
   113    1  0
   127    1  0
   141    1  0
   155    1  0
   169    1  0
   183    1  0
   197    1  0
   211    1  0
   225    1  0  1
   14     1  1
   28     1  1
   42     1  1
   56     1  1
   70     1  1
   84     1  1
   98     1  1
   112    1  1
   126    1  1
   140    1  1
   154    1  1
   168    1  1
   182    1  1
   196    1  1
   210    1  1
   224    1  1
E  238    1  1
   1  12  1
   181 192 3
   222 232 2
   222 232 1
   222 232 3
   222 232 4
   13  0  4
   25  0  4
   37  0  4
   49  0  4
   61  0  4
   73  0  4
```

```
   85  0   4
   97  0   4
   109 0   4
   121 0   4
   133 0   4
   145 0   4
   157 0   4
   169 0   4
   181 0   4
   12  0   2
   24  0   2
   36  0   2
   48  0   2
   60  0   2
   72  0   2
   84  0   2
   96  0   2
   108 0   2
   120 0   2
   132 0   2
   144 0   2
   156 0   2
   168 0   2
   180 0   2
E  192 0   2
   2   0   0   0   0   1   1   0.05     1
   1   225             -0.195
   1   226  235         -0.39
E  1   236             -0.195
   3   0   0   0   0   1   0   0.05     1
   1   225             -0.195
   1   226  235         -0.39
E  1   236             -0.195
   4   0   0   0   0   1   0   0.05     1
   1   225             -0.195
   1   226  235         -0.39
E  1   236             -0.195
   5   0   0   0   0   1   0   0.05     1
```

```
   1  225          -0.195
   1  226  235      -0.39
E  1  236          -0.195
   6  0  0  0  0  1  0  0.05    1
   1  225          -0.195
   1  226  235      -0.39
E  1  236          -0.195
   7  0  0  0  0  1  0  0.05    1
   1  225          -0.195
   1  226  235      -0.39
E  1  236          -0.195
   8  0  0  0  0  1  0  0.05    1
   1  225          -0.195
   1  226  235      -0.39
E  1  236          -0.195
   9  0  0  0  0  1  0  0.05    1
   1  225          -0.195
   1  226  235      -0.39
E  1  236          -0.195
  10  0  0  0  0  1  0  0.05    1
   1  225          -0.195
   1  226  235      -0.39
E  1  236          -0.195
  11  0  0  0  0  1  0  0.05    1
   1  225          -0.195
   1  226  235      -0.39
E  1  236          -0.195
  12  0  0  0  0  1  0  0.05    1
   1  225          -0.195
   1  226  235      -0.39
E  1  236          -0.195
  13  0  0  0  0  1  0  0.05    1
   1  225          -0.195
   1  226  235      -0.39
E  1  236          -0.195
  14  0.0  0  0  1  0  0.05    1
   1  225          -0.195
   1  226  235      -0.39
```

```
E  1  236          -0.195
  15  0  0  0  0  1  0  0.05    1
   1  225          -0.195
   1  226  235      -0.39
E  1  236          -0.195
  16  0  0  0  0  1  0  0.05    1
   1  225          -0.195
   1  226  235      -0.39
E  1  236          -0.195
  17  0  0  0  0  1  0  0.05    1
   1  225          -0.195
   1  226  235      -0.39
E  1  236          -0.195
  18  0  0  0  0  1  0  0.05    1
   1  225          -0.195
   1  226  235      -0.39
E  1  236          -0.195
  19  0  0  0  0  1  0  0.05    1
   1  225          -0.195
   1  226  235      -0.39
E  1  236          -0.195
  20  0  0  0  0  1  0  0.05    1
   1  225          -0.195
   1  226  235      -0.39
E  1  236          -0.195
  21  0  0  0  0  1  1  0.05    1
   1  225          -0.195
   1  226  235      -0.39
E  1  236          -0.195
  22  0  0  0  0  0  0  5.0     1
  23  0  0  0  0  0  1  5.0     1
  24  0  1  0  0  0  1  0.05    1
  -205
  -206
  -207
  -208
  -209
  -210
```

```
   -211
   -212
   -213
   -214
   -215
   -216
   -217
   -218
   -219
   -220
E  -221
   25  0  0  0  0  0  1  10.0    1
   26  0  0  0  0  0  1  100.     1
   27  0  0  0  0  0  1  1440.    1
   28  0  0  0  0  0  1  1440.    1
   29  0  0  0  0  0  1  1440.    1
   30  0  0  0  0  0  1  1440.    1
   31  0  0  0  0  0  1  1440.    1
   32  0  0  0  0  0  1  1440.    1
   33  0  0  0  0  0  1  1440.    1
   34  0  0  0  0  0  1  1440.    1
   35  0  0  0  0  0  1  1440.    1
   36  0  0  0  0  0  1  1440.    1
   37  0  0  0  0  0  1  1440.    1
   38  0  0  0  0  0  1  1440.    1
E  39  0  0  0  0  0  1  1440.    1
```

BIBLIOGRAPHY

AASHTO Standard Specifications for Highway Bridges, 15th edition (1992), AASHTO subcommittee on Bridges and Structure.

Allen, T.M., Christopher, B.R., and Holtz, R.D. (1992) "Performance of a 12.6 m High Geotextile Wall in Seattle, Washington," International Symposium on Geosynthetic-Reinforced Soil Retaining Walls, Balkema Publishers, Natherlands, pp. 81-100.

Bathurst, R.J., Simac, M.R., Christopher, B.R., and Bonczkiewicz (1993),"A Data Base of Result from a Geosynthetic Reinforced Modular Block Soil Retaining Wall," International Symposium: Soil Reinforcement: Full Scale Experiment of the 80's, Paris, France, pp. 341-365.

Billiard, J.W. and Wu, J.T.H. (1991), "Load Test of a Large-Scale Geotextile-Reinforced Retaining Wall," Proceedings of Geosynthetics 1991 Conforence, Atlanta, Georgia, pp. 537-548.

Chou, N.N.S. (1992), "Performance of Geosynthetic Reinforced Soil Walls," Ph.D. Thesis, Department of Civil Engineering, University of Colorado, Denver, CO, USA.

Collins, J.G., Bright, D.G., and Berg, R.R. (1994), "Performance Summary of the Tanque Verde Project-Geogrid Reinforced Soil Retaining Walls," Proceedings, Earth Retaining Session, ASCE National Convention, Atlanta, GA., 1994.

Findley, Lai and Onaran (1976), "Creep and Relaxation of Nonlinear Viscoelastic Materials," North-Holland series in Applied Mathemetics and Mechanics, Vol. 18, North-Holland Publishing Company.

Helwany, M.B. and Wu, J.T.H. (1995), "A Numerical Model for Analyzing Long-Term Performance of Geosynthetic Reinforced Soil Structures," Geosynthetics International, Vol. 2, No. 2, pp. 429-453.

Helwany, M.B. (1994), " A Deep Patch Technique for Landslide Repair," Report No. CTI-UCD-2-94, Colorado

Transportation Institute.

Helwany, M.B. and Wu, J.T.H. (1992), "A Generalized Creep Model for Geosynthetics," Earth Reinforcement Practice, Ochiai, H., Hayashi, S. and tani, J., Eds., Balkema, 1992, Proceedings of the International Symposium on Earth Reinforcement Practice, Fukuoka, Kyushu, Japan, Vol. 1, Nov 1992, pp. 79-84.

Iizuka, A. and Ohta, H. (1987), "A Determination Procedure of Input Parameters in Elasto-Viscoplastic Finite Element Analysis," Soils and Foundations, Vol. 27, No. 3, pp. 71-87.

Morgan, C.J. and Ward, I.M. (1971), "The Temperature Dependence of Nonlinear Creep and Recovery in Oriented Polypropylene," J. Mech. Phy. Solids, Vol. 19, pp. 165-178.

Ohta, H. (1971), "Analysis of Deformation of Soils Based on the Theory of Plasticity and its Application to Settlement of Embankments," Doctor of Engineering Thesis, Kyoto University, Japan.

Ohta, H. and Hata, S. (1971),"A Theoretical Study of the Stress-Strain Relations for Clays," Soils and Foundations, Vol. 11, No. 3, pp. 65-90.

Roscoe, K.H., Schofield, A.N. and Thurairajah, A. (1963),"Yielding of Clays in State Wetter Than Critical," Geotechnique, Vol. 13, No. 3, pp. 211-240.

Sekiguchi, H. (1989),"Theory of Undrained Creep Rupture of Normally Consolidated Clay Based on Elasto-Viscoplasticity," Soils and Foundations, Vol. 24, No. 1, pp. 129-147.

Sekiguchi, H. and Ohta, H (1977),"Induced Anisotropy and Time Dependency in Clays," Proceedings of the 9th International Conference on Soil Mechanics and Foundation Engineering, Special Session 9, Vol. 3, Tokyo, Japan, pp. 542-544.

Shibata, T. (1963),"On the Volume Changes of Normally Consolidated Clays," Annuals of Disaster Prevention Research Institute, Kyoto University, No. 6, pp. 128-134.(in Japanese).

Simac, M.R., Christopher, B.R., and Bonczkiewicz, C. (1990),"Instrumented Field Performance of a 6 m Geogrid Soil Wall," Proceedings of the Forth International Conference on Geotextiles, Geomembranes and Related Products, The Hague, Vol. 1, pp. 53-59.

Tatsuoka, F., Molenkamp, F., Torii, T. and Hino, T. (1984),"Behavior of Lubrication Layers of Platens in Element Tests," Soils and Foundations, Vol. 24, No. 1, pp. 113-128.

Wu, J.T.H. and Helwany, S.M.B. (1996),"A Performance Test for Assessment of Long-Term Creep Behavior of Soil-Geosynthetic Composites," Geosynthetic International, Journal of International Geotextile Society, Vol. 3, No. 1.

Wu, J.T.H. (1994),"long-Term Creep Behavior," Discussion, International Symposium on Recent Case Histories of Permanent Geosynthetic-Reinforced Soil Retaining Walls, Tokyo, Japan, 1992, A.A. Balkema Publishers, Natherlands, pp. 343-344.

Wu, J.T.H. (1992a),"Predicting Performance of the Denver Walls: General Report," Geosynthetic-Reinforced Soil Retaining Walls, Denver, CO, Balkema publisher, pp. 3-20.

Wu, J.T.H. (1992b),"Construction and Instrumentation of the Denver Walls," Geosynthetic-Reinforced Soil Retaining Walls, Denver, CO, Balkema publisher, pp. 21-30.

Wu, J.T.H. (1991),"Measuring Inherent load Extension Properties of Geotextiles for Design of Reinforced Structure," ASTM Geotechnical Testing Journal, Vol. 14, No. 2, pp. 157-165.